This is to certify that the
thesis entitled

INFLUENCE OF A COARSE-GRAINED INCISED-VALLEY FILL ON GROUNDWATER FLOW IN FLUVIAL FAN DEPOSITS, STANISLAUS COUNTY, MODESTO, CALIFORNIA, USA

presented by

Amy LeVan Lansdale

has been accepted towards fulfillment
of the requirements for the

M.S. degree in Geological Sciences

Major Professor's Signature

12-15-05

Date

INFLUENCE OF A COARSE-GRAINED INCISED-VALLEY FILL ON GROUNDWATER FLOW IN FLUVIAL FAN DEPOSITS, STANISLAUS COUNTY, MODESTO, CALIFORNIA, USA

By

Amy LeVan Lansdale

A THESIS

Submitted to
Michigan State University
in partial fulfillment of the requirements
for the degree of

MASTER OF SCIENCE

Department of Geological Sciences

2005

ABSTRACT

INFLUENCE OF A COARSE-GRAINED INCISED-VALLEY FILL ON GROUNDWATER FLOW IN FLUVIAL FAN DEPOSITS, STANISLAUS COUNTY, MODESTO, CALIFORNIA, USA

By

Amy LeVan Lansdale

A relatively coarse grained incised-valley fill (IVF) was identified beneath the city of Modesto, California using geophysical logs. The Tuolumne River fluvial fan IVFs are the result of periods of degradation followed by rapid aggradation due to cycles of Quaternary climate change. These IVFs were located through the use of driller's well logs. Results indicate that the location of the relatively coarse grained IVF can be reasonably approximated by identifying the basal gravel unit of the IVF in the driller's well logs. From the well log analysis and the use of topographic maps, the wedge shaped IVFs are approximately 0.7 to 1.6 km wide and approximately 3 to 30 meters thick with a 5 to 9 meter gravel base that thins down fan. The influence of these IVFs on the regional groundwater flow was tested using a steady-state saturated groundwater model adapted from a USGS model (S. Phillips, unpublished model, 2005). Groundwater flow and contaminant transport models with and without the IVF deposits of the Tuolumne River show IVFs significantly influence groundwater flow and contaminant transport. Specifically, results indicate that the Tuolumne River IVFs provide potential for (1) increased groundwater production rates (2) rapid contaminant transport within the IVF sediments and (3) rapid contaminant movement from the IVF into the contiguous aquifer sediments. The presence of an IVF beneath the city of Modesto, in particular, may have implications for artificial aquifer recharge and regional water quality.

ACKNOWLEDGEMENTS

This thesis could not have been completed with the dedication and countless hours of guidance from my adviser Gary Weissmann. I also want to thank my other committee members, David Hyndman and Phanikumar Mantha for their contributions. I especially would like to thank Dave for his role as my stand in adviser, and for always making time to answer my "quick questions". This research was also made possible by the U.S. Geological Survey (USGS) in Sacramento, California, which afforded access to office space for a summer as well as a substantial amount of data (driller's well logs, core samples, and digital spatial data). USGS employees Karen Burow, Steve Phillips, Barb Dalgash, George Bennett, and Jen Shelton especially provided guidance during my summer of research in California.

Funding for this research was provided by Michigan State University. Acknowledgment is made to the Donors of the American Chemical Society Petroleum Research Fund, for support of this research (PRF#37731-G8).

Significant contributions were also made by the students and faculty of the Michigan State University Hydrostratigraphy and Hydrogeology research groups. A special thanks to Nick Welty, Anthony Kendall, Dush Jaywickreme, and Cheryl Kendall for all of your suggestions. Finally, I want to thank my family and friends who supported me through the long thesis writing process. Thank you Mom and Dad, Garrett, Beth, and Karen for your endless patience.

Table of Contents

List of Tables

List of Figures

Chapter 1: Introduction and Scope of the Study

INTRODUCTION

Modeling in heterogeneous fluvial aquifers can be a very difficult venture. Heterogeneities often exist at various scales within aquifer sediments and have the potential to largely impact or entirely control the direction and velocity of groundwater flow and contaminant movement.

Without detailed field investigations of the spatial distribution of hydraulic conductivity (K), aquifer heterogeneity is significantly more difficult to replicate in groundwater models. For this reason, many studies have begun to employ more qualitative information into approaches that generate K distributions in fluvial aquifer deposits, utilizing known geologic relationships to develop aquifer conductivity fields (e.g. Fogg, 1986; Schiebe and Freyberg, 1995; Webb and Anderson, 1996; Weissmann *et* al, 2004). These studies highlight the importance of preserving the influence of geologic structure in modeling groundwater flow and contaminant transport.

Maintaining the geologic structure within a fluvially deposited aquifer becomes particularly important in scenarios where the contrast between the hydraulic conductivities of the aquifer deposits is high (Webb and Anderson, 1996). Results from Webb and Anderson (1996) showed that in these types of settings, the geologic structure that coincides with the hydraulic conductivity (in their study the braided channel forms) can control regional groundwater flow and particle movement.

In this study, I will examine a similar scenario to determine the influence of a relatively coarse grained incised valley fill (IVF) on groundwater flow in the Modesto area in California. Within the study area, there is a lack of detailed field data on aquifer heterogeneity, but the geological framework is reasonably well understood (Janda, 1966; Marchand, 1977; Huntington, 1980; Marchand and Allwardt, 1981, Lettis, 1988; Burow *et al.*, 2004; Weissmann *et al.*, 2006). Despite the deficiency in detailed aquifer data, we were successfully able to adapt a pre-existing groundwater model to incorporate the geologically-based, geometrical relationship of the relatively coarse-grained IVF. The IVF is added using techniques which preserve the valley geometry and the internal stratigraphy to asses the influence of this discrete geologic structure on the regional groundwater flow and contaminant transport.

PURPOSE OF STUDY

The main purpose of this study is to understand the impact IVF deposits in the Tuolumne River fluvial fan aquifer around Modesto, California, can have on regional groundwater flow, contaminant transport, and artificial aquifer recharge. This was accomplished by (1) assessing the stratigraphic character of the study area with well logs and core, (2) constructing model domains that capture this stratigraphic character, and (3) simulating groundwater flows and solute tracers through these models to evaluate the influence IVFs have on groundwater and contaminant transport. This work provides the foundation for future studies that will better define and model the IVF.

This study area along the Tuolumne River was chosen because geophysical well logs revealed the presence of a relatively coarse grained IVF deposit within Tuolumne River fluvial fan deposits directly beneath the city of Modesto, California (Burow et al., 2004). Groundwater flow and contaminant transport models in previous studies of similar IVF deposits of the Kings River near Fresno, California, showed that IVFs significantly influence groundwater flow and contaminant transport (Weissmann *et al.*, 2004). Specifically, results indicated that the Kings River IVF provides potential for (1) increased groundwater flow and production rates (2) rapid contaminant transport within the IVF sediments and (3) rapid contaminant movement from the IVF into the contiguous aquifer sediments. If the identified IVF beneath the Modesto area has a similar effect, then it may have implications for artificial aquifer recharge and regional water quality in that area.

Current models of the hydrogeology in the Modesto, California, area are being developed by the USGS. The main source of model inputs is previously collected data (driller's logs, geophysical logs, and a few continuous cores) which are used to characterize the hydrogeology of the Modesto area (*Burow et al.*, 2004) and create a regional scale model of the geology (*Burow et al.*, 2004) and groundwater flow (S. Phillips, unpublished model, 2005). While the model that has been developed is a reasonable representation of the region's geology and hydrologic regime, it does not implicitly include the IVFs. The USGS model may be largely improved with the additional application of sequence stratigraphic concepts, described by Weissmann *et al.* (2002b, 2006), to depict and include IVF geometry and character into the groundwater flow model. An understanding of sequence stratigraphy in the area can aid in more accurately modeling the geology to illustrate various hydrofacies and their influence on the groundwater flow.

The model developed for this study utilizes an understanding of the area's sequence stratigraphy to develop multiple conceptual models to test the influence of IVFs. Using the same data the USGS used to develop models of the Modesto area, four geologic realizations of various combinations of IVF locations were developed for this study. A comparison among groundwater models of these realizations and the recently developed USGS groundwater model will improve the current understanding of regional groundwater and contaminant transport trends in the Modesto area.

THESIS OUTLINE

This thesis is divided into three main sections with subsequent appendices:

1. The first section, chapter 2, discusses the development and results of the Modesto area groundwater model and flow and transport simulations. I plan to submit this chapter for publication.
2. The final section of this thesis, chapter 3, is the conclusion where I describe major results of this work and suggest ideas for future work.
3. Subsequent appendices that support this work include:
   a. Appendix A: Delineating the IVF and study area geology
   b. Appendix B: Unconsolidated Sediment Core Description
   c. Appendix C: Driller's logs
   d. Appendix D: Sequence Boundary Surface Generation
   e. Appendix E: Opening USGS MODFLOW Model In GMS
   f. Appendix F: Adapted Model Generation
   g. Appendix G: IVF Fortran Code
   h. Appendix H: Vertical Hydraulic Conductivity and Anisotropy Ratio Fortran Code
   i. Appendix I: General Head Boundary Fortran Code
   j. Appendix J: Well Fortran Code

Chapter 2: Influence of a Coarse-Grained Incised-Valley Fill on Groundwater Flow in Fluvial Fan Deposits, Stanislaus County, Modesto, California, USA

INTRODUCTION

A relatively coarse grained incised-valley fill (IVF) deposit was identified in geophysical well logs beneath the city of Modesto, California (Burow *et al.*, 2004). A recent investigation by Weissmann *et al.* (2004), showed the impact of a similar IVF in the King's River area. To gain insight to the potential impact the IVF can have on regional groundwater flow and contaminant transport in the Modesto area, an investigation of the subsurface geometry, position, and hydrogeologic significance of the valley fill was conducted. Recommendations based on this research are made for further, higher resolution studies. The investigation includes : (1) development of multiple geologic realizations which test different potential locations of the IVF, (2) production of a corresponding number of flow and transport groundwater models, (3) particle pathline analyses that examine the potential for artificial recharge in the IVF, and (4) recommendations for further investigation in the area.

To test the impact of the IVFs on the regional groundwater flow and illustrate the importance of understanding and using sequence stratigraphic concepts at this site, this chapter reports on comparisons of realizations that include various scenarios of IVF locations, as described in Appendix A, with an adaptation of a model generated by the USGS that does not implicitly include the IVF deposits (Burow *et al.*, 2004; S. Phillips, pers. comm., 2005). In this chapter, the development of the USGS groundwater flow model, the modifications made to the model (inclusive of the addition of the IVFs), and various simulations of solute transport are described.

STUDY AREA

Regional and Local Geology

The San Joaquin Basin is located within the California's Great Valley, an approximately 700 km long (north to south) by 100 km wide (east to west) valley that is bound on the east by the Sierra Nevada and on the west by the Coast Ranges. The valley is divided into two sub-basins by the Stockton Arch, a buried transverse arch, with the Sacramento Basin in the north and San Joaquin Basin in the south. The basin is underlain by crystalline basement rock and approximately 9 km of Mesozoic and Cenozoic sedimentary rocks and sediments (Bartow, 1988). Structurally, the basin is asymmetric with a gently sloping eastern margin that abuts the Sierra Nevada, and the more steeply sloping western edge adjacent to the Coast Ranges. This study focuses on the Tuolumne River fan located in the northeast portion of the San Joaquin Basin (Figure 1 *NOTE: Some of the figures included in this thesis are presented in color.*). The fan was formed where the Tuolumne River flows west out of the Sierra Nevada into the San Joaquin Basin.

Quaternary fluvial fan deposits from numerous rivers along the eastern San Joaquin Valley, including the Tuolumne River fan, preserve evidence of past phases of aggradation and degradation from varying amounts of sediment supply and discharge in response to recurring glacial periods in the Sierra Nevada (Janda, 1966; Marchand, 1977; Huntington, 1980; Marchand and Allwardt, 1981, Lettis, 1988; Weissmann *et al.* 2002b, 2006). Fluvial fans are differentiated from alluvial fans in this study to emphasize that fluvial fans are characterized by perennial fluvial processes, while alluvial fans are characterized more by ephemeral debris flows or sheetfloods.

To understand the climatically induced cycles of deposition in the fluvial fans, Weissmann *et al.* (2002b) investigated the fluvial fan deposits on the Kings River fan and applied a sequence stratigraphic model. This sequence stratigraphic model describes changes in *accumulation space* and *preservation* space (after Blum and Törnqvist, 2000) that resulted in the cyclic deposits in the area. Accumulation space is defined as one component of accommodation space and refers to the volume of space available to be filled with sediment on a process-scale. It is dependent on the balance of sediment supply and stream discharge as well as channel geometry. Preservation space is also a component of accommodation space, and, in this case, is a more long-term, net accommodation and is controlled by the subsidence rate. It is the space below the lowest level of sediment removal.

On the Kings River fan, packages of relatively rapidly deposited fluvial fan deposits, or open fan deposits, separated by paleosols indicate periods of aggradation across the fan, or increased accumulation space, punctuated by periods of degradation and fan incision, or restricted accumulation space and quiescence on the upper parts of the fan. Preservation space was created by constant subsidence in the area, which lowered the deposits below the lowest level of erosion. Sequence boundaries in this model are identified as the paleosol surface and respective IVF base that divide the fluvial fan deposits into five stratigraphic units.

The five sequences mark distinct periods of regional aggradation and degradation. Specifically, fluvial fan aggradation or degradation on the Kings River fan occurred as sediment supply to discharge ratios increased or decreased with changes from glacial to interglacial climate. Interglacial periods are marked by limited aggradation, a low accumulation space, and an intersection point located distally on the fan (Figure 2) (Weissmann *et al.,* 2002b). This portion of the cycle is when deposition occurred only at the distal end of the fan allowing paleosols to form in the exposed upper fan outside the incised valleys. Glacial periods are characterized by a large amount of laterally extensive aggradation on the fan, a high accumulation space, and an intersection point proximally located to the apex of the fan. Weissmann *et al.* (2002b) suggested that this sequence stratigraphic model can assist in the prediction of facies distributions and stratigraphic relationships in areas exposed to similar conditions.

Due to the similar cyclic depositional character among the fans in the eastern San Joaquin Basin, the sequence stratigraphic model described in the Kings River fan study can be applied to other fans in the basin (Weissmann *et al.*, 2006). However climate and sediment supply to stream discharge ratios are only two of the controls on the deposition of the fluvial fans in the valley (Weissmann *et al.*, 2006). Factors that control the overall amount of accumulation space available during periods of climate fluctuation and hence sequence geometry development are: (1) the sediment supply to stream discharge ratio, (2) the rate of basin subsidence, (3) the amount of local base level change, and (4) the basin width (Weissmann, *et al.*, 2006). These controls vary within the San Joaquin Basin and influence the sequence geometry on individual fans.

Controls on the Tuolumne River sequence geometry in particular are (1) glacial influence in the drainage basin (2) relatively low subsidence rates (approximately 30cm/ 1000 yrs, Lettis, 1988) due to the river's location in the northern portion of the San

Joaquin Valley, and (3) the San Joaquin River local base level control on Tuolumne River elevation (Weissmann *et al.,* 2006). The Tuolumne River drainage basin in the Sierra Nevada was glaciated during the Quaternary, which resulted in cycles of significant fluctuations in the sediment supply and stream discharge. Because the Tuolumne River is in the north, where the valley is narrower and subsidence rate is relatively low, sequence thickness and lateral extent were thinner and smaller than observed in southern portions of the valley. This resulted in an overall reduction in accumulation and preservation space, which caused the lateral progression of apexes and the thinner fluvial fan units deposited along the Tuolumne River than were seen along the Kings River (Weissmann *et al.* 2006; Bennett *et al. in press*) (Figure 2). The local base level is connected to the San Joaquin River and ultimately sea level. This resulted in deeper incision and sediment bypass in the distal portions the fan during interglacial periods, also reducing the overall amount of accommodation space available to be filled.

The area within the scope of this study is delineated by the Sierra Nevada and the San Joaquin River to the east and west, respectively, and by the Stanislaus and Merced Rivers to the north and south (Figure 3). The study area is approximately 48 km (30 miles) long (west to east) and 19 km (12 miles) wide (north to south). Dissecting the site is the Tuolumne River, which flows east to west through the middle of the study area (Figure 3). Deposits at the site are composed mainly of Cenozoic sedimentary deposits (Marchand and Allwardt, 1981). These thick, slightly westward dipping fluvial fan deposits along the Tuolumne River decrease in age to the west, toward the San Joaquin Basin center (Figure 1). Uplift and erosion have exposed older fan units in the eastern portion of the basin. This study of the Modesto area will focus on the Quaternary

Pleistocene fluvial deposits: the Turlock Lake Formation, the Riverbank Formation and the Modesto Formation. A more comprehensive description of the older units in the area can be found in Marchand and Allwardt (1981).

GENERATING GEOLOGIC REALIZATIONS TO BE MODELED

Each stratigraphic unit of open-fan deposits is bound at the top and bottom by a paleosol and is composed of silty, sandy, and clayey sediments with discrete coarser-grained channel deposits (Figure 4). Nestled among the relatively fine-grained open-fan sediments are the relatively coarse-grained IVFs, characterized by a thick basal gravel lag (5 to 9 meters) that gradually fines up to the surface (Figure 5).

Characterization of hydrofacies within the fluvial fan deposits was done by using methods similar to those described in Weissmann *et al.* (2002b) where we utilized several sources of geologic data, including driller's well logs, geophysical logs, and lithology from continuous core samples. Cooperation with the U.S. Geological Survey (USGS) in Sacramento, California afforded access to several thousand paper copies of the Department of Water Resources (DWR) driller's logs within the study area, geophysical well logs from city wells, and recently obtained, relatively-continuous, soft sediment core. Also available from the USGS were digitized spatial data of the area hydrology, geology, soils, topography, and approximate pumping rates of the city of Modesto municipal wells (S. Phillips, unpublished data, 2005).

Multiple geologic scenarios were created using two soft sediment cores (a total of 155 meters (509 ft) of core—Appendix B) and lithologic descriptions from approximately 10,000 driller's well logs. The lithology from the soft sediment core samples was used to better understand the overall character of the fluvial fan deposits, and the driller's well logs were used to identify the IVF in the area.

Open Fan Deposit Character

Continuous core samples collected by the USGS from two well locations were assessed: one located in a proximal fan position and the other on a distal portion of the fan (Figure 3). The proximal well, MREA, was drilled to a depth of 96 m (315 ft) and the distal well, MRWA, was drilled to a depth of 59 m (195 ft).

Hydrofacies observed in these cores include: (1) gravel channel deposits (not recovered in these cores but observed in drillers' logs and described by Weissmann *et al.*, 2002b) (2) sand channel deposits (3) silty sands, silty clays, and clay overbank deposits, and (4) pedogenically altered deposits. The core descriptions show that the western extent of the study area contained more fine-grained sediments of the distal fluvial fan deposits, while the eastern extent of the study area contained the more coarse-grained proximal fluvial fan sediments. More detailed descriptions of these hydrofacies are in Appendix A.

Incised-Valley Fill Geometry

Through the interpretation of approximately 10,000 drillers' well logs and geophysical well logs, we were able to locate the originally identified IVF along with several other plausible additional valley fills. Further analysis of the location and depth of the IVFs was completed by mapping selected well logs in ArcMap.

The well logs that note gravels of sufficient thickness (> 3 meters) were assigned a rank of 1 to 4 in 0.5 increments based on how accurately the log's description of the stratigraphy resembled the fining-upward prototype characterization of the IVF, as observed in the geophysical well logs by Burow *et al.* (2004) and described for the Kings River fluvial fan by Weissmann *et al.* (2002b) (See Appendix C). A well assigned a rank of 1 denotes the best representation of the IVF, with a thick gravel base fining upward to sand then silt and clay, while a well ranked 4 contains thick gravel but does not resemble the ideal fining-upward succession contained within the IVF deposits. The drilling method and the consistent quality of individual drillers were also used to determine the rank of the well.

The geometry of the IVF was approximated through the analysis of well logs and assessment of the modern Tuolumne River valley geomorphic configuration in topographic maps, which is assumed analogous to the interglacial character of the paleovalleys to be modeled. The IVF is estimated to (1) be 0.7 to 1.6 kilometers wide, (2) range from approximately 30 meters thick at the apex of the fan to approximately 3 meters thick at the toe of the fan, giving it a wedge-shaped appearance, and (3) have a 5 to 9-meter-thick gravel base near the fan apex that thins down fan (Figure 5).

Using the database of well logs, a map of the various ranked wells was created within ArcGIS. Because each plotted well does not represent the IVF, a subsequent map exclusively of the highest ranked wells, 1 through 2, was generated to emphasize any elongate channel patterns (Figure6A). General trends indicate presence of (1) a paleovalley trending northwest from beneath the city of Modesto in the west side of the site, (2) a paleovalley trending just north of and paralleling the current Tuolumne River, (3a) a shallow paleovalley as a short meander loop in the eastern portion of the site, and (3b) a shallow paleovalley trending to the southwest, also in the eastern extent of the study area.

Further analysis to determine which geologic formation these valleys correlate to was conducted by looking at the basal gravel depths (Figure 6B). The gravel depths were mapped in intervals of the expected depths of the IVF base. A 6 m (~20 ft) resolution was allotted for possible error or variation in accuracy among drillers. A depth of 24 to 38 m (80 to 125 ft) was expected for the Modesto Formation IVF basal gravel, and a depth of 43 to 61 m (~140 to 200 ft) was expected for the Riverbank Formation IVF basal gravel depth. From this map, the previously identified four IVF trends are still prevalent; however four valleys can be segregated. The possible valleys interpreted to exist from this map are: (1) a Riverbank Formation IVF from the Stanislaus River to the north that may trend beneath the city of Modesto, (2) a Riverbank Formation IVF from the Tuolumne River that appears to be clearly marked adjacent to the current river valley and may potentially cross the modern river valley in the eastern reach of the river, and (3) the two potential positions for the Modesto Formation IVF—(A) a small loop adjacent to the modern Tuolumne River in the eastern reach of the river (identified in an aerial photo of the current surface—See Figure 7) and (B) a southwestern trending IVF projecting from the same location as position A. These trends are reemphasized when slightly lower ranked wells (rank 2.5) were added to the map.

Because significant uncertainty exists as to whether these trends are real, this study focuses on addressing multiple conceptual scenarios of valley fill orientation and geometries. Initial interpretations of the various locations for the Modesto IVF (positions A and B) and the potential Stanislaus River IVF influence from the north provide a foundation for the following four geologic scenarios that test the combinations of these channel positions. The resulting four realizations are summarized in Table 1, and include: (a) Riverbank IVF from Tuolumne River and the Modesto IVF *A*, or the small loop adjacent to the modern Tuolumne River(RB/MS), (b) Riverbank IVF from Tuolumne River and the Modesto IVF *B* the large IVF that projects southwest from the apex (RB/ML) (c) Riverbank IVF from the Stanislaus River and the Tuolumne River and the Modesto IVF *A* the small loop (RB/ST/MS) and (d) Riverbank IVF from the Stanislaus River and the Tuolumne River and the Modesto IVF *B* (RB/ST/ML).

GROUNDWATER MODEL DEVELOPMENT

Steady-state groundwater and transport models were produced using Groundwater Modeling System 5.1 (GMS 5.1) and were modified from a MODFLOW 2000 model developed by the US Geological Survey (S. Phillips, unpublished model, 2005, Burow *et al,* 2004). The Stanislaus, Merced, and San Joaquin Rivers provide relatively natural hydrologic boundaries on the north, south and west sides of the model domain, respectively. The Sierra Nevada is approximated as a no–flow boundary to the east. The steady-state model includes the influence of pumping in the city of Modesto and is calibrated to match measured water levels in the region. Along with the groundwater flow and contaminant transport models of the multiple geologic realizations, simulations testing the artificial recharge potential of the IVF scenarios were also assessed. Based on the results of the flow and transport models and the artificial recharge model, recommendations are made on where future more comprehensive investigations should be conducted. Methods for generating numerical models of these realizations are described below.

USGS Model

The framework for the model used in this study of the influence of the IVF was generated by the USGS (S. Phillips, unpublished model, 2005). The finite difference steady-state model (produced in MODFLOW) was constructed based on the hydrogeologic characterization of the Modesto area described in Burow *et al.* (2004). Included in the report by Burow *et al.* (2004) is a description of how the model area geology was characterized using existing data and how the area water budget was calculated using information about water deliveries, pumping, and recharge within several subwatersheds.

A coarse-fine geologic model was produced by Burow *et al.* (2004) using geophysical logs and lithologic descriptions from driller's well logs to develop representative percent coarse sediment fractions (F_{coarse}) for the model area (F_{fine} was subsequently calculated as the remaining percent). To determine F_{coarse}, a binary texture classification of "coarse grained" or "fine grained" was used to assign either 100 or 0 percent coarse grained: gravels and sands were assigned 100 percent and silts and clays as well as more consolidate sediments were assigned 0 percent. The percent coarse fractions were then determined using a weighted average for 1-meter (3.3 feet) depth intervals. Horizontal and vertical hydraulic conductivities (Kh and Kv) across the study area were calculated with these percent coarse fractions and various combinations of end-member conductivities (a K_{coarse} and a K_{fine}). Equivalent conductivities were calculated using the arithmetic mean for Kh and the harmonic mean for Kv shown below in equations 1 and 2.

Arithmetic Mean for Kh

$$K_{equiv} = (F_{coarse} \times K_{coarse}) + (F_{fine} \times K_{fine}) \quad \textbf{(1)}$$

Harmonic Mean for Kv

$$K_{equiv} = \frac{1}{\frac{F_{coarse}}{K_{coarse}} + \frac{F_{fine}}{K_{fine}}} \quad (2)$$

The groundwater model was run systematically with equivalent conductivities for several combinations of end-member K values and calibrated to wells in various locations of the model (wells below the Corcoran Clay, above the Corcoran Clay but below the water table, and east of the Corcoran Clay as well as some shallow wells in the western portion of the model) (S. Phillips, pers. comm., 10/4/05). The root-mean squared error (RMSE) was determined and plotted for each end-member combination to determine the combination with the least amount of error. The final end-members used to assign K values are 80 m/day (262 ft/day) for K_{coarse} and 0.008 m/day (0.02624 ft/day) for K_{fine}.

The 1 meter interval data set of equivalent K values was smoothed within a 10 meter (32.8 feet) vertical window (+ or -5 meters (16.4 feet) from the point being sampled) and then resampled every 5 meters (16.4 feet). The 10 meter smoothed data set was kriged using two nested structures: (1) Gaussian variogram model and (2) exponential variogram model. This kriged grain size-to-K model implicitly includes the IVFs, which is evident by regions of coarse grained deposits in various locations, especially south of the Tuolumne River.

From the data included in the report by Burow *et al.* (2004), a 16-layer model was created. The model area is approximately 62 km long and 55 km wide and has a maximum thickness of ~420 meters. The model uses the Block Centered Flow (BCF) package and the PCG2 (preconditioned conjugate gradient 2) solver. The vertical discretization of the USGS model was developed as various percentages of the total thickness between two halves of the model. The top half was discretized between the top of layer 8 (the Corcoran Clay) and the top of the model (the land surface). The bottom half was discretized as percentages of thickness from the bottom of layer 8 to the bottom of the model (an artificially generated surface). Layer 8 top and bottom in the western portion of the model were assigned based on thickness estimates of the Corcoran Clay from Page (1986).

Boundary Conditions

The boundary conditions in the USGS model are defined by general head boundary (GHB) cells. The boundaries along the perimeter of the northern, southern, and western portion of the model represent the expected vertical gradient in the aquifer. In the top model layer, the rivers are GHBs. The San Joaquin River is denoted completely by GHB cells. The other three westward flowing rivers (Stanislaus, Tuolumne, and Merced Rivers) in the area are represented as a combination of GHB cells and specified flux cells. In the western portion of the model area, these westward flowing rivers are GHBs because they are connected to the water table, where the depth to the water table is relatively low. However, in the east, the rivers are no longer connected to the water table and are denoted with a specified flux cell (described below in recharge). Each general head boundary cell requires two inputs: (1) a head value and (2) a conductance value.

Initial head values for the GHB representing rivers were determined from stream gage data and the area topography. The lateral boundary GHB heads that represent the expected vertical gradient were estimated from water-level data (S. Phillips, pers. comm.

8/1/05 and 12/5/05). A vertical gradient of 0.05 meters of head per meter of depth (thickness) was applied to the initial head values to produce the head elevations for the GHB (ghbhead). The gradient applied was based on vertical gradients observed in nested wells northeast of Modesto and generalized flow directions based on the approximate average elevation of the perforated interval of deep production wells in the area (S. Phillips, unpublished data, 9/26/05 and 9/20/05).

The average elevation of the perforated interval of deep production wells is estimated to be within layer 9 of the model. This heavy pumping generates a complex vertical gradient with downward flow from layer 1 to layer 9 and upward flow from layer 16 to layer 9. To recreate the influence of deep production wells on the flow regime, a gradient of 0.05 meters of head per meter of depth was multiplied by the depth to the cell center. This value was then *subtracted* from head levels in layer 1 for layers 2 through 9 (the layer below the Corcoran Clay), reducing the head elevations with depth and creating a downward flow. Conversely, the gradient was multiplied by the depth of the center of the cell and *added* to the head assigned to layer 9 for layers 10 through 16, increasing the head elevations with depth creating upward flow toward layer 9. Additionally, to prevent the head value calculated for layers 10 through 16 from exceeding the head value in layer 1, mathematically possible but physically implausible, head levels that were calculated to be greater than the head elevation in layer 1 were set equal to the head elevation in layer 1.

The conductance (ghbcond) through the GHB cells was determined depending on the location of the cell in the model: the top layer river cells had different conductance calculations than the rest of the GHB cells. In general, conductance is calculated using two variables: (1) the horizontal hydraulic conductivity assigned to the cell and (2) the cell thickness. Constants also included in the calculation are: (1) cell size (400m) and (2) general head boundary distance (400m).

$$\mathbf{ghbcond = KH*thick*cellsize/\ ghbdist} \qquad (3)$$

For the GHB cells that delineate rivers in layer 1, this boundary allows a small amount of vertical flow, while below layer 1 along the western model edge and for all layers along the north and south extent of the model, the boundary reflects the overall lateral flow from the east. To implement this condition, the conductance through layer 1 GHB cells at the location of the rivers was calculated using the vertical hydraulic conductivity, riverbed thickness (1m), river width (25m), and a vertical conductivity multiplier of 10.

$$\mathbf{ghbcond = KV * ((cellsize*rivwidth)\ /bedthick)*\ vkrivmult} \qquad (4)$$

<u>Recharge</u>

Recharge to the aquifer was assigned from the 2000 water budget reported by Burow *et al.* (2004), and was determined with a land use approach. Burow *et al.* (2004) divide the study area (same as the model area) into the 47 sub-regions (the smallest possible) where the amount of surface water deliveries could be evaluated. Separate water budgets were evaluated for each of the 47 sub-areas containing non-urban (crop and vegetation) and urban settings. Recharge in non-urban settings was estimated with crop demand (calculated from National Oceanic and Atmospheric Administration (NOAA) and the California Department of Water Resources data), surface water deliveries (from local irrigation district data), and precipitation (from NOAA data) in combination with land use surveys for Stanislaus and San Joaquin counties. Urban area recharge was approximated using estimates of applied water, leakage from distribution lines, and precipitation. Recharge from rivers is assumed to be 0.005 m/d in locations where the river was not connected to the water table. Although this recharge value is the best current approximation, recharge rates over the rivers could not accurately be estimated with the available data, and calibration of this parameter was poorly constrained (S. Phillips, pers. comm., 08/01/05).

Base-soil Evaporation

Transpiration for this model was accounted for separately in the water budget from *Burow et al.* (2004). Thus, the evapotranspiration package (ET) was used in this groundwater model to account for base-soil evaporation with a maximum evaporation rate of 1.6 m/yr at land surface. This rate was determined from pan evaporation estimates; however significant uncertainty exists around this value. The maximum extinction depth is 2.1 meters below the land surface.

Wells

Pumping from three types of wells (urban-supply, agricultural, and water-table-control, or have known "drainage") is accounted for in the model. (Water table control wells are shallow pumping wells located mostly in the western portion of the model that prevent the water table from rising to a point where it can interfere with crop roots.) Although domestic wells are numerous in the area, pumpage from wells in this category is extremely small compared to pumpage from urban supply, agriculture and water-table-control wells, so it was ignored.

Pumpage was distributed by dividing the three types of wells in the model to one of two categories: (1) actual wells with measured pumpage values and (2) imaginary wells that account for unmeasured private agricultural pumpage. The measured wells were assigned an annual pumping rate for the water year 2000 (i.e. from October 1, 1999 to September 30, 2000). The imaginary wells representing the private agriculture wells were assigned annual pumping rates estimated from the water budget described in *Burow et al.* (2004), where this rate is generally estimated as the residual between sources and demand for crop water assumed to be met by private pumpage. The amount of pumpage was distributed among imaginary wells within each sub-area defined in the water budget calculation (Burow *et. al.*, 2004).

Reservoirs

This model also incorporates the recharge from local reservoirs through use of the reservoir package. This package is similar to the river package. The reservoirs included in this model are the Wood Reservoir (to the northeast), the Modesto Reservoir (to the east), and Turlock Lake (to the southeast) (Figure 8). Turlock Lake is only partially within the model boundaries, but still contributes leakage to the region and was included.

Leakage from the reservoirs is calculated by the reservoir package as the product of the hydraulic conductance of the reservoir bed sediments and the difference between the stage of the reservoir and the head in the groundwater system. However, once the reservoir and groundwater are no longer connected, the recharge rate from the reservoir is constant, not head-dependent. Reservoir bed conductance is calculated from estimates of vertical hydraulic conductivity of the reservoir bed (m/day), thickness of the reservoir bed (m), and the model cell's row and column dimensions. The modeled total inflow volume of 192,701 m^3 (6,805,171 ft^3) from all three reservoirs was based on an estimate made by the Modesto Irrigation District (MID) for the Modesto Reservoir, and the assumption that the other reservoirs had similar leakage rates (S. Phillips, pers. comm., 8/31/05).

Modifications to the USGS Model

The USGS model of the Modesto area was generated to obtain a better understanding of the regional flow and water budget. The model for our study aims to specifically show the influence of the IVF within this regional approximation of groundwater flow. Alterations made to the original USGS model, described in more detail below, include: (1) the addition of the IVFs, (2) altered slope of the uppermost layers in the model, (3) increased vertical discretization, (4) use of the Layer Property Flow (LPF) package, (5) addition of GHB conditions along the upper reaches of the river, (6) removal of GHB cells from the northeastern portion of the model, (7) slight alteration of the vertical head gradient calculation in the GHB, and (8) reduced vertical conductance of the reservoirs.

<u>Addition of the IVF</u>

Each of the four IVF scenarios (RB/ML, RB/MS, RB/ST/ML, and RB/ST/MS) was modeled in an adaptation of the USGS model (Figure 9). To add these IVFs to the model, a code was developed to assign IVF hydraulic conductivity values to the cells within the IVF (Appendix G). The code uses the elevation at the center of the cell and the lateral location of the cell to assign either the original USGS hydraulic conductivity or an IVF hydraulic conductivity. The code also accounts for the fining upward character of the valley by assigning K values that differentiate between cells that represent basal gravel, sand, or the uppermost fines (see Appendix F and G). This internal IVF stratigraphy was modeled as an elevation percentage between the top and bottom of the valley (total valley thickness). Gravel represented the basal 40% of the IVF, sand the middle 45% of the IVF, and fines the top 15% of the total valley thickness. The Kh values for the gravel and the fines sections of the IVF with values used in Weissmann *et al.* (2004), with gravel = 864 m/d and fines = 0.0864 m/d. The sand in the IVF was assigned a K of 220 m/d, instead of the 86.4 m/d used by Weissmann *et al.* (2004). We deviated from the values in Weissmann *et al.* (2004) and chose a K of 220 m/d to maintain consistency with our conceptual model which asserts that the IVF is more coarse-grained than the surrounding sediments. The reasons for increasing the K of the sand in the IVF are discussed in more detail in the results.

Slope of Upper Model Layers and Vertical Discretization

To best preserve the continuous nature and fining upward character of the IVF deposits to test their impact on the groundwater flow, the vertical discretization and slope of the layers in the upper portions of the model were changed from the original USGS model. The original 16 layer model was converted to a 27 layer model, described in detail in Appendix F. The top of USGS layer 1 and layers 12 through 16 (23 to 27 in the new model) were not changed in the modified version of the model. Layers 2 through 16 in the modified model (USGS layers 2 through 7) have slight to drastic variations in cell thickness and/ or slope of the layer elevations. The slope of these upper layers matches the gradient of the base of the IVF (Figure 10). In this modified model, the slope of the layers 2 through 5 match the Modesto small IVF base and 6 through 16 match the slope of the Riverbank IVF base.

Adaptations to the vertical discretization and the slope of the USGS model for use in this study serve to improve the model's ability to simulate the influence of the IVF while preserving as much of the original model as possible. The finer vertical discretization in the modified model best preserves the IVF stratigraphic character and geometry in the model (See Appendix F). The initial coarser vertical discretization of the model would not allow for accurate representation of the IVF fining upward stratigraphy, which is an important geologic attribute to maintain because it is vital to assessing the influence of the IVFs on groundwater flow. Additionally, because the layers that contain the IVF have the same gradient as the IVF in this model version, the Kh data imported from the IVF code preserves the continuous nature of the IVF.

Layer Property Flow (LPF) versus Block Centered Flow (BCF)

Another difference between the model generated for this study and the USGS model of the Modesto area is the flow process package used. The model generated for this study uses "Layer Property Flow" package (LPF). The LPF simplifies parameter input because it utilizes the cell elevations, as specified in the discretization file, to calculate cell thickness and ultimately the flow through each cell. The Block Centered Flow package (BCF) does not use the cell elevation values to calculate the cell thickness and flow through each cell.

For example, the LPF package only requires model inputs of hydraulic conductivity for each cell and will use cell top and bottom elevations to calculate thickness and then transmissivity values for confined model layers prior to running the model. Using the BCF package, cell thickness are not be calculated prior to the model run; therefore, model inputs for use with the BCF package require the thickness component already be incorporated in parameter values. In practice, this means that the BCF requires a combination of hydraulic conductivities and transmissivities be assigned to the model cells. While both methods of flow calculation offer comparable results, the LPF allows more flexibility for adaptations to the model discretization and parameters (such as changing confined/ unconfined layers and vertical conductivities).

Another example of the benefits of using the LPF in this case is illustrated in the use of an anisotropy factor instead of a leakance value. The leakance term is required as an input in the BCF package, and is the product of vertical hydraulic conductivity and the thickness of the cell. In the LPF, an anisotropy factor (Kh/Kv) is used instead of leakance and does not include the cell thickness, which means that these values can remain the same, despite any subsequent changes in cell thickness. For the modified model, Kh/Kv was calculated using a FORTRAN code (See Appendix H).

Addition of GHB Conditions along the Upper Reaches of the River

The northern, southern, and western general head boundary cells in the modified model are the same as those in the USGS. However, the specified flux cells that represent the Stanislaus, Tuolumne, and Merced Rivers in layer 1 of the USGS model were changed to GHB cells in the modified model (Figure 8). Despite the USGS justification that the rivers are disconnected from the aquifer in the area, the lack of a boundary in this portion of the model causes unrealistic volumes of water to collect within the river valleys. Water filled the valley up to 10 meters above the valley base. Addition of the GHB conditions in the river valley was implemented to rectify this problem. Head elevations at these new GHB cells were assigned based on the ground surface elevation, using National Geographic TOPO! California.

To preserve the condition that the rivers are disconnected from the aquifer in the eastern portion of the model even with the addition of the GHB cells, flow between the river and the aquifer was reduced by assigning lower conductance values to the new GHB cells. The lower conductances were calculated with the same equation as the original river cells (explained above), but the vertical-K river multiplier (vkrivmult) of 10 was not included. Additionally, the uppermost reaches of the river near the reservoir were assigned even lower cell conductance values to reflect the lower conductivities of the more consolidated geologic deposits in that area. These cells were also calculated without the vertical K river multiplier and then divided by 2 as well. Reducing the conductance still allows unrealistic volumes of water to fill the river valley, 5 to 8 meters (16 to 26 ft) at most; the river still maintains losing and gaining reaches, which is the most parsimonious condition that could be achieved for the model in this study.

Removal of GHB Cells from the Northeastern Portion of the Model

Along the northeastern-most edge of the USGS model, GHB cells are dry down to an elevation of 10 to 17 meters (33 to 56 feet). While a solution can still be calculated despite the presence of dry boundary cells, it is not practical to set a boundary condition artificially high and allow the cell to dry. To avoid the drying of the peripheral GHB cells, GHB conditions were removed from layer 1 through layer 4 (Figure 8). The exact cells where the GHB condition was removed include:

- **Layer 1: I** 1; **J** 76 to 153
- **Layer 2: I** 1; **J** 81 to 153
- **Layer 3: I** 1; **J** 96 to 153
- **Layer 4: I** 1; **J** 111 to 153

Alteration of Vertical Head Gradient in GHB

General head boundaries in the modified model were also assigned around the perimeter of the model to represent the vertical gradient in the area that is caused by deep production wells. The head and conductance values required as input for the GHBs were calculated in a manner similar to the method used for the USGS model. The vertical head gradient applied to the GHB cells, however, was calculated using slightly different methods. This modified approach produced a comparable vertical gradient.

Similar to the USGS vertical head gradient, downward flow was produced by reducing the set head elevations in layer 1 by a gradient of 0.05 meters per meter of depth (thickness) for layers 2 through layer 17 (the Corcoran Clay). Initial set head values for layer 1 GHB were determined from gage data and the area topography (S. Phillips, pers. comm., 8/1/05). One variation between the USGS GHB gradient and mine is that layer 18 heads were set equal to the heads in layer 17. This was changed to prevent an unrealistic (at this model scale) head change between the low conductivity Corcoran Clay (layer 17) and the layer below it (18). The upward flow gradient was applied to the head assigned to layers 19 through 27. To generate upward flow in these layers, the gradient of 0.05 meters of head per meter of depth (thickness) multiplied by the depth of the cell center from was added to the head values from layer 18. In a manner similar to the USGS approach, this increasing head value was constrained with the condition that the calculated head value could not exceed the assigned head value in layer 1. If this condition occurred, the calculated head value for that layer would be ignored and the cell would be assigned the layer 1 head value instead.

Conductance calculations were made with the same methods used in the USGS model. Variations in the actual conductance values between the USGS model and the model used in this study are a result of thinner layers in areas with finer discretization or the presence of the IVF that intersects the western-most boundary.

Reduced Vertical Conductance of the Reservoirs

Another method used to reduce the volume of water that collects within the river valleys in the model, the vertical conductivities of the reservoir bed sediments were lowered in the reservoir package. Manual trials of various vertical conductivities were used to constrain the value that not only best matched the USGS estimate of the volume of inflow from the reservoirs, but also reduced the volume of water within the river valleys. The values of 0.003 (for the Wood and Modesto Reservoirs) and 0.006 m/day (for Turlock Lake) assigned to the reservoir bed sediments in the original USGS model were divided by 1.2. The resulting vertical conductances used in the adapted model are 0.0025 (for the Wood and Modesto Reservoirs) and 0.005 m/day (for Turlock Lake).

Flow Model Simulations, Particle Tracking, Solute Transport Simulation

Six steady-state flow models were run in MODFLOW 2000 for this study. They include the USGS model, the modified model without the IVFs, and a model for each of the four geologic realizations. Comparison of the head solutions, particle pathways, and transport simulations for each of these realizations gives insight into the influence the addition the IVFs have on the groundwater flow in the Modesto area.

RESULTS AND DISCUSSION

Results of the flow model simulations for this study first examine the impact that changes made to the original USGS model have in the flow solution by comparing the USGS model and the modified model without the IVFs. Once the impact of changes made to the original model is evaluated, the influence of the IVFs will be assessed with particle tracking and solute transport simulations. Although models and results were generated for each geologic realization, model results are similar for the four different IVF realizations; therefore we illustrate the influence of IVF deposits using results from the RB/ST/ML, and briefly describe variability between IVF realizations at the end of this section. The RB/ST/ML realization was chosen to illustrate the influence of the IVF, because it incorporates the influence of three potential locations of the IVFs and most clearly shows the degree of influence of the IVFs may have on the groundwater flow.

Groundwater Modeling – Comparison of models without the IVF deposits

Changes made to the USGS model (altered slope of the uppermost layers in the model, increased vertical discretization, use of the Layer Property Flow (LPF) package, addition of GHB conditions along the upper reaches of the river, removal of GHB cells from the northeastern portion of the model, and slight alteration of the vertical head gradient calculation in the GHB) appear to have little impact on the model solution.

Both models show the general trend of groundwater flow is to the west-southwest with the highest hydraulic head elevations in the east (Figure 11A and B). For the modified model without the IVF, the head solution has slightly lower heads in the reservoir area, and the head gradient appears slightly more gradual in the central portion of the model near the Tuolumne River. The large depression in the water table in the southeast corner is observed in both models. This depression is caused by a heavy dependency on local groundwater and limited recharge through application of non-local irrigation water in this area (a significant source of recharge in other areas of the model) (Burow *et al.*, 2004; S. Phillips pers. comm., 11/9/05).

Though the USGS and the modified flow model solutions are similar, some minor variation in the flow statistics was observed. The volumetric budgets are comparable with a total volume in and out of the USGS model at approximately 5.40 million meters^3 (190.7 million feet^3) and the modified model at 5.42 million meters^3 (191.4 million feet^3). The discrepancy between the inflow and outflow of the model is smaller in the modified model relative to the USGS model, but both discrepancy values are less than a tenth of a percent (<<0.01%) of the total budget. The USGS model has a difference of 14 m^3 (494 ft^3) while the modified model has a difference of 0.34 m^3 (12 ft^3).

More specific comparison shows the USGS model has a maximum head value of 70.9 meters (232.6 feet) at the Modesto Reservoir and a minimum of -2.4 meters (-7.9 feet). The modified model has a slightly lower maximum and a similar minimum head value: a maximum of 60.2 meters (197.5 feet) at the Modesto Reservoir and a minimum of -2.2 meters (-7.2 feet). The maximum head values have a 15% difference and the minimum values ~8.9%. The mean simulated head in the USGS model is slightly lower at 19.7 meters (64.6 feet) relative to the modified model's mean head of 21.5 meters (70.5 feet) (Table 2).

Although the volumetric budget and regional flow appear similar, local variation between the two models does exist. The addition of the GHB to the upper reaches of the Tuolumne River in the modified model did not eliminate flooding within the river valley. In the USGS model, because the river was not denoted as a boundary, less water accumulated within the channel specifically in the uppermost (eastern) reaches. Along the entire length of the river valley, however, comparable flooding is observed within both models. While the Tuolumne River is thought to be losing water to groundwater in the upper reaches, as are the Stanislaus and Merced Rivers, (based on water-level contour maps developed by the CA Dept. of Water Resources, S. Phillips, pers. Comm., 11/1/05), model results indicate that the Tuolumne River may have both gaining and losing reaches (see Advective Pathline Analysis section below). However, further refinement of our groundwater model may also be necessary in order to more accurately capture the surface water – groundwater interaction. Aside from the changes within the river, the results from both of these models indicate that the changes made to the modified model without the IVFs did not impact the overall flow model significantly as the flow budgets only varied by 0.4% and the regional head solution is approximately the same.

Influence of the IVF Deposits on Groundwater Model Results

The results from the Modesto area model that includes the wedge-shaped, coarse-grained IVFs indicate that the IVFs have a hydrogeologic significance and are capable of acting like a regional "pipeline" for groundwater flow and contaminant transport in the area. The influence of the IVF on the groundwater flow is illustrated by comparing the modified model without the IVFs (i.e. the model without the IVFs) to the model with the IVFs (specifically, the RB/ST/ML model, which is representative of results seen in the other geologic scenarios) using three methods: (1) a calculation of the head difference between the model with and without the IVF, (2) advective pathline analysis, and (3) solute transport simulation.

Head Difference

The head difference between the model with and without the IVF highlights the influence the IVF may have on the regional head distribution. The head difference was obtained by subtracting the head solution of the model with the IVFs from the head solution of the model without the IVFs (Figure 12), and allows us to visualize the extent as well as the magnitude of the influence of the IVF. It also highlights the nature of the head difference: positive or negative.

As expected, the magnitude of the head difference decreases with distance from the IVF and is illustrated in figure 12. The areas significantly influenced by the presence of the IVFs, a head difference > 10 cm, are adjacent to the IVFs. In areas farther away from the IVFs, the head difference, and therefore the influence of the IVFs on the head elevation, decreases.

The location of positive and negative head difference values also provides significant insight into the influence of the IVFs. Areas with a positive head difference mark locations where the model without the IVF has higher head elevations than the model with the IVFs. A negative head difference indicates areas where the model without the IVFs has lower head elevations than the model with the IVFs.

In the eastern portion of the model domain, the head difference is positive. Farther west, from the location where the RB and ST IVFs (Tuolumne River and Stanislaus River Riverbank Formation IVFs) intersect to the western extent of the model, the head difference is negative. Positive head differences in the eastern portion of the model are high, approximately 1 to 4 meters, where the RB and ST IVFs are located (Figure 12). The head difference is positive all along the eastern portion of the model, but the magnitude of the head difference decreases radially with distance from the IVFs.

In the western portion of the model domain, negative head differences radiate out from the intersection of the RB and ST IVFs. The most negative head differences (approximately -2 meters) are located in the area where the IVFs intersect (Figure 12).

Farther west, the influence of the IVF remains, but the extent and magnitude of the negative head difference surrounding the RB IVF decreases.

This pattern of head differences, positive in the east transitioning to negative toward the west along the IVF, indicate that the RB and ST IVFs create areas of convergent and divergent flow. Thus, at the head of the valley, hydraulic head elevations are lower (where head difference is positive) due to the addition of the thick, coarse-grained IVFs that allow a significant amount of flow through the area. Farther down the IVFs to the west, head elevations are higher (where head difference is negative) than were observed in the model without the IVF, indicating flow is being diverted from the IVFs. In the steady-state conditions specified in this model, water flows into the IVFs at the head, but once the maximum volume of water capable of flowing through the IVF fills the valley, the water "backs-up" within this coarse "pipeline", and raises the hydraulic heads in the western portion of the model. This in turn causes flow that is initially following the IVF to divert into the contiguous aquifer sediments.

The convergent and divergent flow regions can be inferred to represent an equilibrium plane. The transition from convergent to divergent flow along this plane shows the location in the IVF where the hydraulic conductance has reached a balance with the volume of water that can pass through. Above this point, the hydraulic conductance of the IVFs is sufficiently high to allow the volume of water entering the IVFs to pass through. Below the transition point, the hydraulic conductance of the IVFs is not large enough to allow the entire volume of water entering the IVF to pass through and the water "backs-up" and is pushed out of the IVF deposits into the surrounding aquifer sediments.

One limitation on testing the influence of the IVFs on groundwater flow in the model is the presence of artificially generated coarse areas in the USGS grain size to K model, which are a result of the implicit inclusion of the IVFs. The impact of the shallower Modesto Formation IVF (ML), in particular, on groundwater flow is dampened by surrounding coarse grained regions across the area south of the Tuolumne River. Here, the Kh of the gravels in the IVF are almost an order of magnitude greater than the surrounding deposits, while the sand is approximately the same Kh as the deposits around it. The result of this is a more localized impact on the hydraulic heads. Head elevations do not show a distinct area dividing convergent and divergent flow along the valley as can be seen with both of the Riverbank Formation IVFs (RB and ST). Instead, this valley appears to highlight local areas where the connectivity of coarse sediments is improved (Figure 12).

In some areas along the ML IVF, there is only a small positive head difference. These areas highlight where there was little improvement in the connectivity of the aquifer with the addition of the IVF and head difference varies only slightly. Areas that show little improvement in aquifer connectivity were already well connected due to the presence of coarse sediments prior to the addition of the IVF.

In other areas along the ML IVF, the head difference is negative. These areas highlight where the connectivity of the aquifer is improved locally by the addition of the IVF. Replacement of relatively finer sediments with the addition of the coarser ML IVF creates a local area of preferential flow, which displays the "back-up" of water.

The presence of the IVF within both relatively coarser and finer sediments is contrary to our conceptual model, where the IVF is thought to be relatively coarse compared to the surrounding sediments. The USGS grain size-to-K model data indirectly preserve the coarse grained nature of the IVF. Because this data set is kriged across the model, the coarse grained nature of the IVF was probably interpolated across a large area, artificially increasing K values. Thus, the USGS method of generating K values from grain size does not exclude the IVFs and may not provide the best representation of the deposits around the IVFs to illustrate the influence of IVFs on groundwater flow.

Along the deeper Riverbank Formation IVFs to the north of the Tuolumne River (the RB and ST IVFs), the IVF is surrounded by significantly finer sediments (low K values) relative to the coarse grained sediments of the IVF (high K values). This allows for a more regional increase in aquifer connectivity with emplacement of an IVF and shows a single point of transition from convergent flow into the IVF to divergent flow out of the IVF. Implications of the varying influence on groundwater flow are described below with the results of advective pathline analysis in the model.

Advective Pathline Analysis

Simple pathline tracking in the flow models with and without the IVFs were used to show the impact the IVFs have on the groundwater flow in the Tuolumne River area. Pathline tracking allows an analysis of the advective flow pathways within the groundwater model.

Using MODPATH within GMS 5.1, 1000 particles were assigned and released from the same 4 cells in layer 1 of each model (the model without the IVF and the model with the IVF) (Figures 13, 14, 15). The 4 cells were chosen because they are located in each of the IVFs: 1 cell in the RB, 1 cell in the ST, and 2 cells in the ML (proximal and distal). The particles were tracked in both models to their ultimate fate within the steady state flow conditions.

In the model without the IVF, pathlines from particles released in the central and southern portion of the model tend to be located in the upper unconfined portions of the aquifer, while other pathlines from particles released farther north, follow the vertical gradient and trend down into the confined portions of the aquifer (Figures 13A, 14A, and 15A). The addition of the IVF shows that pathlines extend farther westward into the basin as well as deeper into the aquifer (Figures 13B, 14B, and 15B). As illustrated by the pathlines that follow the IVF trend, the IVF provides a conduit for water to flow through. The addition of the IVF also allows pathlines to spread into aquifer sediments that they previously would not reach. The vertical flow gradient from heavy pumping in the area contributes to the spread of pathlines, or water, throughout the area.

The implications of changes in head gradients through the addition of the IVF are discernible from the results of the pathline analysis. The addition of the IVF sufficiently changes the head gradients to generate areas of convergent and divergent flow. This flow pattern redirects pathlines or groundwater flow into the IVF and then diverts flow out of the IVF, thus causing the pathlines (or groundwater) to spread into contiguous aquifer sediments.

Advective pathline analysis was also used to illustrate the impact of the IVF on recharge to the aquifer from the rivers. Figures 16A and B shows a map view of pathlines from particles released within the general head boundary cells that delineate the Tuolumne River. Losing and gaining reaches of the stream can be identified by the trends of the pathlines. The Tuolumne River shows intermittent losing and gaining reaches along the stream in this model. A cross-section through the area (Figure 17A and B) shows pathlines from the losing part of the stream, at the head of the stream in the model with and without the IVF. In the model with the IVFs, the pathlines illustrate the flow into the IVF and westward (Figure 16 and 17B). In the model without the IVFs, the pathlines have very little lateral movement and extend downward into the aquifer with the vertical gradient (Figure 16 and 17A). Particle pathlines released from along the losing portion of the stream near the Modesto area, in the model with the IVFs, show flow into the IVF and under the city (Figure 17B). Pathlines in the same area in the model without the IVF show some lateral movement beneath the city, but not to the extent shown in the model with the IVFs (Figure 17A). Comparison of pathlines in the models with and without the IVFs illustrates that the presence of the IVF near the river allows the IVF to gain recharge from the river. This is important, especially at the head of the valley where artificial recharge to the aquifer could provide a water supply for wells pumping in the Modesto area.

Solute Transport Simulation

Transport simulations were conducted using MT3DMS to run a potential transport scenario in the modified model without the IVFs and the model with the IVFs. A constant concentration of 100 mg/L of an unspecified conservative solute was released from the same location in layer 1 in simulations for both of the models (Figure18A and B). Data requirements for the transport simulation include groundwater flow solution from the MODFLOW simulation, longitudinal dispersivity (α_L), ratio of transverse to longitudinal dispersivity, ratio of vertical to longitudinal dispersivity, effective molecular diffusion (D^*), and effective porosity. The longitudinal dispersivity was assigned a value of 1 meter, which is based on work by Gelhar *et al.* (1992) who indicate that 1 meter is a reasonable value for a 400 meter cell size. The ratios of transverse and vertical diffusivity to longitudinal were both set equal to 1. Effective molecular diffusion was assigned a value of 5.9616 x 10^{-5} m^2 /day (Weissmann *et al.*, 2002a). The effective porosity assigned to these transport simulations was 33% (0.33). This porosity was chosen because it provides a good average estimate for the porosity in the unconsolidated fluvial fan sediments (Weissmann *et al.*, 2002a, c). To maintain simplicity, the consolidated deeper, confined aquifer cells were assigned the same porosity. Transport simulations were run in the model with the IVF and without the IVF for 100 years.

The variation in plume morphology in these transport simulations clearly depicts the influence the IVF can have on solute transport. The model without the IVF shows a more uniform plume front that spreads laterally and vertically over a smaller area, while the model with the IVF, displays preferential lateral and vertical movement through the IVF. An interesting observation in Figure 18A is the southern most plume front shows some preferential spreading in the coarse grained areas south of the Tuolumne River. This is the area that likely has artificially high conductivity values due to the implicit inclusion of the IVF in the USGS grain size-to-K model.

Because of the vertical gradient, both models show a significant amount of vertical movement of the plume. However, in the model with the IVF, a distinct elongate lobe of the plume develops in the location of the IVF which spreads areas of the plume farther westward than they do in the model without the IVF (Figure 18B). The results show the contaminant plume front follows the IVF and moves farther to the west in the model with the IVF.

This relatively rapid plume movement within the IVF indicates that the IVF will have a large role in water quality and remediation schemes. The presence of these valleys will significantly increase contaminant residence times, which could drastically affect efforts to develop effective remediation schemes in the area. These results also indicate the aquifer is more susceptible to widespread contamination due to the presence of the IVFs. These results are similar to those observed by Weissmann *et al.* (2004) on the Kings River.

Comparison among Geologic Realizations

Head differences among the IVF realizations show that that addition of IVFs in different spatial locations can alter the head solution. Table 3 shows that while the overall statistics of the head solution appear similar, very different local head variations are apparent when the difference between heads solutions is calculated.

Comparing head differences of the various geologic scenario head solutions allows for analysis of the impact each additional IVF has on the groundwater flow. The resulting head difference plots show the same pattern observed by adding the IVFs to the model without the IVF: lower hydraulic heads at the head of the fan and higher heads where the flow has "backed-up" in the IVF. The location of the positive and negative head differences varies depending on the IVF location. The addition of the ST valley reduces the head elevations more over a larger area in the eastern portion of the model than in models without the ST IVF. Figure 19A and B show a smaller positive head difference in the northeastern portion of the model without the ST valley. The addition of the MS valley instead of the ML valley results in a similar pattern of patchy areas of positive and negative head differences highlighting where the IVF lowers or raises the local head elevation instead of continuous regions of convergent and divergent flow along the IVF (Figure 19A and B).

While the results are similar for each of the IVF scenarios, the various locations of the IVF do highlight the potential for drastic local variation in groundwater flow. The location of the IVF will have implications for how the IVF can best be utilized for artificial recharge (i.e. where to drill wells to obtain the maximum groundwater production rates). The areas of the aquifer most susceptible to rapid and widespread contaminant transport through the IVF will be controlled by its location. As an essential component of the groundwater system, the exact location of the IVF should be integrated into remediation schemes.

CONCLUSION

From this investigation into the influence of the IVF, we can make several conclusions about this work, including the methods used to delineate the IVF and the impact the addition of the IVF has on the groundwater flow in the Modesto area.

Our results indicate that the IVF has a significant influence on the ground water flow in the Modesto area. We found that the IVF significantly influences regional hydrogeology by:

- acting as a regional "pipeline" of coarse sediment for groundwater flow,
- providing a preferential pathway that has the potential to provide artificial recharge to the Modesto area as well as create a conduit for contaminants to follow,

- increasing the dispersion of particle pathlines into the aquifer sediments surrounding the IVF, and
- enabling solute plumes to move farther distances more rapidly through the IVF making the aquifer susceptible to widespread contamination.

These results are consistent with those observed by Weissmann et al. (2004). They found that the IVF geometry allows it to significantly impact the ground water flow and solute transport due to the continuous and relatively thick basal cobble unit. The continuous, course-grained nature of the valley fill creates a highly conductive conduit for groundwater flow, cutting across any laterally bounding confining units.

The four geologic scenarios developed in our study from the drillers' well logs allowed the influence of the IVF to be assessed along with the impact of uncertainty in geologic model. Comparisons among these four scenarios give insight to the impact of incorrectly developing a conceptual model and substantiate the need to better constrain the location of these IVFs.

Future Recommendations

While these models provide a good preliminary understanding of the influence of the IVF, they should be used as a basis for further investigation into the area stratigraphy and hydrologic regime. The geologic model could use some improvement by (1) using more reliable methods for identifying the location of the IVF (2) obtaining core through several locations of the IVF to better understand IVF lithologic character, (3) collecting additional continuous core in the open fan deposit areas, and (4) more studies of the Tuolumne River's flow differential down-stream during stable flow conditions.

Further investigation into the location of the IVF should be conducted. Although the driller's logs were successfully applied, this method of locating and defining the IVFs could be significantly improved. Although multiple potential IVFs within the same stratigraphic range (i.e. two potential Modesto Formation IVFs) were identified, it is unlikely that they both exist. While driller's well logs provide a good approximate location of the IVF, to more effectively model the IVF, more reliable geophysical data should be acquired. Seismic data across the area will help better constrain the location and geometry of these features, providing more dependable estimates of the width, depth, and length of the IVF.

In this study, no core was collected within the IVF. This made modeling of the lithologic character more challenging. The character of the proximal and distal portions of the IVF need to be investigated as these are the principle areas of recharge and discharge for groundwater and will impact the location of the divergent flow from the valley. Investigation into the toe of the fan may provide insight into the influence of local base level (sea level) and the basin width on the preservation (or lack of) of the distal fan deposits. Currently, the IVF code does not account for the fact that gravels are not likely present in the distal portion of the model. With further constraints on the distal character in the IVF, this portion of the model could be improved. Additional studies near the apex of the fan will provide further insight into the geometry of the stacked IVF deposits believed to exist. This may have a significant influence on the ability to artificially recharge the aquifer.

Additional continuous core data across the fan will also help to better capture the aquifer heterogeneity outside of the IVF. One significant improvement in this area would be to add the sequence bounding paleosols. While this model does not include the paleosols, they may have an impact on the regional or local groundwater flow, acting as no or low flow barriers which could potentially increase the influence of the IVF and their ability to influence the aquifer connectivity (Weissmann *et al.,* 2004).

Studies to better constrain the differential flow during stable flow conditions along the Tuolumne River will give insight into the true potential for artificial recharge into the aquifer through the IVF. Detailed characterization of reaches along the Tuolumne River where recharge occurs is needed in order to understand the nature of groundwater-surface water interaction and conductance between the river and groundwater system. While our model highlights flow from the river as a potential pathway for recharge to access the IVF, further studies would be needed to confirm this potential.

The groundwater and contaminant transport models produced enhance understanding of the groundwater flow and the potential for contaminant movement through the Modesto area. The models also provide a preliminary understanding of the potential influence these incised-valley fills may have on artificial recharge in the incised-valley fill.

Tables

Table 1: Summary of the geologic scenarios developed from the locations of thick gravels in the drillers' well logs delineating potential IVF locations. These scenarios will be incorporated into multiple, steady-state, saturated groundwater flow models.

IVF Age		**Riverbank Incised-Valley Fill (IVF)**	
		*Tuolumne River (**RB**) and Stanislaus River (**ST**)*	*Tuolumne River (**RB**)*
Modesto Incised-Valley Fill (IVF)	*Large IVF (**ML**)*	RB/ST/ML	RB/ML
	*Small IVF (**MS**)*	RB/ST/MS	RB/MS

Table 2: Summary of the hydraulic head maximum, minimum and mean elevations for the USGS model and the modified model without the IVF. Percent differences between the USGS model and the adapted model and between the adapted model and the model with IVFs are also included.

Head Elevation Statistics

Hydraulic Head Elevations	**USGS**	**No IVF**	**% difference from USGS**	**IVF (RB/ST/ML)**	**% difference from the model without the IVF**
Minimum Value (m)	-2.37	-2.08	12.2	-2.06	1.0
Maximum Value (m)	70.94	60.37	14.9	60.06	0.5
Mean Value (m)	19.68	22.15	12.6	22.03	0.5

Table 3: Summary of the hydraulic head maximum, minimum and mean elevations for the four geologic scenario models. Percent differences between the USGS model and the adapted model and between the adapted model and the model with IVFs are also included.

Hydraulic Head Elevations	**RB/ ML**	**RB/ MS**	**RB/ST/ ML**	**RB/ST/ MS**	***Average IVF Scenarios***	**Modified Model without the IVF**	**% difference from Modified Model without the IVF**
Minimum Value (m)	-2.07	-2.07	-2.06	-2.07	-2.07	-2.08	0.60
Maximum Value (m)	60.10	60.12	60.06	60.07	60.09	60.37	0.47
Mean Value (m)	22.07	22.07	22.03	22.03	22.05	22.15	0.60

Figures

Figure 1: Generalized stratigraphy of the Great Valley of California, with the white and black dashed boxes showing the approximate study area of the Tuolumne River area near Modesto, California in the Eastern San Joaquin Valley. The geologic map, based on soil surveys, shows the fluvial fan deposits in the eastern portion of the San Joaquin Valley (adapted from Weissmann *et al.,* 2006). Thick, slightly westward dipping fluvial fan deposits along the Tuolumne River decrease in age to the west, toward the San Joaquin Basin center. Uplift and erosion have exposed older fan units in the eastern portion of the basin. This study focuses on the Turlock Lake, Riverbank, and the Modesto deposits. Geologic map shown in color.

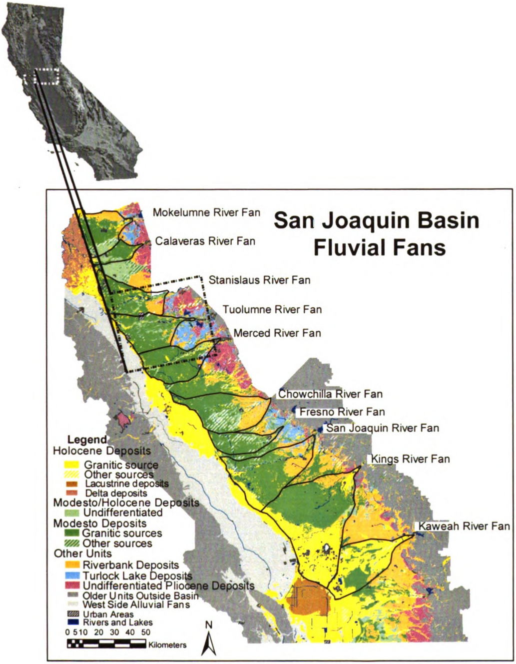

Figure 2: Schematic profile of the Tuolumne River fan stratigraphy showing the westward stepping, thin, stacked, fluvial fan units (Weissmann *et al.* 2006).

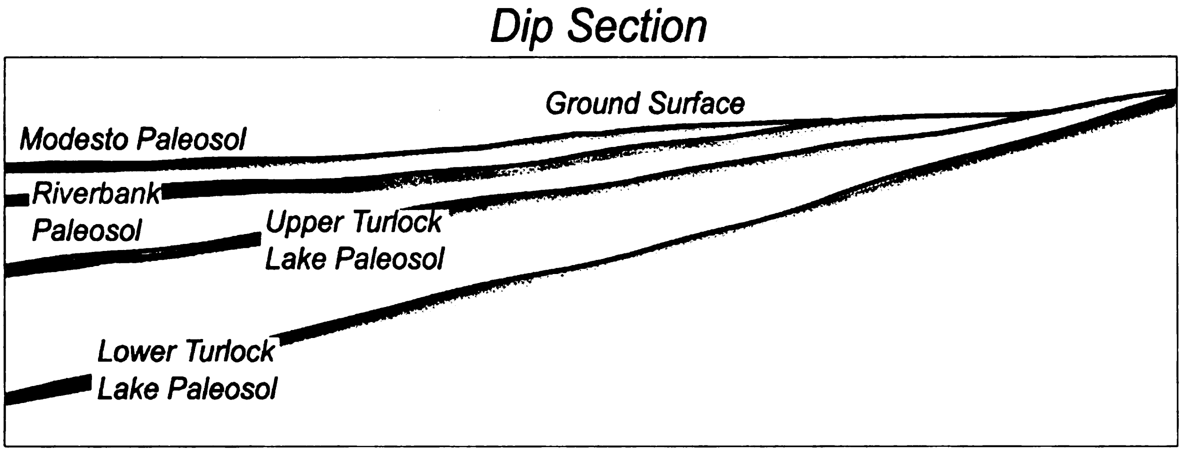

Figure 3: The Tuolumne River area near Modesto, California in the Eastern San Joaquin Valley. The black solid box denotes the entire study area. The dashed line outlines the area shown in Figure 13.

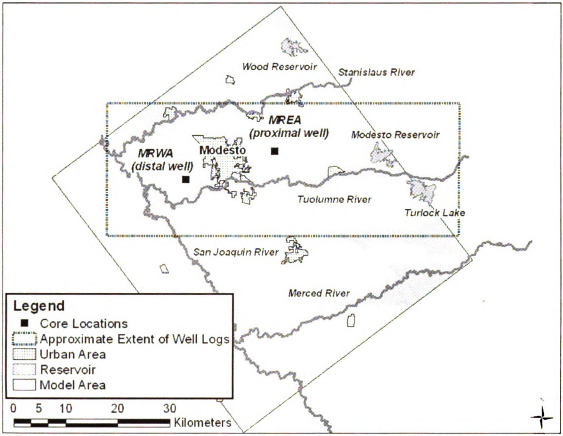

Figure 4: Each cyclic Quaternary deposit contains a relatively coarse-grained IVF nestled within finer open fan deposits of silt, clay and some sand. The IVF has a thick gravel base that fines upward to sand then fines.

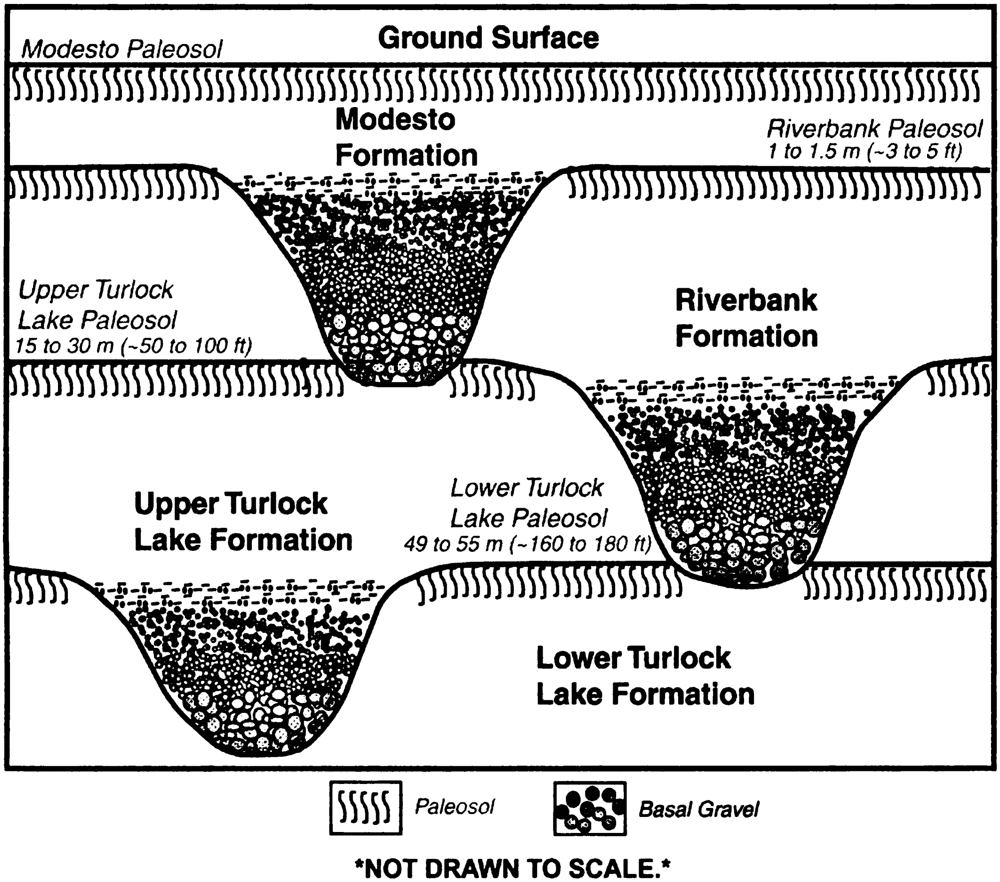

Figure 5: Conceptual model of the Riverbank IVF. The valley fill is 0.7 to 1.6 km wide and ranges from approximately 30 meters thick at the apex to 0.3 meters at the toe. It has a 5 to 9 m thick gravel base that fines down fan.

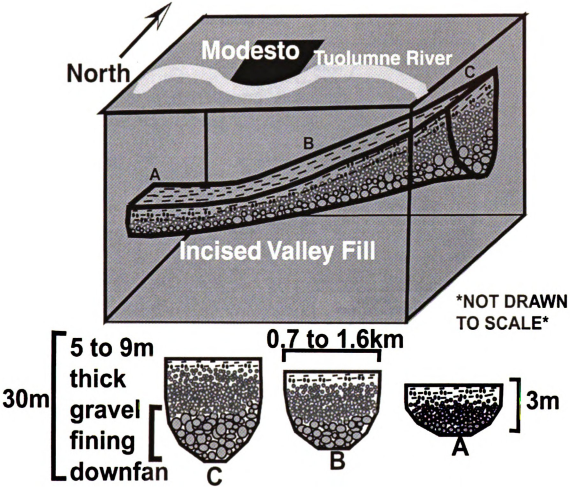

Figure 6: Wells assigned a rank of 1 and 2, plotted spatially, roughly show a few east-west elongate trends. The areas of particular interest are (1) the northwest trending line of wells that runs beneath Modesto, (2) the line of wells that trends along just north of the modern Tuolumne River, (3) a short string of wells that create a small loop to the south in the eastern portion of the river, and (4) the line of wells that begins on the southeastern part of the river and trends to the southwest.

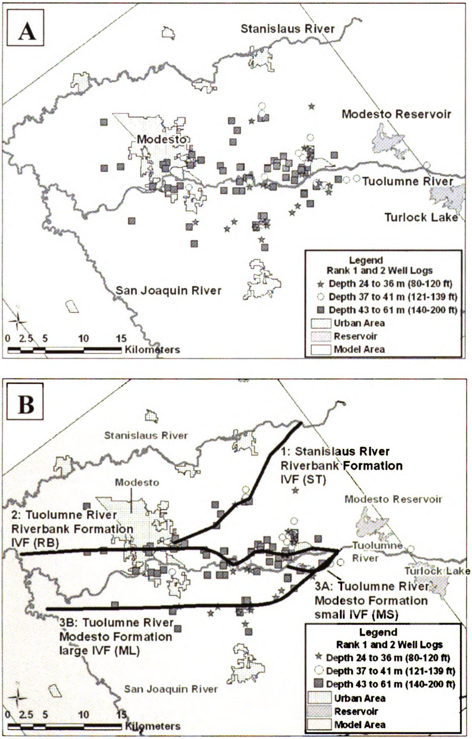

Figure 7: Aerial photograph showing the potential location of the Modesto small IVF loop (outlined by the light gray dashed line). The solid white line represents the current river valley.

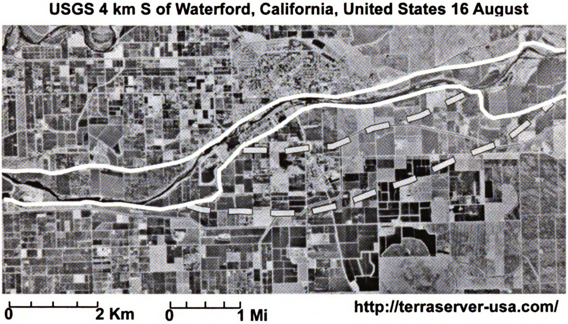

Figure 8: The specified flux cells that represent the Stanislaus, Tuolumne, and Merced Rivers in layer 1 of the USGS model were changed to GHB cells in the adapted model. The locations of the reservoirs are outlined with a thin black line. The GHB cells are represented by the dark gray dots around the perimeter of the model and over the locations of the rivers. The light gray squares represent wells.

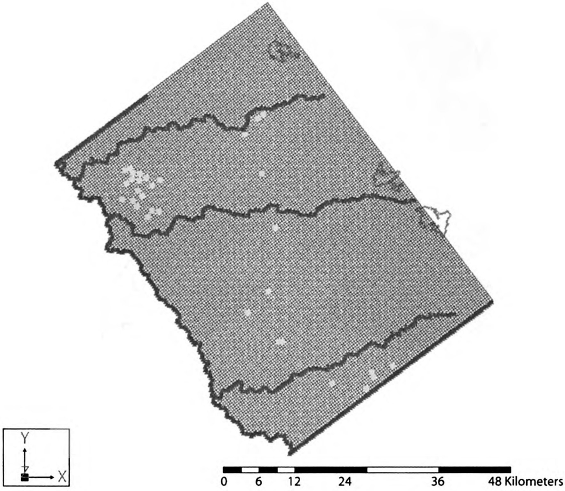

Figure 9: Four geologic scenarios were created to test the influence of the IVF: (from top left to bottom right) RB/ST/ML, RB/ML, RB/ST/MS, and RB/MS. Vertical exaggeration of 100.

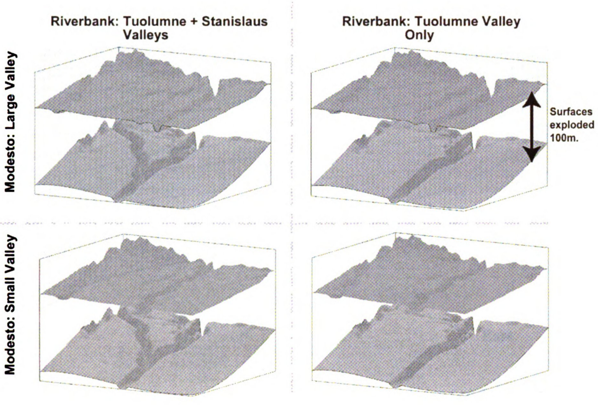

Figure 10: Row 60 (I60) in **A:** the USGS model and **B:** the newly discretized model. Vertical exaggeration is 50. Each cell is 400 meters wide.

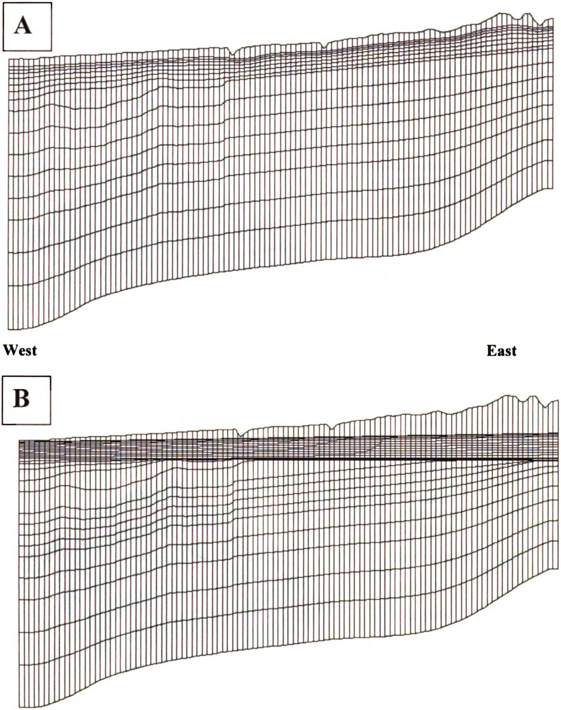

Figure 11: Comparison of (A) the USGS model and (B) the adapted model without the IVF MODFLOW hydraulic head solutions. **A:** USGS head solution. The regional groundwater flow is to the west-southwest. The large depression in the water table in the southeast corner of the model is due to a heavy dependency on local groundwater with little recharge from application of irrigation water. **B:** Adapted model without the IVF head solution. The general flow direction is the same. The heads in the area of the reservoir are slightly lower and the head gradient is slightly more gradual. The large depression in the southeast corner is maintained in this adapted model. (Elevations are in meters and the vertical exaggeration is 50). Shown in color.

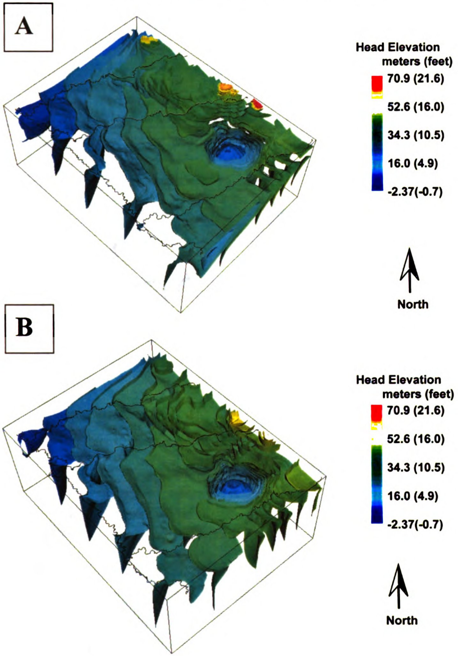

Figure 12: Head differences between the model without IVFs and the IVF model (RB/ST/ML). Positive residuals (yellow to red) indicate areas of the model where the head elevations are lower in the IVF model than in the model without the IVF. Negative residuals (green to blue) indicate areas were the head elevation is higher in the IVF model than in the model without the IVF. (Elevations are in meters and the vertical exaggeration is 50). **A:** 63 isosurfaces. **B:** 20 isosurfaces (rotated for improved view). Shown in color.

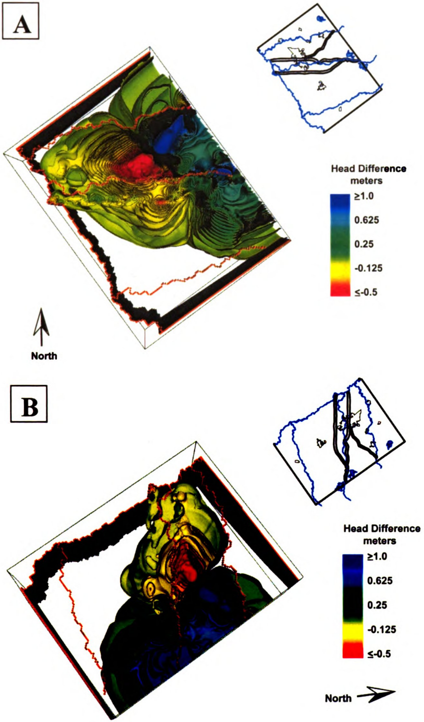

Figure 13: Pathline analysis was done using MODPATH. The light gray triangles indicate where the particle started and the black circles indicate where the particle ultimately ends up. **A:** Map view of the model without the IVF. Pathlines have the same trend along the hydraulic gradient across the model. **B:** Map view of the model with the IVF (RB/ST/ML). Pathline analysis in the model with the IVFs (RB/ST/ML) shows that pathlines extend farther to the west and spread laterally to the north and south.

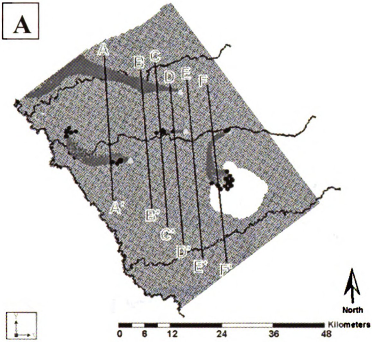

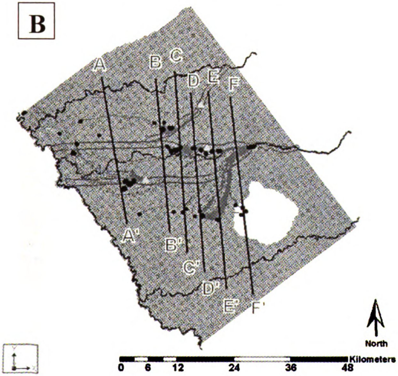

Figure 14: A cross-section of the particle pathlines displayed in the previous figure. The yellow triangles indicate where the particle path started and the black circles indicate where the particle pathline ultimately ends. Vertical exaggeration is 50. **A:** No IVF cross-section showing a view of the pathlines looking north. Particles released in the northern portion of the model have pathlines that trend downward near the bottom extent of the model. The other pathlines remain relatively shallow, but do move from the unconfined to the confined portion of the aquifer. **B:** IVF (RB/ST/ML) cross-section showing a view of the pathlines looking north. The pathlines from particles released in the north are redirected into the IVF and do not flow as deep into the aquifer as they do in the model without the IVF. The other particle pathlines also follow the path of the IVF then disperse into the aquifer. Shown in color.

WEST **EAST**

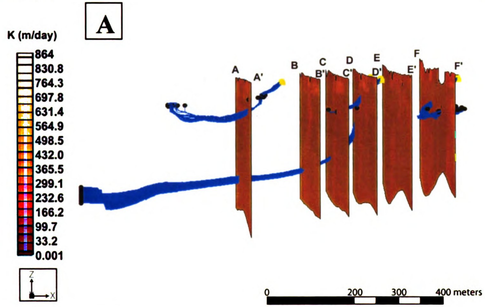

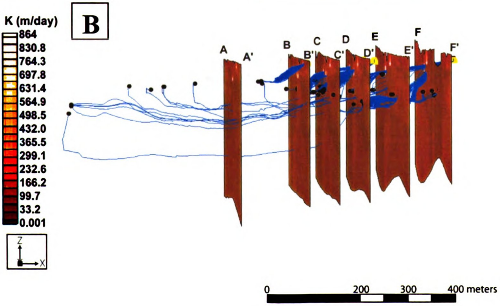

Figure 15: Cross-section of the particle pathlines shown in the previous two figures viewed obliquely from above the south edge. The yellow triangles indicate where the particle path started and the black circles indicate where the particle path ultimately ends. Vertical exaggeration is 50. **A:** In the model without the IVF, the particle pathlines follow a similar trend through the aquifer and move deep into the confined portion of the aquifer. .**B:** In the model with the IVF (RB/ST/ML) the particle pathlines follow the IVF then spread out displaying the various flow paths into the deeper portions of the aquifer. Shown in color.

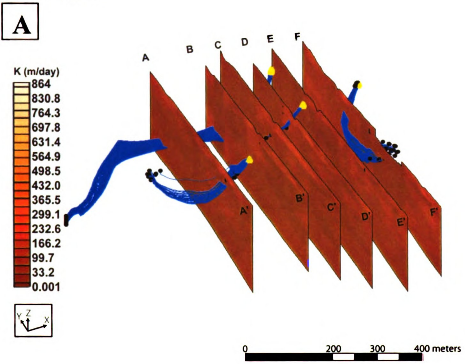

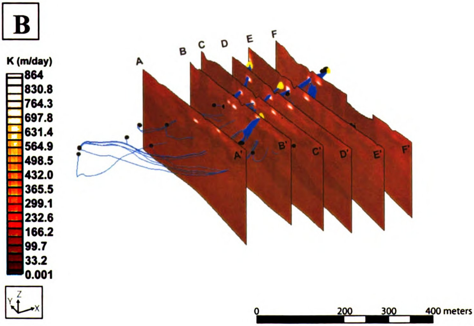

Figure 16: Map view of particles released within the general head boundary cells that delineate the Tuolumne River: **A:** In the model without the IVF the advective pathlines are short and follow the hydraulic gradient and **B:** In the model with the IVF, the advective pathlines are longer and follow the IVF. Vertical exaggeration is 50. Shown in color.

A

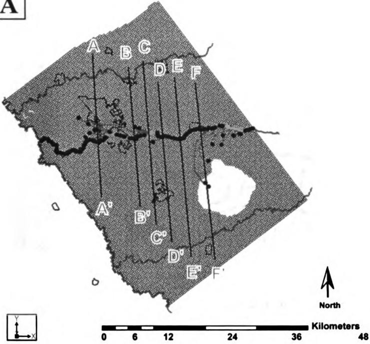

B

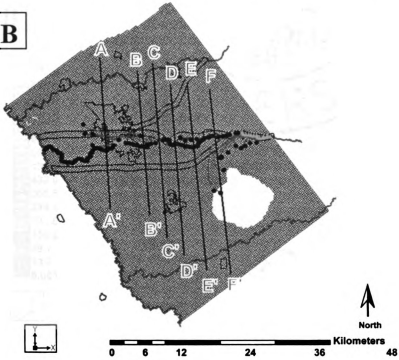

Figure 17: Cross-section of particles released within the general head boundary cells that delineate the Tuolumne Rivers. Vertical exaggeration is 50. **A:** In the model without the IVF the advective pathlines are short and follow the hydraulic gradient and **B:** The model with the IVF shows, in losing portions of the stream, the advective pathlines move from the river into the IVF. Advective pathlines from particles released within the river also migrate beneath the city of Modesto. Shown in color.

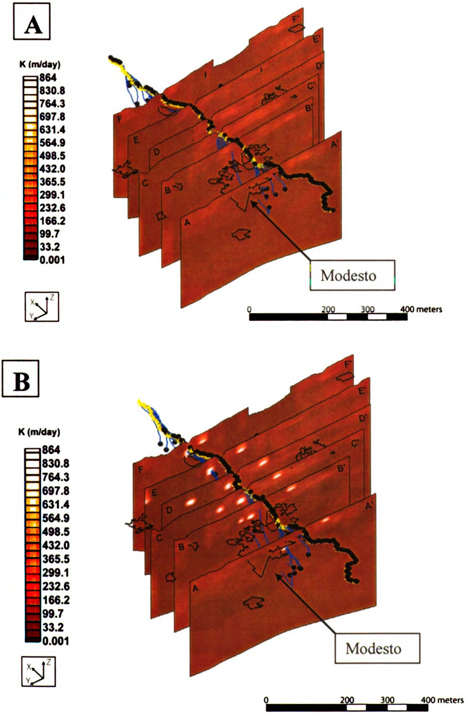

Figure 18A: Solute transport simulations were run for 150 years. **A:** Shows the uniform plume morphology in the modified model without the IVF. NOTE: The IVFs are NOT in this model. The IVF outline is shown only to facilitate reference between figures. **B:** Shows the plume morphology in the model with the IVFs. The plume preferentially follows the IVF and allows higher concentrations of the contaminant to move farther distances and more deeply into the aquifer in the same amount of time as the modified model without the IVFs. Shown in color.

A*

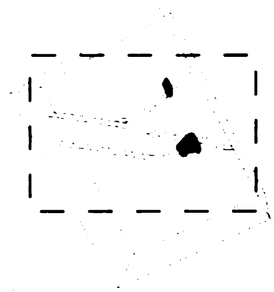

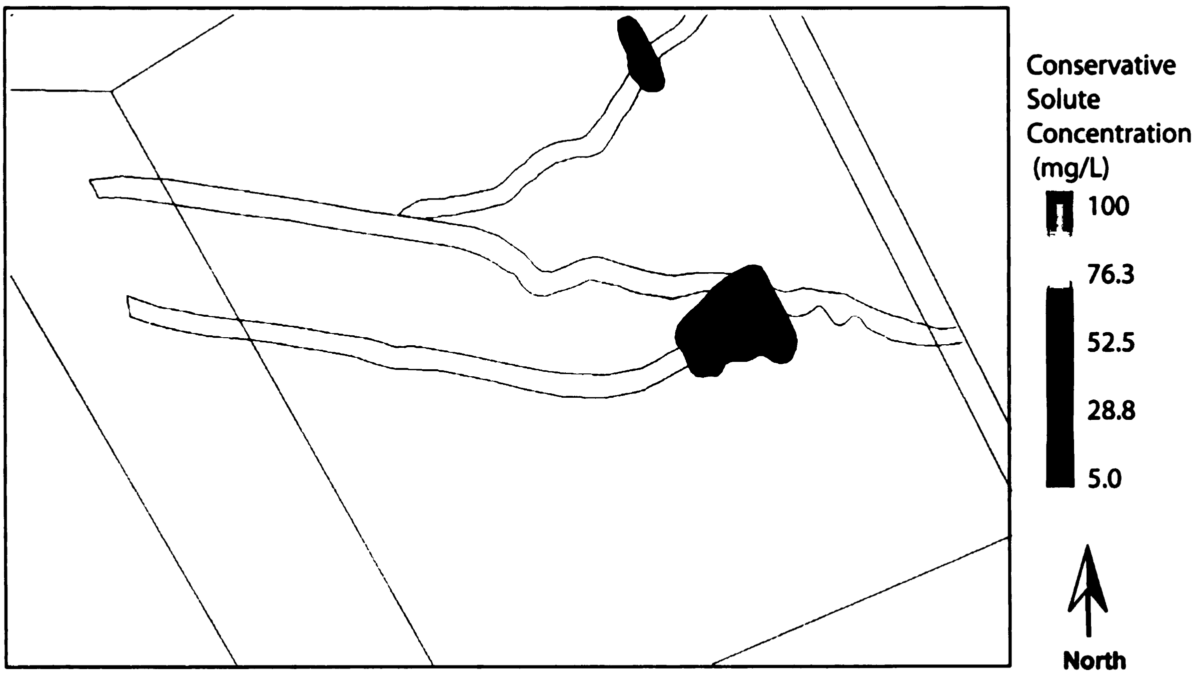

*NOTE: In figure A, the IVF outline is only shown for reference.

Figure 18B: Solute transport simulations were run for 150 years. **B:** Shows the plume morphology in the model with the IVFs. The plume preferentially follows the IVF and allows higher concentrations of the contaminant to move farther distances and more deeply into the aquifer in the same amount of time as the modified model without the IVFs. Shown in color.

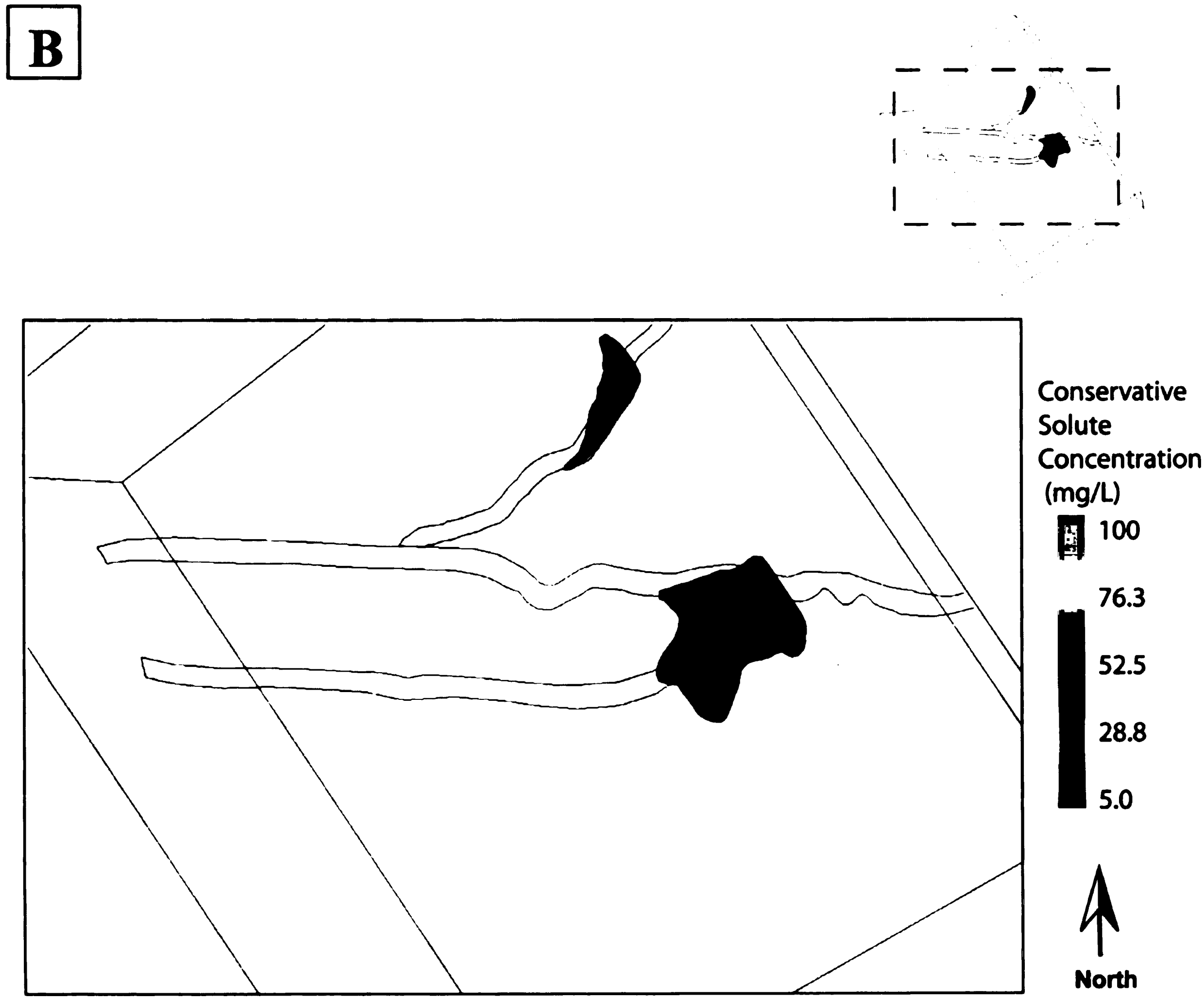

Figure 19: Head differences between the model without IVFs and the IVF model (RB/ MS). Positive residuals (yellow to red) indicate areas of the model where the head elevations are lower in the IVF model than in the model without the IVF. Negative residuals (green to blue) indicate areas were the head elevation is higher in the IVF model than in the model without the IVF. (Elevations are in meters and the vertical exaggeration is 50). **A:** 63 isosurfaces. **B:** 20 isosurfaces. Shown in color.

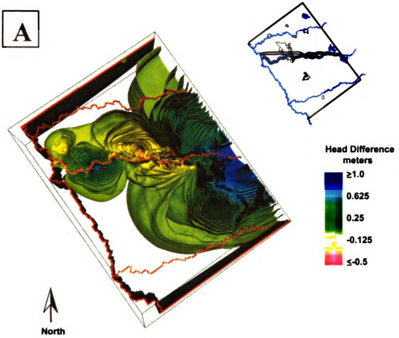

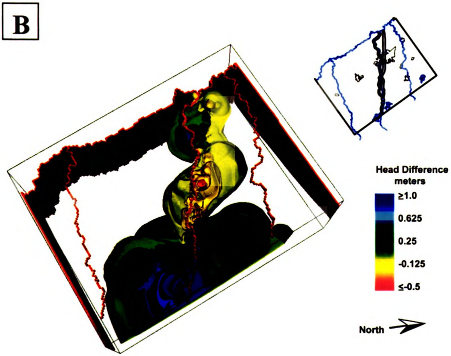

Chapter 3: Conclusions and Future Work

CONCLUSIONS

The primary purpose of this study was to understand the impact incised-valley fills (IVFs) have on regional groundwater flow, contaminant transport, and the potential for artificial aquifer recharge in the Tuolumne River fluvial fan aquifer around Modesto, California. This task was accomplished by (1) assessing the stratigraphic character of the study area with well logs and core in order to construct model domains that capture this character and then (2) simulating groundwater flows and solute tracers through these models.

The most current regional scale groundwater model in the Modesto, California area, developed by the USGS (S. Phillips, unpublished model, 2005), used previously collected data (driller's logs, geophysical logs, and a few continuous cores) to characterize the area's hydrogeology (Burow *et al.*, 2004). While this model is a reasonable representation of the area geology and hydrologic regime, it does not implicitly include the IVFs.

By adapting the existing USGS model to incorporate the IVFs, this thesis shows that the IVFs are critical to understanding the regional hydraulic regime. To include the IVFs in the model, sequence stratigraphic concepts, by Weissmann *et al.* (2002b), were applied to characterize IVF geometry and character for integration into the USGS groundwater flow model. With a sequence stratigraphic model, a more accurate model of the regional geology could be generated, even in areas where little subsurface data were available. Addition of the IVF improves the geologic model of the Modesto area and in turn the understanding of regional groundwater flow and solute transport.

Assessment of Stratigraphic Character

Stratigraphic character assessment was completed through the analysis of two soft sediment continuous cores and many (>10,000) driller's well logs. The continuous cores were used to develop a better understanding of the fan deposits surrounding the IVF. The use of a ranking scheme for driller's well logs and subsequent analysis in this study helped to find several potential locations for the IVF. The thick gravel base of the IVF provided a means to identify the location of the IVF.

While it would have been ideal to incorporate more core data into this model, the two cores that were described in the study area did not provide a sufficient amount of data to generate statistical realizations of the area. The two cores were used to supplement the understanding of the surrounding IVF deposits.

Two conclusions come from the investigation of driller's logs: (1) such driller's logs can be used with reasonable success to generally identify the position of IVFs by focusing on presence or absence of thick gravel units and (2) multiple (four) geologic scenarios were developed to help assess the influence of the IVF on regional groundwater flow and assess the impact of model uncertainty.

While the quality of driller's logs is often unreliable, there are certain instances where these logs can be used with relative confidence. The use of the driller's logs as an initial attempt to delineate the IVF and identify the thick, gravel base of the IVF provides a good example of the appropriate application of driller's logs. Because of the coarse grained nature and significant thickness of these deposits, the driller's reliability to properly identify the interval increases.

Although the driller's logs were used in this study with some success, they should be employed for subsurface analysis with caution. For example, I was able to identify several IVF locations, which may or may not actually exist. The geometry of the IVF was inferred from the current topography. These trends need to be validated with further geophysical survey (e.g. seismic reflection) studies to better locate and describe the IVF geometry and stratigraphy.

Simulation of Groundwater Flow and Solute Tracers

The groundwater models developed to test the influence of the IVF resulted in four main conclusions. The addition of the IVF (1) changes regional hydraulic heads regimes (2) allows pathlines (water) to move more rapidly to a greater lateral extent and deeper into the aquifer (3) allows flow (illustrated by particle pathlines) to spread into the aquifer sediments adjacent to the IVF and (4) creates a preferential pathway for contaminant plumes, decreasing solute transport times in areas where the IVF is located.

The creation of a preferential pathway from the addition of the IVF is not easily identified simply through the measurement of head elevations. As was shown by the slight variation in head elevations in the model with and without the IVF, measurements of groundwater levels alone would not indicate the presence of these preferential pathways. Examining the model head solutions alone also provided very little insight into the influence of the IVF on groundwater flow. To better illustrate the influence of the IVF, the head difference between the model with and without the IVF was used to show the areas of convergent and divergent flow. Areas where the head levels are lower in the model with the IVF indicate that the flow in that area converges on the IVF. In steady-state conditions represented by this model, the IVF is "funneling" the maximum amount of water through the available effective pore space, which causes the water to "back-up" and diverge from the IVF.

Pathline analysis experiments were used to asses the advective flow in the model and illustrate the impact of flow changes along the IVF. Pathlines in the model without the IVF have little lateral movement and vertically tend to follow with the local gradient. Pathlines in this model do not disperse in various directions in the aquifer; rather, they all have similar trends that reflect the regional head gradients. In the model with the IVF, however, pathlines follow the IVF and are dispersed into the contiguous aquifer sediments.

Transport experiments reaffirm the pathline analysis results. In the model without the IVF, transport simulations reveal that the plume expands in a uniform radial pattern from the constant contaminant source. In the model with the IVFs, the solute transport simulations clearly illustrate the changes in the plume morphology with the addition of the IVF. The contaminant plume preferentially follows the path of the IVF. The IVF increases the distance the plume can travel in the same amount of time, thus resulting in a transport time that would be shorter than predicted using the model without the IVF.

These results show that the IVF provides a pathway of preferential flow for groundwater as well as contaminants. In the terms of managing the regional water quality, this is both beneficial and detrimental. The IVF provides the benefit of potentially providing a conduit to artificially recharge the aquifer. Recharge will be important to provide sustainable water supply to the city of Modesto. While the IVF provides a good source for artificial recharge, unfortunately, it also creates a pathway for

contamination to enter and disperse into the aquifer, exposing the entire aquifer to potential contamination.

RECCOMMENDATIONS FOR FUTURE INVESTIGATIONS

While the realizations generated in this study provide a good preliminary understanding of the influence of the IVF, these realizations should be used as a basis for further investigation into the area stratigraphy and hydrologic regime. The geologic realizations could be improved by (1) using more reliable methods for identifying the location of the IVF (2) obtaining core through several locations of the IVF to better understand IVF lithologic character and (3) collecting additional continuous core in the open fan deposit areas.

Further investigation into the location of the IVF should be conducted. While analysis from driller's well logs provides a good approximate location of the IVF more reliable geophysical data should be accrued, to effectively model the IVF. Seismic data across the area will help better constrain the location and geometry of these features, providing more dependable estimations of the width, depth, and length of the IVF.

In this study, no core was collected within the IVF. This made modeling of the lithologic character more challenging. The character of the apex and toe of the IVF need to be investigated as these are the principle areas of recharge and discharge for groundwater and will impact the location of the divergent flow from the valley. Investigation into the toe of the fan may provide insight into the influence of local base level (sea level) and the basin width on the preservation (or removal) of the distal fan deposits. Currently, the IVF code does not account for the fact that gravels are not likely

present in the distal portion of the model. With further constraints on the distal character in the IVF, this portion of the model could be improved. Additional studies near the apex of the fan will provide further insight into the geometry of the stacked IVF deposits believed to exist. This may have a significant influence on the ability to artificially recharge the aquifer.

Additional continuous core data across that fan will also help to better capture the aquifer heterogeneity. One significant improvement in this area would be to add the sequence bounding paleosols. While this model does not include the paleosols, they may have an impact on the regional or local groundwater flow, acting as no or low flow barriers, as noted on the Kings River fluvial fan (Weissmann *et al.*, 2004).

The groundwater and contaminant transport models generated in this study enhance understanding of the groundwater flow and the potential for contaminant movement through the Modesto area. The models also provide a preliminary understanding of the potential influence these incised-valley fills may have on artificial recharge in the incised-valley fill.

SUMMARY

The coarse-grained continuous nature of the IVFs indicates that the IVF in the Modesto area is capable of acting like a regional conduit for groundwater flow and contaminant transport. Our results support those reported by Weissmann *et al.* (2004) who created groundwater flow and contaminant transport models in studies of similar IVF deposits of the Kings River near Fresno, California. They showed that IVFs significantly influence groundwater flow and contaminant transport specifically by providing the potential for (1) increased groundwater flow and production rates (2) rapid contaminant transport within the incised-valley fill sediments and (3) rapid contaminant movement from the incised-valley fill into the contiguous aquifer sediments. Based on the results of this study, the identified IVF beneath the Modesto area has a similar effect. Continued and more detailed studies on the influence of the IVF will help to fully explore the potential role the IVF plays in artificial aquifer recharge and regional water quality in that area.

Furthermore, implications of these conclusions are directly applicable to the current and continuing USGS investigation into the groundwater status and long term quality, for which the original model was created. The eastern fluvial fans in the San Joaquin valley have been primarily agricultural land and subjected to substantial amounts of fertilizer application and irrigation since the early 1900's (Gronberg *et al.,* 2004). An investigation of the transport of anthropogenic and natural contaminants to community supply wells by the USGS is already underway in the Modesto area. The main question motivating this USGS investigation of the groundwater status is, "What are the primary man-made and natural contaminant sources, aquifer processes, and well characteristics that control the transport and transformation of contaminants along flow paths to community supply wells in representative water-supply aquifers?" (Gronberg *et al.*, 2004, p.4). The specific objectives of the study are to (1) characterize the regional geologic setting to determine the preferential or most common, groundwater pathways to community supply wells and (2) gain an understanding of the sources of contaminants in the aquifer and the processes that impact the transport and potential transformation of the contaminants (Gronberg *et al.*, 2004). The addition of the IVF into the USGS model will greatly improve the current groundwater model's ability to illustrate the dominant pathways for transport. Areas where contamination of the Tuolumne River can migrate deep into the groundwater would also be highlighted in a groundwater model that incorporates the IVFs. In terms of remediation, it is vital to understand the sources and pathways of the chemicals to better treat or remove the contaminant. The IVF provides a preferential path for water flowing downward through the river bed thus creating a potential conduit for runoff contaminants like fertilizers that will degrade water quality and should be addressed. The realizations developed in this study show that the IVFs significantly influence the groundwater flow by acting as a regional "pipeline" of coarse sediment that creates the potential to provide artificial recharge to the Modesto area and a conduit for contaminants to follow, increasing the dispersion of particle pathlines into contiguous aquifer sediments and enabling solute plumes to move farther distances more rapidly leaving the aquifer susceptible to widespread contamination.

References

Bartow, J. A., 1988, The Cenozoic evolution of the San Joaquin Valley, California: U.S. Geological Survey, v. Professional Paper 1501.

Bennett V, G. L., 2003, Estimating the nature and distribution of shallow subsurface paleosols on fluvial fans in the San Joaquin Valley, California [MS Thesis]: Michigan State University.

Bennett V, G. L., Weissmann, G. S., Baker, G. S., and Hyndman, D. W., in press, Regional-scale assessment of a sequence bounding paleosol on fluvial fans using ground penetrating radar, Eastern San Joaquin Valley, California: Geological Society of America Bulletin.

Blum, M. D., and T.E. Tornqvist, 2000, Fluvial responses to climate and sea-level change: a review and look forward: Sedimentology, v. 47, p. 2-48.

Bull, W. B., 1991, Geomorphic Responses to Climatic Change: New York, Oxford University Press, 326 p.

Burow, K. R., Shelton, J.L., Hevesi, J.A., and Weissmann, G.S., 2004, Hydrogeologic characterization of the Modesto Area, San Joaquin Valley, California, 2004-5232.

Fogg, G. E., 1986, Groundwater-Flow and Sand Body Interconnectedness in a Thick, Multiple-Aquifer System: Water Resources Research, v. 22, no. 5, p. 679-694.

Gelhar, L.W., Welty, C., and Rehfeldt K.R., 1992, A Critical Review of Data on Field-Scale Dispersion in Aquifers: Water Resources Research, v. 28, no. 7, p. 1955-1974.

Harden, J. W., 1986, Soils Developed in Granitic Alluvium near Merced, California: U.S. Geological Survey, Bulletin 1590-A.

Houston, J., 2004, High-resolution sequence stratigraphy as a tool in hydrogeological exploration in the Atacama Desert: Quarterly Journal of Engineering Geology and Hydrogeology, v. 37, p. 7-17.

Huggenberger, P., and Aigner, T., 1999, Introduction to the special issue on aquifer-sedimentology: problems, perspectives and modern approaches: Sedimentary Geology, v. 129, no. 3-4, p. 179-186.

Huntington, G. L., 1980, Soil-Land Form Relationships of Portions of the San Joaquin River and Kings River Alluvial Depositional Systems in the Great Valley of California [unpublished Ph.D. Dissertation]: University of California at Davis, 147 p.

Janda, R. J., 1966, Pleistocene history and hydrology of the upper San Joaquin River, California [unpublished Ph.D. Dissertation]: University of California, Berkley, 293 p.

Jervey, M. T., 1988, Quantitative geological modeling of siliciclastic rock sequences and their seismic expressions, *in* Wilgus, C. K., Hastings, B. S., Kendall, C. G. S. C., Posamentier, H. W., Ross, C. A., and Van Wagoner, J. C., eds., Sea-level Changes: An Integrated Approach, SEPM (Society for Sedimentary Geology) Special Publication, p. 47-69.

Koltermann, C. E., and Gorelick S.M., 1992, Paleoclimatic signature in terrestrial flood deposits: Science, v. 256, p. 1775-1782.

Lettis, W. R., 1982, Late Cenozoic stratigraphy and structure of the western margin of the central San Joaquin Valley, California: U.S. Geological Survey, 82-526.
-, 1988, Quaternary geology of the Northern San Joaquin Valley, *in* SEPM, Pacific Section, p. 333-351.

Lettis, W. R., and Unruh, J.R., 1991, Quaternary geology of the Great Valley, California, *in* Geological Society of America, Geology of North America, Conterminous U.S., p. 164-176.

Marchand, D. E., and Allwardt, A., 1977, The Cenozoic history of the San Joaquin Valley and the adjacent Sierra Nevada as inferred from the geology and soils of the eastern San Joaquin Valley, *in* Singer, M. J., ed., Soil Development Geomorphology, and Cenozoic History of the Northeastern San Joaquin Valley and Adjacent Areas, California, University of California Press, Guidebook for Joint Field Session.

-, 1981, Late Cenozoic Stratigraphic Units, North Eastern San Joaquin Valley, California: Soil Science Society of America and Geological Survey of America, 1470.

Page, R. W., Geology of the fresh ground-water basin of the Central Valley, California, with texture maps and sections, 1401-C.

Scheibe, T. D., and Freyberg, D. L., 1995, Use of sedimentological information for geometric simulation of natural porous media structure: Water Resources Research, v. 31, no. 12, p. 3259-3270.

Schumm, S. A., 1993, River response to baselevel change-implications for sequence stratigraphy: Journal of Geology, v. 101, no. 2, p. 279-294.

Unruh, J. R., 1991, The Uplift of the Sierra-Nevada and Implications for Late Cenozoic Epeirogeny in the Western Cordillera: Geological Society of America Bulletin, v. 103, no. 11, p. 1395-1404.

Webb, E. K., and Anderson, M. P., 1996, Simulation of preferential flow in three-dimensional, heterogeneous conductivity fields with realistic internal architecture: Water Resources Research, v. 32, no. 3, p. 533-545.

Weissmann, G. S., and Fogg, G. E., 1999, Multi-scale alluvial fan heterogeneity modeled with transition probability geostatistics in a sequence stratigraphic framework: Journal of Hydrology, v. 226, no. 1-2, p. 48-65.

Weissmann, G. S., Carle, S. F., and Fogg, G. E., 1999, Three dimensional hydrofacies modeling based on soil surveys and transition probability geostatistics: Water Resources Research, v. 35, no. 6, p. 1761-1770.

Weissmann, G. S., Zhang, Y., LaBolle, E. M., and Fogg, G. E., 2002a, Dispersion of groundwater age in an alluvial aquifer system: Water Resources Research, v. 38, no. 10.

Weissmann, G. S., Mount, J. F., and Fogg, G. E., 2002b, Glacially driven cycles in accumulation space and sequence stratigraphy of a stream-dominated alluvial fan, San Joaquin valley, California, USA: Journal of Sedimentary Research, v. 72, no. 2, p. 240-251.

Weissmann, G. S., Yong, Z., LaBolle, E. M., and Fogg, G. E., 2002c, Modeling environmental tracer-based groundwater ages in heterogenous aquifers: Water Resources Research, v. 38, p. 1198-1211.

Weissmann, G. S., Zhang, Y., Fogg, G.E., and Mount, J.F., 2004, Influence of Incised Valley-Fill Deposits on Hydrogeology of a Stream-Dominated Alluvial Fan, *in* Bridge, J., and Hyndman, D. W., eds., Aquifer Characterization, SEPM (Society for Sedimentary Geology) Special Publication, p. 15-28.

Weissmann, G. S., Bennett, G. L., and Lansdale, A. L., 2006, Factors controlling sequence development on Quaternary fluvial fans, San Joaquin Basin, California, *in* Harvey, A. M., Mather, A. E., and Stokes, M., eds., Alluvial Fans: Geomorphology, Sedimentology, Dynamics, Geological Society, London, Special Publications, p. 169-186.

Zhang, Y., and Fogg, G. E., 2003, Simulation of multi-scale heterogeneity of porous media and parameter sensitivity analysis: Science in China Series E-Technological Sciences, v. 46, no. 5, p. 459-474.

Appendix A: Geologic Setting and Stratigraphic Character

INTRODUCTION

Through this study, we intend to show the influence of relatively coarse-grained incised-valley fills (IVFs) on groundwater flow, contaminant transport, and potential artificial recharge in the Modesto, California area. To assess the influence of the IVFs, an investigation of the area geology was conducted to locate and characterize the IVFs and the surrounding sediment.

In this appendix, I first describe the regional geology and stratigraphy. Next, the local geology is described with the findings of geologic investigations using sediment core and driller's well log data. The results of this investigation are then incorporated into four geologic realizations.

BACKGROUND GEOLOGY

San Joaquin Basin and Regional Geologic Setting

The San Joaquin Basin is located within the California's Great Valley, an approximately 700 km long (north to south) by 100 km wide (east to west) valley that is bound on the east by the Sierra Nevada and on the west by the Coast Ranges. The valley is divided into two sub-basins by the Stockton Arch, a buried transverse arch, with the Sacramento Basin in the north and San Joaquin Basin in the south (See Figure 1 from Chapter 2). The basin is underlain by crystalline basement rock and approximately 9 km of Mesozoic and Cenozoic sedimentary rocks and sediments (Bartow, 1988). Structurally, the basin is asymmetric with a gently sloping eastern margin that abuts the Sierra Nevada, and the more steeply sloping western edge adjacent to the Coast Ranges.

This study focuses on the Tuolumne River fan, located in the northeast portion of the San Joaquin Basin (Figure 1). The fan was formed where the Tuolumne River flows west out of the Sierra Nevada into the San Joaquin Basin.

Climate Effects on Quaternary Deposits in the Eastern San Joaquin Valley

Quaternary fluvial fan deposits along the eastern San Joaquin Valley preserve evidence of past phases of aggradation and degradation from varying amounts of sediment supply and discharge in response to recurring glacial periods in the Sierra Nevada (Janda, 1966, Marchand 1977, Huntington 1980, Marchand and Allwardt 1981, Lettis 1988, and Weissmann *et al.* 2002b, 2006). Fluvial fans are differentiated from alluvial fans in this study to emphasize that fluvial fans are characterized by perennial fluvial processes, while alluvial fans are characterized more by ephemeral debris flows or sheetfloods. Similarities among the fluvial fans along the eastern portion of the valley have allowed for basin-scale comparisons of these fans (Weissmann *et al.*, 2006).

Weissmann *et al.* (2002b) investigated the fluvial fan deposits on the Kings River fan and use a sequence stratigraphic model to understand the climatically induced cycles of deposition. In the model, they apply the traditional definition of a sequence as "…a relatively conformable succession of genetically related strata bounded at its top and base by unconformities, or their correlative conformities" (Mitchum, 1977, p. 210). Sequence boundaries in this model are identified as the paleosol surface and respective IVF base that divide the fluvial fan deposits into five stratigraphic units.

In this sequence stratigraphic model, concepts of *accumulation* and *preservation* space (after Blum and Törnqvist, 2000) are used to understand the stratigraphy. Accumulation space is defined as one component of accommodation space and refers to the volume of space available to be filled with sediment and is dependent on the balance of sediment supply and stream discharge as well as channel geometry. Preservation space is also a component of accommodation space and is the space below the lowest level of sediment removal. In the Kings River and Tuolumne River areas, it is a long-term, preservation space controlled by the local subsidence rate. The five sequences marked distinct periods of regional aggradation and degradation, or accumulation space change. Packages of relatively rapidly deposited fluvial fan deposits separated by paleosols indicate periods of aggradation across the fan, or increased accumulation space, punctuated by periods of degradation and fan incision, or restricted accumulation space and quiescence on the upper parts of the fan. Preservation space was created by constant subsidence in the area, which lowered the deposits below the lowest level of erosion (sequence stratigraphic model described in more detail in the next paragraph). Sequence boundaries in this model are identified as the paleosol surface and respective IVF base that divide the fluvial fan deposits into five stratigraphic units.

Specifically, fluvial fan aggradation or degradation occurred on the Kings River fan as sediment supply to discharge ratios increased or decreased as a result of changes from glacial to interglacial climate. Interglacial periods are marked by limited aggradation, a low accumulation space, and an intersection point located distally on the fan (Figure A1) (Weissmann *et al.,* 2002b). During this portion of the cycle, paleosols formed in the exposed upper fan outside the incised valleys. Glacial periods are characterized by a large amount of laterally extensive aggradation on the fan, a high accumulation space, and an intersection point proximally located near the apex of the fan (Figure A2). Weissmann *et al.* (2002b) indicated that this sequence stratigraphic model can serve as a means to predict facies distributions and stratigraphic relationships in areas exposed to similar conditions.

Due to the similar cyclic depositional character among the fans in the eastern San Joaquin basin, the sequence stratigraphic model described in the Kings River fan study can be applied to other fans in the basin. However climate and sediment supply to stream discharge ratios are not the only controls on the deposition of the fluvial fans in the valley (Weissmann *et al.*, 2006). Factors that control the overall amount of accumulation space available during periods of climate fluctuation and hence sequence development are: (1) the sediment supply to stream discharge ratio, (2) the rate of basin subsidence, (3) the amount of local base level change, and (4) the basin width (Weissmann, *et al.*, 2006). These controls vary within the San Joaquin Basin and influence the sequence geometry on individual fans.

Controls on the Tuolumne River fluvial fan sequence geometry in particular are (1) glacial influence in the drainage basin (2) relatively low subsidence rates (approximately 30cm/ 1000 yrs, Lettis, 1988) due to the river's location in the northern portion of the San Joaquin Valley, and (3) the San Joaquin River aslocal base level control on Tuolumne River elevation (Weissmann *et al.,* 2006). The Tuolumne River drains the Sierra Nevada which resulted in cycles of significant fluctuations in the sediment supply and stream discharge from Quaternary glaciations. Because the Tuolumne River is in the north, where the San Joaquin Valley is narrower and the subsidence rate is relatively low (30 cm/1000 yrs, Lettis, 1988), sequence thickness and lateral extent were thinner and smaller than found in southern portions of the valley. This resulted in an overall reduction in accumulation and preservation space, which caused the lateral progression of apexes and the thinner fluvial fan units observed here (Weissmann *et al.* 2006; Bennett *et al. in press*; See Figure 2 in Chapter 2). The local base level is connected to the San Joaquin River and ultimately sea level. This resulted in deeper incision and sediment bypass in the distal portions the fan during interglacial periods, also reducing the overall amount of accumulation space available to be filled.

LOCAL GEOLOGIC INVESTIGATION

Study Area

The study area is delineated by the Sierra Nevada and the San Joaquin River to the east and west, respectively, and by the Stanislaus and Merced Rivers to the north and south (See Figure 3 in Chapter 2). It is approximately 48 km (30 miles) long (west to east) and 19 km (12 miles) wide (north to south). Dissecting the site is the Tuolumne River, which flows east to west through the middle of the study area (See Figure 3 in Chapter 2). Deposits at the site are composed mainly of Cenozoic sedimentary deposits (Marchand and Allwardt, 1981). This study of the Modesto area will focus on the Quaternary Pleistocene fluvial deposits: the Turlock Lake Formation, the Riverbank Formation and the Modesto Formation (See Figure 1 in Chapter 2). A more comprehensive description of the older units in the area can be found in Marchand and Allwardt (1981).

Stratigraphic Units

Each unit of open-fan deposits is bound at the top and bottom by a paleosol and is composed of silty, sandy, and clayey sediments with discrete coarser-grained channel deposits. Nestled among the relatively fine-grained open-fan sediments is the relatively coarse-grained IVF, characterized by a thick basal gravel lag (5 to 9 meters) that gradually fines up to the surface (See Figure 4 in Chapter 2).

Characterization of hydrofacies within the fluvial fan deposits was done by using methods similar to those described in Weissmann *et al.* (2002b) where we utilized several sources of geologic data, including driller's well logs, geophysical logs, and lithology from continuous core samples. Cooperation with the U.S. Geological Survey (USGS) in Sacramento, California afforded access to several thousand paper copies of the Department of Water Resources (DWR) driller's logs within the study area, geophysical well logs from city wells, and recently obtained, relatively-continuous, soft sediment core. Also available from the USGS are digitized spatial data of the area hydrology, geology, soils, topography, and approximate pumping rates of the city of Modesto municipal wells (S. Phillips, unpublished data, 2005).

Open-fan Deposit Character

Four hydrofacies were identified within the study area from two continuous soft sediment cores collected by the USGS (See Figure 3 in Chapter 2) and well logs from the California Department of Water Resources (DWR) (See Appendix B for detailed descriptions). Included in the core descriptions are a visual estimation of grain size, grain shape, grain sorting, color, primary sedimentary structures, and secondary alterations (including pedogenic alteration). The core descriptions were used to better understand hydrofacies in the proximal (eastern) and distal (western) open-fan deposits. The core data were also used to help generate the fan surfaces used in the IVF fill code in Appendix G. The hydrofacies include: (1) gravel channel deposits (not recovered in these cores but observed in drillers' logs and described by Weissmann *et al.*, 2002b) (2) sand channel deposits (3) silty sands, silty clays, and clay overbank deposits, and (4) pedogenically altered deposits. The core descriptions show that the western extent of the study area contained more fine-grained sediments of the distal fluvial fan deposits, while the eastern extent of the study area contained the more coarse-grained proximal fluvial fan sediments.

Gravel Channel Deposits

Although the gravel channel deposits of the IVF were not seen in these cores, descriptions by Weissmann *et al.* (2002b) indicate that the gravel is composed of clast-supported gravel and cobbles and are commonly found at the channel base.

A few thin intervals of poorly sorted, matrix supported, gravel flood deposits were observed in the core (Figure A3). The matrix is coarse to very coarse sub-angular sand with some granules. The gravel is 1 to 4 cm (0.4 to 1.6 inches). The deposits do not show any primary structures and tend to be heavily iron stained. In both the proximal and distal portions of the fan, these thin gravels are sparse and were located at depth: MREA at 70 meters (230 ft) and MRWA at 55 meters (180 ft). The proximal gravels overall are more coarse than the distal deposits and have less matrix material. The gravel in the distal deposits has fewer large clasts of gravel within the coarse matrix.

Sand Channel Deposits

The channel sand facies (Figure A4) are well sorted, mica rich quartz and feldspathic arenites. The mica is present in large unweathered flakes giving the core a "glittery" appearance. They range in grain size from very fine to coarse sand and are sub-rounded to sub-angular. These channel sands were commonly noted to have a poorly-sorted matrix-supported pebbles at the basal contact. These deposits are typically cross-stratified but were also observed without any primary structures (massive). The channel sand deposits also commonly display a fining upward trend. Proximal fan deposits are more coarsely grained (medium to coarse or very coarse sand) while distal deposits tend to have a finer grain size (very fine to medium grained). Distal deposits showed less evidence of secondary alteration and tended to show more distinct heavy mineral banding along cross-bedding planes.

Overbank Deposits

Overbank deposits (Figure A5) characterized in the cores was silty fine to very fine sand, silty clay, or clayey silt. They are gray to light brown in color with occasional sandy lenses. Slight to no pedogenic alteration was observed. These deposits were commonly thinly laminated, although some massive deposits were observed. Root traces and/or burrows were also observed within the overbank deposits. Iron staining/ mottling was also a very common characteristic among the overbank deposits. Proximal overbank deposits have more silty sands a smaller fraction of silt and clay than was observed in the distal deposits. The distal deposits are most commonly sandy or clayey silt.

Pedogenically Altered Deposits

Reddish colored pedogenically-altered sand with medium to thick clay coats was also present in the cores (Figure A6). Hues range 2.5YR to 10YR in the proximal and 5YR to 10YR (mostly 7.5YR). Value ranges from 4 to 5 in the proximal and 5 to 6 in the distal, and chroma ranges from 3 to 6 in the proximal and 2 to 4 in the distal. These deposits are the most developed paleosols observed in the core samples. Slickensides and root traces are also present in these deposits. Proximal paleosols are better developed with thicker clay coats (thick to medium) and have a stronger reddish coloring. The distal paleosols are less well developed with thinner clay coats (medium to light) and do not always exhibit the distinct reddish coloring seen in the proximal paleosols.

Incised-Valley Fill Geometry

Core was not collected within the targeted IVF deposit. However, Weissmann *et al.* (2002b, 2004) noted that the incised-valley fill could be recognized in driller's logs by a thick gravel or cobble base with overlying sandy facies. These coarse-grained deposits form approximately two-thirds of the fill deposit. Burow *et al.*, (2004) indicated that the IVF could also be recognized in geophysical logs by a relatively high resistivity and a correspondingly low gamma ray response. This method was adapted and applied to locate and describe the IVF character in the Modesto area using available driller's well logs and geophysical well logs. .

Identification of Incised-Valley Fill with Driller's Well Logs

Approximately 10,000 well logs from the study area were examined. The well logs used for this investigation are the same as those initially filtered by the USGS to develop a database (described in *Burow et al.* (2004)). Logs containing gravels of sufficient thickness (> 3 meters) were assigned a rank of 1 to 4 based on how well the log's description of the stratigraphy resembled the fining-upward prototype characterization of the incised-valley fill. A well assigned a rank of 1 denotes the best representation of the incised-valley fill, with a thick gravel base fining upward to sand then silt and clay, while a well ranked 4 contains thick gravel but does not resemble the ideal fining-upward succession contained within the incised-valley fill deposits. Examples of driller's well logs of various ranks are included in Appendix C. The drilling method and the consistent quality of individual drillers were also used to determine the rank of the well.

Once all of the wells had been ranked, a database of these well logs was generated in ArcGIS to locate the incised-valley fill (Figure A7). Wells were located using reported addresses and descriptors on logs, and then well location coordinates were obtained by plotting them as waypoints in National Geographic TOPO! California. Information that was entered into the database of wells includes (1) the well identification number (2) the rank of the well, (3) the elevation of the well, (4) the depth of the gravel lag deposit, (5) whether or not the well had previously been selected for a USGS database, (6) the relative depth of the gravel (shallow or deep), and (7) general notes about the log. The results of IVF delineation is described in Chapter 2 and Appendix C.

A potential source for uncertainty in this method of delineating the IVFs is created by using driller's well logs as the primary data set. There is significant uncertainty when identifying the basal gravel lag within the IVF through interpretation of the driller's logs. The quality and accuracy of the logs may be questionable and somewhat unreliable for detailed subsurface correlation. Quality strongly depends on the driller's ability and conscientiousness, and even under the best circumstances, carries significant uncertainty. More easily drilled units, such as sand and clay, may not be noted accurately during drilling, as there is no variation in the rig character or drilling techniques required. However, well logs are successfully used in this study to identify thick gravel deposits. These thick basal gravel lag deposits result in a distinct change in the rig behavior. For this reason, it is assumed that the depth of the gravel units, as well as their thicknesses, will be consistently more correctly described in the log than sand, silt, or clay, thus allowing more reasonable identification of the incised-valley fills.

Construction of Sequence Bounding Surfaces

Prior to generating the groundwater models, digital spatial data were used to generate surfaces for the model layers and for use in FORTRAN codes to insert the IVF in the model. Surfaces depicting the incised channel were developed by (1) adapting the modern Tuolumne River valley from the digital elevation model (DEM) for the Riverbank Formation fan surface and (2) by using ArcGRID to interpolate the older Turlock Lake Formation fan surface (See Appendix D). The present ground surface was assumed to be a sufficient estimate of the Riverbank fan surface outside the IVF, because the Modesto formation that covers the area is only a thin veneer over the fan surface (Bennett, 2003; Weissmann *et al.*, 2006; Bennett *et al. in press*), . The Turlock Lake Formation surface was developed with data from well logs, digital soil maps, and core data. Surfaces were combined to match the four geologic scenarios described in Chapter 2 (See Table 1 in Chapter 2).

CONCLUSION

Two conclusions come from the analysis of the IVF and surrounding open fan deposits: (1) driller's logs can be used with reasonable success to generally identify the position of IVFs by focusing on presence or absence of thick gravel units and (2) multiple (four) geologic scenarios were developed to help assess the influence of the IVF on regional groundwater flow and assess the impact of model uncertainty.

While the driller's logs were successfully applied, there are still significant improvements that can be made to locating and defining the IVFs. It is unlikely that multiple potential IVFs within the same stratigraphic range (i.e. two potential Modesto Formation IVFs) exist, although were identified. Using four geologic scenarios, the influence of the IVF can be assessed as along with the impact of uncertainty in geologic model. Comparisons among these four scenarios may give insight to the impact of incorrectly developing a conceptual model.

To improve this analysis of the Tuolumne River fluvial fan sediments and stratigraphy, further collection of geologic data is needed. This data collection effort might help constrain the location and the geometry of the IVF. Suggestions for investigation include: seismic studies to delineate the extent of the IVF and additional continuous core data from the area to provide a better definition of the character of the IVF sediments and their variation proximally or distally on the fan. Supplementing the current characterization of the open-fan deposits from more continuous core would be vital to generate a geostatistical model to illustrate the distribution of hydrofacies and supply information to parameterize the deposits that surround the incised-valley fills. While it would have been ideal to use the core descriptions to generate geostatistical realizations for this study, the data set (inclusive of the two wells described above) was not large enough for proper statistical analysis.

The geologic analysis described in this appendix provides the framework for the groundwater flow and solute transport models described in Chapter 2 of this thesis. The groundwater and contaminant transport models produced are expected to enhance understanding of the groundwater flow and the potential for contaminant movement through the Modesto area. Additionally, the models are also expected to provide a preliminary understanding of the potential influence these incised-valley fills may have on artificial recharge in the incised-valley fill.

Figure A1: Map and cross-sectional view of the balance between aggrading and degrading reaches in deposits on the Kings River. Changes in accumulation space are inferred by a shifting intersection point that marked the aggrading (lower fan) and degrading reaches (incised channel) of the river. (adapted from Weissmann *et al.*, 2002b).

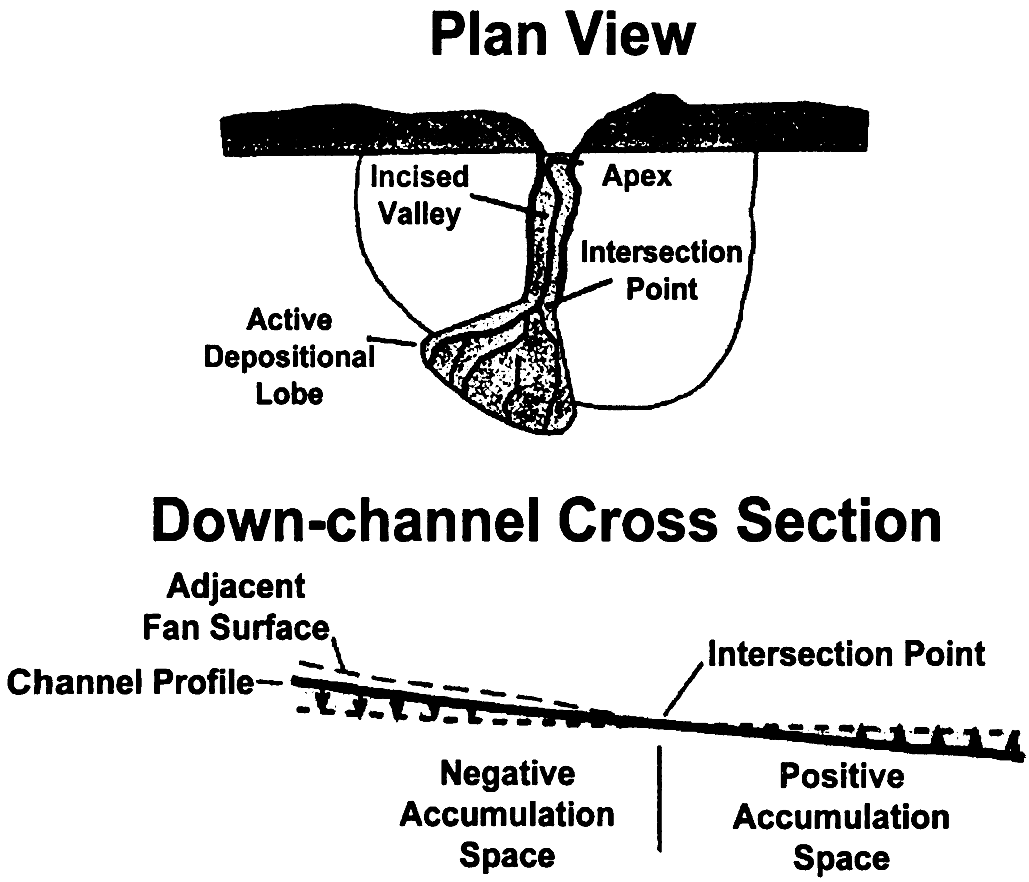

Figure A2: Four diagrams of various depositional regimes though a full glacial to interglacial cycle. The intersection point of the fan, or the transition between aggrading and degrading reaches, will shift up and down the fan as sediment supply:discharge ratios increase and decrease, respectively, with changes from glacial to interglacial episodes. (adapted from Weissmann *et al.*, 2002b).

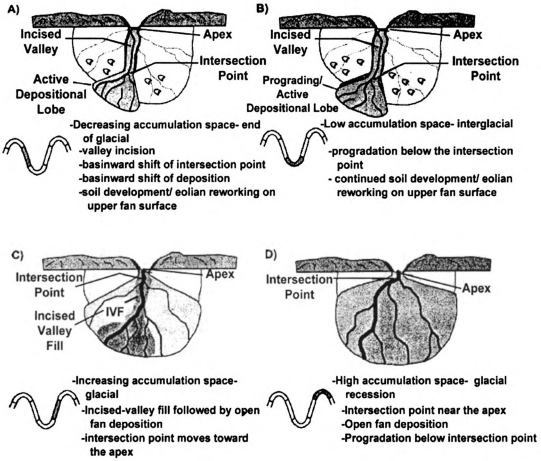

Figure A3: An example of the infrequent matrix-supported gravel facies. This facies represents only a small portion of the core samples and is presumed to be rare. Shown in color.

DISTAL

PROXIMAL

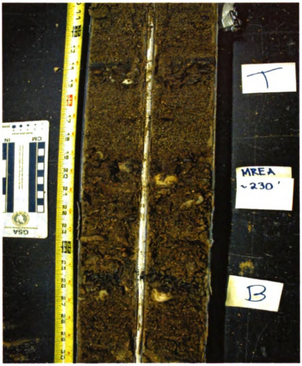

Figure A4: Typical distal and proximal fan examples of the channel sand facies. The distal sediments are typically more fine grained and display less iron staining. Shown in color.

DISTAL **PROXIMAL**

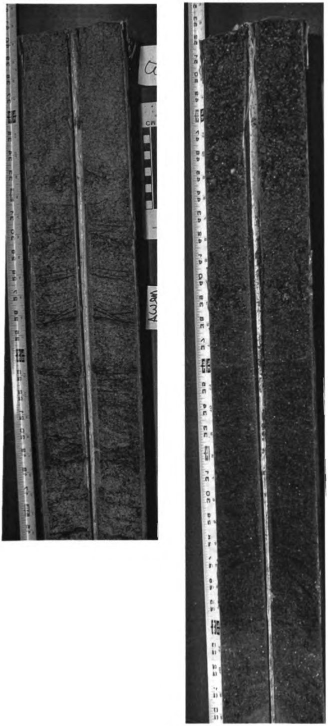

Figure A5: Typical distal and proximal fan examples of the overbank silty clay deposits. These deposits are typically composed of silty fine to very fine sand, silty clay, clayey silt. They are usually gray to light brown with some sandy lenses, slight to no pedogenic alteration, and can be thinly laminated or massive. Some deposits displayed root traces or burrows and iron staining or mottling. Shown in color.

DISTAL **PROXIMAL**

Figure A6: Typical distal and proximal fan examples of the pedogenically altered facies. This facies is typically reddish in color with significant pedogenic alteration (sand with medium to thick clay coats). Some slickensides and root traces were also noted in descriptions of this facies. Shown in color.

DISTAL **PROXIMAL**

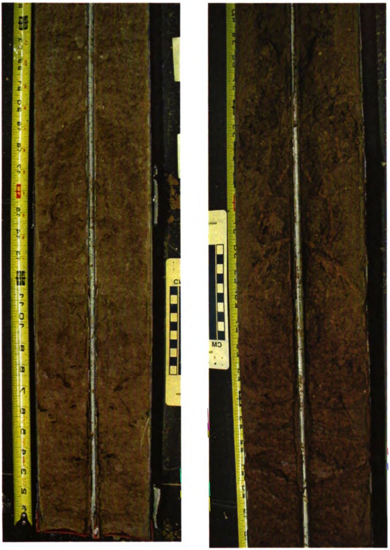

Figure A7: All driller's log wells entered in the ArcMap database ranked 1 through 4.

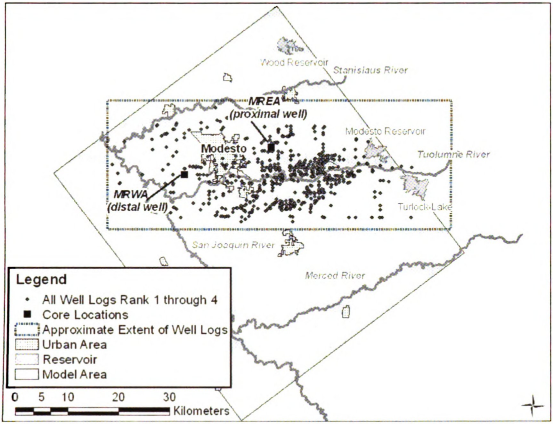

Appendix B: Open Fan Deposit Character Core Description

In order to better understand the character of the open-fan deposits surrounding the incised-valley fill, continuous core, collected by the USGS from two well locations was assessed—one located in a proximal fan position and the other on a distal portion of the fan (See figure 3 in Chapter 2). The proximal well, MREA, was drilled to a depth of 96 m (315 ft) and the distal well, MRWA, was drilled to a depth of 59 m (195 ft). Core was collected in 2.5 cm (1 inch) diameter tubes in 1.5 m (5 ft) increments. The cumulative 155 m (~500 ft) were described with visual assessments of grain size, sorting, shape; lithologic composition; color; primary structures; and secondary alterations. Descriptions verify the western extent of the study area contained more fine-grained sediments of the distal fluvial fan deposits, while the eastern extent of the study area contained the more coarse-grained proximal fluvial fan sediments. See Table B1 and Table B2 for detailed lithologic descriptions for MREA and MRWA, respectively.

Table B1: Lithologic descriptions of the proximally located soft sediment core MREA. The facies column uses a number to denote the hydrofacies and areas where core was not recovered. The numbers include: (0) no core recovered, (1) gravel flood deposits, (2) sandy channel deposits, (3) silty sands, silty clays, and clay overbank deposits, (4) pedogenically altered deposits.

See table on following page.

Top Depth (ft)	Top Depth (m)	Basal Depth (ft)	Basal Depth (m)	Thickness (ft)	Thickness (m)	Grain Size	▲ or ▼ **	Facies	Sorting	Roundness	Color	Basal Contact	Primary Structures	Secondary Alteration	Comments	Driller's Log
20.0	6.1	20.2	6.2	0.2	0.1	pebbles, 1-3 cm diameter	▼	1	well	subrounded to rounded		sharp			feldspar and other lithics	
20.2	6.2	21.0	6.4	0.8	0.2	sand: very coarse-coarse sand		2	well	subangular to subrounded	overall 2.5Y 5/3	sharp contact at grain size change	massive		90% quartz (arenite), felspathic, lithics, some chert, muscovite. Some heavy mineral banding.	
21.0	6.4	21.8	6.6	0.8	0.2	sand: medium to coarse sand		2	well	subangular to subrounded	overall 2.5Y 5/3	end of core	massive		90% quartz (arenite), felspathic, lithics, some chert, muscovite. Some heavy mineral banding.	
21.8	6.6	25.0	7.6	3.2	1.0	NO DATA		0								
25.0	7.6	26.2	8.0	1.2	0.4	sand: coarse to medium sand		2	well	subangular to subrounded	overall 10YR 5/6	sharp	interbeds of silty clay	some iron staining in the sands	same comp.	
26.2	8.0	27.8	8.5	1.6	0.5	sand: coarse to medium sand interbedded with silty clay		2			2.5Y 4/3	sharp	interbeds of silty clay with micrometer scale laminae			
27.8	8.5	28.6	8.7	0.8	0.2	sand: medium to fine sand		3	well	subangular to subrounded	overall 10YR 5/6	sharp	thin bed of silty clay at 28.2	heavily iron stained		
28.6	8.7	29.2	8.9	0.6	0.2	silty clay to clayey silt		3			2.5Y 5/2	end of core	thin laminae			
29.2	8.9	30.0	9.1	0.8	0.2			0								
30.0	9.1	32.2	9.8	2.2	0.7	clayey silt		3			2.5Y 5/3	gradational	mostly massive, thin interbeds of medium sand	heavy iron staining, mostly around root traces or burrows		

Top Depth (ft)	Top Depth (m)	Basal Depth (ft)	Basal Depth (m)	Thickness (ft)	Thickness (m)	Grain Size	▲ or ▼ ••	Facies	Sorting	Roundness	Color	Basal Contact	Primary Structures	Secondary Alteration	Comments	Driller's Log
32.2	9.8	33.0	10.1	0.8	0.2	sandy silt: sandy (medium to fine grained) silt with some clay that		4			7.5YR 5/3	gradational				
33.0	10.1	33.4	10.2	0.4	0.1	drill mud					2.5YR 5/4				very fine grained and soft, looks like peanut butter, a little sandy with specks of dark brown, approximately 4-5 inches	
33.4	10.2	33.6	10.2	0.2	0.1	sandy silt		4			7.5YR 5/3	gradational				
33.6	10.2	35.0	10.7	1.4	0.4	sand with clay coats: coarse to very coarse sand with medium clay coats		4			10YR 5/3	end of core				
35.0	10.7	35.4	10.8	0.4	0.1	clay: red clay		4			7.5YR 4/6	sharp			thin 1 mm white clay layer below at the contact with the sand with thick clay coats	
35.4	10.8	38.2	11.6	2.8	0.9	sand with clay coats: coarse to medium sand with thick clay coats		4	moderately well	subangular to subrounded	5YR 4/6	gradational		thin black bands of manganese oxide, also some larger blotchy stains that makes the sediment very hard and creates a blocky breakage pattern.		

Top Depth (ft)	Top Depth (m)	Basal Depth (ft)	Basal Depth (m)	Thickness (ft)	Thickness (m)	Grain Size	▲ or ▼ ••	Facies	Sorting	Roundness	Color	Basal Contact	Primary Structures	Secondary Alteration	Comments	Driller's Log
38.2	11.6	40.0	12.2	1.8	0.5	sand with thick clay coats: medium to fine sand with medium to thick clay coats		4	moderately well	subangular to subrounded	10YR 4/4	end of core			occassional pebble present; less induration then above due to reduction in MnO alteration	
40.0	12.2	40.4	12.3	0.4	0.1	gravel: granule to pebble 1-4cm diameter		1				sharp			top 6 inches of the barrel are not full, the gravel is loose	
40.4	12.3	43.0	13.1	2.6	0.8	drill mud					10YR 5/4	sharp			medium to fine sand mixed with drill mud	
43.0	13.1	45.0	13.7	2.0	0.6	sand with clay coats: medium to coarse sand with thick clay coats		4			7.5YR 4/6	end of core		heavy metal bands	some finer grains intermixed with the coarser grains	
45.0	13.7	45.2	13.8	0.2	0.1	clay: red clay		4			10YR 4/6	gradational				5" missing: red sand and gravel in the shoe
45.2	13.8	48.0	14.6	2.8	0.9	sand with clay coats: medium to fine sand with thick clay coats		4	well	subangular to subrounded	10YR 4/6	gradational		MnO (especially from 47-49') makes the sedimnets well indurated.	occassional rounded pebble (1-5mm)	
48.0	14.6	50.0	15.2	2.0	0.6	sand with clay coats: medium to coarse sand with thick clay coats		4	moderately well		7.5YR 4/6	end of core		MnO (especially from 47-49') makes the sedimnets well indurated.	more frequent pebbles than above	
50.0	15.2	50.2	15.3	0.2	0.1	sand with clay coats: medium to coarse sand with thick clay coats and gravel at base (1-2cm)		4			7.5YR 4/6	sharp			Top two inches are reddish in color. Gravel composition is chert, quartz, lithics in a sandy clay matrix.	6" missing

Top Depth (ft)	Top Depth (m)	Basal Depth (ft)	Basal Depth (m)	Thickness (ft)	Thickness (m)	Grain Size	▲ or ▼ **	Facies	Sorting	Roundness	Color	Basal Contact	Primary Structures	Secondary Alteration	Comments	Driller's Log
50.2	15.3	51.4	15.7	1.2	0.4	silty sand: medium to fine sand with some silt		3	well		10YR 4/4 overall	sharp	massive	Basal inch of this layer is heavily chemically altered: iron staining and MnO bands of well indurated sand	composition is mostly quartz, feldspar, and muscovite	
51.4	15.7	55.0	16.8	3.6	1.1	silty sand: very fine to fine sand with some silt		3	well- coarser at top and finer at the base		10YR 5/3	end of core	thin millimeter to micormeter laminations	slight iron staining along the laminae (faint orange color); small patches of dark brown to black stains	friable; composition is mostly quartz, feldspar, and muscovite	
55.0	16.8	56.0	17.1	1.0	0.3	silty sand: very fine to fine sand with some silt, coarsens to fine sand at base		3	well	subangular to subrounded	2.5Y 4/3	sharp	massive, friable		composition is mostly quartz, feldspar, and muscovite	
56.0	17.1	57.8	17.6	1.8	0.5	clay: light brown clay		3			10YR 6/3	gradational	thinly laminated (core split along these making them conspicuous)	iron staining in patches and along the laminae	core split into large blocks on each half of the core (well indurated)	
57.8	17.6	58.2	17.7	0.4	0.1	sand: coarse to very coarse		3	well	subangular to subrounded		sharp			clay above grades into about 1 inch of sand	
58.2	17.7	58.6	17.9	0.4	0.1	silty sand: fine to very fine sand with some silt		3	well		2.5Y 4/3	sharp	massive	some dark red iron stains	similar to the above silty sand ▼	

Top Depth (ft)	Top Depth (m)	Basal Depth (ft)	Basal Depth (m)	Thickness (ft)	Thickness (m)	Grain Size	▲ or ▼ **	Facies	Sorting	Roundness	Color	Basal Contact	Primary Structures	Secondary Alteration	Comments	Driller's Log
58.6	17.9	60.0	18.3	1.4	0.4	clay		3			10YR 6/3	end of core	thinly laminated	upper portion has black MnO stains and is well indurate in these areas	breaks blocky especially where MnO staining	
60.0	18.3	60.2	18.4	0.2	0.1	clay: very malleable clay distinctly different than clay below it		3			10YR 6/3	sharp	massive			
60.2	18.4	65.0	19.8	4.8	1.5	clay		3			2.5Y 6/3	end of core	thinly laminated (breaks along laminations)	some dark brown to black	blocky breaks on either side of the core; the clay is the same all of the way down with no secondary alteration visible	
65.0	19.8	65.8	20.1	0.8	0.2	clay: some sporadic silt lenses	▼	3			2.5Y 5/3	gradational	thinly laminated (mm scale--similar to previous core)	slight iron staining		7" missing
65.8	20.1	67.4	20.5	1.6	0.5	clayey silt		3			2.5Y 5/3	gradational	thinly laminated (mm scale--similar to previous core)	more distinct and frequent iron stains; some iron stains in pockets or root traces, while others are along the laminae		
67.4	20.5	68.2	20.8	0.8	0.2	clay: basal three inches of the clay mix with the underlying sand		3			2.5Y 6/3	sharp	thinly laminated (mm scale--similar to previous core)	sheen of dark black MnO stains and heavily iron stained as well; ▼		

Top Depth (ft)	Top Depth (m)	Basal Depth (ft)	Basal Depth (m)	Thickness (ft)	Thickness (m)	Grain Size	▲ or ▼ **	Facies	Sorting	Roundness	Color	Basal Contact	Primary Structures	Secondary Alteration	Comments	Driller's Log
68.2	20.8	69.6	21.2	1.4	0.4	sand: very coarse to coarse sand that fines to a coarse to medium sand at the base		2	well	subangular to subrounded	10YR 5/6	end of core	massive	iron staining that gives the sand a light orange tint; pockets of more heavily, darker iron staining	▼	
69.6	21.2	70.0	21.3	0.4	0.1			0							↓	
70.0	21.3	70.5	21.5	0.5	0.2	sand: medium to coarse sand that coarsesn to coarse to very coarse sand		2	well	subangular to subrounded		sharp/ erosional (some mixing with underlying silt)	massive	no iron staining, but dark brown/black (2.5Y 3/1) staining at the contact with underlying silty sand	▲	43" missing: gravel in the shoe
70.5	21.5	70.7	21.6	0.2	0.1	silty sand		3			2.5Y 4/3	sharp	thinly laminated	iron staining in root traces throughout; pockets of dark iron staining along basal contact with yellowish clay		
70.7	21.6	71.0	21.6	0.3	0.1	clay		3			2.5Y 6/3 (yellowish)	sharp	none visible			
71.0	21.6	71.2	21.7	0.2	0.1	clay		3			2.5Y 6/3	mixing	thinly laminated			
71.2	21.7	71.4	21.8	0.2	0.1	sand mixed with clay:very coarse to coarse sand with some gravel mixed with		2	moderately to poorly	subangular to subrounded		end of core		dark iron staining throughout	lasy 1" of the core is sand	

Top Depth (ft)	Top Depth (m)	Basal Depth (ft)	Basal Depth (m)	Thickness (ft)	Thickness (m)	Grain Size	▲ or ▼ **	Facies	Sorting	Roundness	Color	Basal Contact	Primary Structures	Secondary Alteration	Comments	Driller's Log
						overlying clay										
71.4	21.8	75.0	22.9	3.6	1.1			0								
75.0	22.9	77.9	23.8	2.9	0.9	silty clay:silt fraction increases from 76' to 77' then decreases toward 77.9'	▲ ▼	3			2.5Y 4/4	sharp		some iron staining near the base	white filaments (2.5Y 8/2) generally arranged in a horizontal linear pattern, no reaction with HCl	15" missing
77.9	23.8	78.9	24.1	1.0	0.3	clayey silt		3			2.5Y 4/3	end of core		well indurated in top 1-2" (breaks blocky) but no color staining.		
78.9	24.1	80.0	24.4	1.1	0.3			0								
80.0	24.4	81.2	24.8	1.2	0.4	silty clay	▲	3			2.5Y 4/4	sharp	massive	root traces, one large crack with white mineral fill, faint iron stains,		7" missing: sandy at the bottom of shoe
81.2	24.8	82.5	25.2	1.3	0.4	silt: becomes more sandy with depth		3			2.5Y 4/3	sharp	massive	very faint blotchy iron stains		

Top Depth (ft)	Top Depth (m)	Basal Depth (ft)	Basal Depth (m)	Thickness (ft)	Thickness (m)	Grain Size	▲ or ▼ **	Facies	Sorting	Roundness	Color	Basal Contact	Primary Structures	Secondary Alteration	Comments	Driller's Log
82.5	25.2	83.4	25.4	0.9	0.3	silty sand: very fine sand to silt		3	well	subangular to subrounded	2.5Y 4/2	sharp	dark black heavy mineral banding along horizontal beds			
83.4	25.4	84.6	25.8	1.2	0.4	sand: medium to fine sand		3	well	subangular to subrounded	overall 2.5Y 5/2	end of core	massive	90% quartz, feldspar, lithics, muscovite		
84.6	25.8	85.0	25.9	0.4	0.1			0								
85.0	25.9	89.8	27.4	4.8	1.5	sand: medium sand coarsens into medium to coarse sand which coarsens into coarse to very coarse sand	▲	2	well	subangular to subrounded	overall 2.5Y 6/2	entire core	massive, some heavy mineral banding, and patches of fining (at 86' approximately 2" of finer material) .			3" missing sandy fresh mica in shoe
90.0	27.4	90.8	27.7	0.8	0.2	drill mud mixed with coarse to very coarse sand		0								6" missing: fine sand in shoe
90.8	27.7	92.8	28.3	2.0	0.6	sand: coarse to very coarse sand and coarsens to very coarse sand toward the base.	▲	2	well	subangular to subrounded	overall 2.5Y 4/2	sharp	thin clay beds near the top of the sand	at 91.7' there is a block of sand that is indurated (made obvious by blocky break).		

Top Depth (ft)	Top Depth (m)	Basal Depth (ft)	Basal Depth (m)	Thickness (ft)	Thickness (m)	Grain Size	▲ or ▼ **	Facies	Sorting	Roundness	Color	Basal Contact	Primary Structures	Secondary Alteration	Comments	Driller's Log
92.8	28.3	94.3	28.8	1.5	0.5	silt: silt with very fine sand, clay content increases toward the base	▼	3			2.5Y 4/2 with bands of 2.5Y 5/2	gradational	massive	sporadic iron stains, small root traces/bioturbation		
94.3	28.8	94.6	28.8	0.3	0.1	clayey silt		3			2.5Y 4/2	end of core	massive	none visible (too thin)		
94.6	28.8	95.0	29.0	0.4	0.1			0								
95.0	29.0	95.1	29.0	0.1	0.0	sand: medium to fine sand		3			2.5Y 5/3	sharp	massive--thin unit	faint iron staining and root traces		full core
95.1	29.0	95.3	29.1	0.2	0.1	silt	▼	3			2.5Y 5/3	sharp	heavy mineral bands	faint iron staining and root traces		
95.3	29.1	95.5	29.1	0.2	0.1	clay		3			2.5Y 5/3	sharp	massive	faint iron staining and root traces		
95.5	29.1	96.8	29.5	1.3	0.4	sandy silt:sandy silt grades to medium to fine sand then back to sandy silt		3			2.5Y 4/2	gradational				
96.8	29.5	97.0	29.6	0.2	0.1	silt		3			2.5Y 4/2	sharp				
97.0	29.6	98.4	30.0	1.4	0.4	clay		3			10YR 5/3	sharp	thin laminations, heavy mineral banding	breaks blocky		
98.4	30.0	99.3	30.3	0.9	0.3	sand: medium to fine sand grades to medium sand	▲	2			overall 10YR 6/2	sharp				

Top Depth (ft)	Top Depth (m)	Basal Depth (ft)	Basal Depth (m)	Thickness (ft)	Thickness (m)	Grain Size	▲ or ▼ **	Facies	Sorting	Roundness	Color	Basal Contact	Primary Structures	Secondary Alteration	Comments	Driller's Log
99.3	30.3	100.0	30.5	0.7	0.2	clay		3			10YR 5/3	end of core	massive	some black mottling (MnO), and breaks in a blocky pattern.		
100.0	30.5	102.0	31.1	2.0	0.6	clay		3			10YR 5/3	gradational	massive, thin (2-3") silt layer at 101' (10YR 4/3)	MnO filled root traces/ burrows		
102.0	31.1	102.5	31.3	0.5	0.2	silt: silt coarsens to fine sand	▲	3			2.5Y 4/2	gradational				
102.5	31.3	103.0	31.4	0.5	0.2	sand: medium to fine sand		2			overall 2.5Y 6/2	sharp	cross-stratified, heavy mineral bands along the cross-strata		quartz, feldspar and mica	8" missing, fresh mica in shoe
103.0	31.4	104.4	31.8	1.4	0.4	silty sand: silt with some fine sand	▲	3			2.5Y 4/3	end of core	heavy mineral banding			
104.4	31.8	105.0	32.0	0.6	0.2			0								
105.0	32.0	106.2	32.4	1.2	0.4	clay		3			10YR 5/3	gradational	massive	some root traces filled with iron stains, some filled with MnO (black mineral)		4" missing
106.2	32.4	108.1	33.0	1.9	0.6	clayey silt: can roll into a stringer, but mostly gritty		3			10YR 4/3	gradational	massive	faint mottled iron staining		

Top Depth (ft)	Top Depth (m)	Basal Depth (ft)	Basal Depth (m)	Thickness (ft)	Thickness (m)	Grain Size	▲ or ▼ **	Facies	Sorting	Roundness	Color	Basal Contact	Primary Structures	Secondary Alteration	Comments	Driller's Log
108.1	33.0	109.7	33.4	1.6	0.5	clay		3			10YR 5/3	end of core	massive	some iron staining but no visible black mineral		
109.7	33.4	110.0	33.5	0.3	0.1			0								
110.0	33.5	111.2	33.9	1.2	0.4	clay		3			10YR 5/4	sharp	massive	some black mineral stains, root traces near the top of the core; some coarse sand mixed in near basal contact with very fine sand; faint orange mottling		5" missing clay and sand contact in shoe
111.2	33.9	112.6	34.3	1.4	0.4	silty sand: very fine sand with some silt		3			10YR 5/3	gradational	massive, thin band o fmedium to coarse sand at 111.4'	faint orange mottling		
112.6	34.3	113.3	34.5	0.7	0.2	silt grades to clayey silt then to clay		3			10YR 5/3	sharp	massive	cracks/ root traces infilled with black mineral; faint orange mottling		

Top Depth (ft)	Top Depth (m)	Basal Depth (ft)	Basal Depth (m)	Thickness (ft)	Thickness (m)	Grain Size	▲ or ▼ **	Facies	Sorting	Roundness	Color	Basal Contact	Primary Structures	Secondary Alteration	Comments	Driller's Log
113.3	34.5	113.8	34.7	0.5	0.2	silt: has some thin clay bands sporadically		3			10YR 5/3	sharp	1" band of medium to coarse sand at 113.6', about 1.5" of silt below the sand layer that is the sharp contact with the underlying sand	faint orange mottling		
113.8	34.7	115.0	35.1	1.2	0.4	sand: medium to coarse		2	well	subangular to subrounded		end of core	massive	composition of mostly quartz, feldspar, mica		
115.0	35.1	115.5	35.2	0.5	0.2	silty clay: clay with some silt		3			10YR 4/3	sharp	massive	some root traces/burrows, breaks blocky		5" missing: coarse sand with pebbles in shoe
115.5	35.2	116.3	35.5	0.8	0.2	sand: medium to coarse sand		2			overall 10YR 6/2	sharp	massive with two distinct clay bands (at 115.9' and 116.1') and some heavy mineral banding			
116.3	35.5	116.7	35.6	0.4	0.1	silty sand: very fine sand with some silt		3			10YR 5/3	sharp	massive			

Top Depth (ft)	Top Depth (m)	Basal Depth (ft)	Basal Depth (m)	Thickness (ft)	Thickness (m)	Grain Size	▲ or ▼ **	Facies	Sorting	Roundness	Color	Basal Contact	Primary Structures	Secondary Alteration	Comments	Driller's Log
116.7	35.6	119.4	36.4	2.7	0.8	clay: some isolated silt lenses		3			10YR 5/3 transitions to 7.5YR 5/3	sharp/erosional	massive	heavy iron stains in root traces/burrows mostly at base of the clay; heavy iron stains also at basal contact with very coarse gravelly sand		
119.4	36.4	119.6	36.5	0.2	0.1	sand: very coarse to coarse gravelly sand		2	moderately	subangular to subrounded	overall 10YR 4/6	end of core	massive	distinct orange tint, heavily iron stained throughout	lithology similar to sands above	
119.6	36.5	120.0	36.6	0.4	0.1			0								
120.0	36.6	122.5	37.3	2.5	0.8	clay		3			10YR 5/3	gradational	massive	faint iron stained root traces; sporadic MnO stains		4" missing: clay in shoe
122.5	37.3	124.0	37.8	1.5	0.5	silty clay: clay with some silt; looks fuzzy/furry		3			10YR 5/3	gradational	thinly laminated	more heavy blotches of iron staining; sporadic MnO stains		
124.0	37.8	124.9	38.1	0.9	0.3	clay: band of coarse to very coarse sand sand at 124.6' that is about an inch thick		3			10YR 5/3	end of core	massive	faint iron stained root traces; band of sand within the clay is heaviy iron stained; sporadic MnO stains		
124.9	38.1	125.0	38.1	0.1	0.0			0								

Top Depth (ft)	Top Depth (m)	Basal Depth (ft)	Basal Depth (m)	Thickness (ft)	Thickness (m)	Grain Size	▲ or ▼	Facies	Sorting	Roundness	Color	Basal Contact	Primary Structures	Secondary Alteration	Comments	Driller's Log
125.0	38.1	128.9	39.3	3.9	1.2	clay		3			10YR 5/4	gradational	mostly massive; breakage pattern indicates thin laminations from ~126-128'	mottled iron staining at the top, MnO in root traces, heavy MnO from 126.5' to 129.5'	at 125.6' there is a thin 0.25" band of off white clay--ash? alteration?	full recovery, hard clay in shoe, possible root traces
128.9	39.3	130.0	39.6	1.1	0.3	silty clay: silt fraction increases towards the base of the core		3			10YR 5/3	end of core	massive	blotches of heavy iron staining in bottom 0.5' as the clay becomes more silty; root traces		
130.0	39.6	131.3	40.0	1.3	0.4	clayey silt: some bands of silt to very fine sand		3			10YR 5/3 to 10YR 4/3	sharp	massive	blotchy iron staining, some dark mineral concetrations		9.5" missing: coarse sand with pebbles in shoe
131.3	40.0	132.0	40.2	0.7	0.2	silt interbedded with sand: 1" beds of silt and very fine sand		3				gradational	cross-bedded	faint orange tint, noticably less iron stained than over and underlying sediments	lots of mica visible	

Top Depth (ft)	Top Depth (m)	Basal Depth (ft)	Basal Depth (m)	Thickness (ft)	Thickness (m)	Grain Size	▲ or ▼ **	Facies	Sorting	Roundness	Color	Basal Contact	Primary Structures	Secondary Alteration	Comments	Driller's Log
132.0	40.2	133.6	40.7	1.6	0.5	sand: medium to fine; some silt		3	well	subangular to subrounded		gradational	cross-bedded	heavily iron stained near the top of the sand with dark black/brown staining along cross-bed planes, sand is also stained a deep burt orange		
133.6	40.7	134.0	40.9	0.4	0.1	sand: coarse to very coarse; some silt		2	well	subangular to subrounded		gradational	massive, band of pebbles and very coarse sand at 133.3'	some iron staining, but not as dark as sands above		
134.0	40.9	134.4	41.0	0.4	0.1	sand: very coarse to pebbly sand, some areas more pebbly than others; pebbles generally 1-2mm diameter (1cm max); some silt		2	moderately	subangular to subrounded		end of core	massive	faint orange tint		
134.4	41.0	135.0	41.2	0.6	0.2			0								
135.0	41.2	135.5	41.3	0.5	0.2	sand: very coarse to pebbly sand, some areas more pebbly than others; pebbles generally 1-2mm diameter; some silt		2	moderately	sand: subangular to subrounded Pebbles: subrounded to rounded	overall 10YR 4/2 at top to 4/3 at the bottom	gradational	massive			11.5" missing: medium to coarse sand in shoe

Top Depth (ft)	Top Depth (m)	Basal Depth (ft)	Basal Depth (m)	Thickness (ft)	Thickness (m)	Grain Size	▲ or ▼ **	Facies	Sorting	Roundness	Color	Basal Contact	Primary Structures	Secondary Alteration	Comments	Driller's Log
135.5	41.3	136.3	41.6	0.8	0.2	sand: coarse to very coarse; some silt		2	well			gradational	massive			
136.3	41.6	138.6	42.3	2.3	0.7	sand: medium to coarse; some silt		2	well	subangular to subrounded		sharp	massive	heavily iron stained bands at contact; dark black and burnt orange stained		
138.6	42.3	139.0	42.4	0.4	0.1	sand: medium to fine, some silt		3	well	subangular to subrounded		end of core	massive		more silt in basal sands than at the tp of the core	
139.0	42.4	140.0	42.7	1.0	0.3			0								
140.0	42.7	140.2	42.7	0.2	0.1	sandy silt: silty very fine sand with thin clay layer at base		3			10YR 5/3	sharp	thin unit		drill mud? 3" very fine silty sand with 1" very malleable light brown clay layer below	8" missing: coarse sand at bottom of shoe fining to medium coarse sand at top of shoe
140.2	42.7	141.5	43.1	1.3	0.4	sand: coarse to very coars sand with pebbles		2				gradational			pebbles are subround to round ~1-2 cm diameter	
141.5	43.1	144.5	44.1	3.0	0.9	sand: coarse to very coarse and fines to coarse sand at the bottom	▼	2	moderately well	subangular to subrounded	10 YR 5/3	end core	thin bands of silt and clayey silt		occassional bands of silt and clayey silt , heavy mineral bands, green minerals throughout , still mostly quartz and feldspar	
144.5	44.1	145.0	44.2	0.5	0.2			0								
145.0	44.2	145.4	44.3	0.4	0.1	sand; very coarse sand mixed with pebbles and some clay (drill mud) that fines to coarse and		2	moderately to poor	subangular to subrounded	10 YR 4/3	sand mixes with clay below			this unit is about the top 5" of the core, fines downward	

Top Depth (ft)	Top Depth (m)	Basal Depth (ft)	Basal Depth (m)	Thickness (ft)	Thickness (m)	Grain Size	▲ or ▼	Facies	Sorting	Roundness	Color	Basal Contact	Primary Structures	Secondary Alteration	Comments	Driller's Log
						then medium sand										
145.4	44.3	146.0	44.5	0.6	0.2	clay: reddish brown clay with medium to coarse sand		3			5 YR 5/3 (reddish brown) to 5 YR 5/4 (pinkish brown)	sharp		146' root traces and iron stains in the clay	very hard	
146.0	44.5	147.5	45.0	1.5	0.5	sand with clay coats: coarse to medium sand with thick clay coats		4?				sharp	massive	root traces filled with black mineral, larger cracks have an off-white colored fill		

Top Depth (ft)	Top Depth (m)	Basal Depth (ft)	Basal Depth (m)	Thickness (ft)	Thickness (m)	Grain Size	▲ or ▼ **	Facies	Sorting	Roundness	Color	Basal Contact	Primary Structures	Secondary Alteration	Comments	Driller's Log
147.5	45.0	149.0	45.4	1.5	0.5	ash layer???		as h			varies (see coomen ts) dark burnt orange: 5YR 5/6 light orange: 5YR 6/6 light brown lenses: 10YR 6/2 off-white: 2.5Y 7/3 dark brown: 10YR 4/3	Sharp / erosional (irregular)			147.6' looks like insitu weathered granite. This layer is ~1' section with ~2" sections of the following: (1) yellow to off white clay with burt orange clay (2.5YR 6/3) with MnO staining. (2) sharp contact with very hard brown (10YR 4/3) clay with MnO filaments (3) sharp contct with peach (7.5 YR 5/6) clay containing lenses of light brown clay (4) sharp contact back to burnt orange (5YR 5/6) clay with MnO stains and patches of yellow to offwhite clay (2.5 Y 7/3) (5) gradual change to light orange or peach colored clay with bands of heavy minerals and some silt	full recovery, clay in shoe
149.0	45.4	150.0	45.7	1.0	0.3	clay: light brown clay grades to silt with very fine sand		3			10YR 6/2 to 10YR 5/2	end core	massive		contains a band of fadded yellowish clay	
150.0	45.7	150.8	46.0	0.8	0.2	clay: light green brown to gray brown clay		3			2.5Y 6/2	sharp	massive	some pinkish red thin layers (iron stains)	very soft	12" missing: sand in the shoe

Top Depth (ft)	Top Depth (m)	Basal Depth (ft)	Basal Depth (m)	Thickness (ft)	Thickness (m)	Grain Size	▲ or ▼ **	Facies	Sorting	Roundness	Color	Basal Contact	Primary Structures	Secondary Alteration	Comments	Driller's Log
150.8	46.0	153.5	46.8	2.7	0.8	sand: very fine to fine sand coarsesn to medium sand with layers of clayey fine sand to silt		3	well	subangular to subrounded	2.5 Y 5/2 (sily areas)	sharp	thin layers of claye fine sand to silt	iron staining around the layers of fines. Heavy mineral banding.	very micaceous! Glittery look.	
153.5	46.8	154.0	47.0	0.5	0.2	sand: medium to coarse sand		2	well	subangular to subrounded		end core		heavy mineral banding and iron staining	composition similar to previous sands (no green mineral)	
154.0	47.0	155.0	47.3	1.0	0.3			0								
155.0	47.3	155.3	47.3	0.3	0.1	clayey silt		3			2.5Y 4/2			mineral banding	u-shaped from drilling?	
155.3	47.3	157.0	47.9	1.7	0.5	sand: very fine sand to silt coarsens to medium to fine sand	▲	3	well	subangular to subrounded		gradational	medium to fine sand is massive. Medium to coarse sand is cross-stratified	heavily iron satined, heavy mineral banding	increase in muscovite creates glittery sheen	
157.0	47.9	158.2	48.2	1.2	0.4	silt: very fine sand grades to silt		3			2.5 Y 5/3	gradational	massive	iron staining		
158.2	48.2	158.6	48.4	0.4	0.1	clay: medium brown clay	▼	3			2.5 Y 4/3	sharp	massive	iron staining and MnO stains	hard	
158.6	48.4	159.2	48.5	0.6	0.2	sand: coarse to medium sand	▼	2	well	subangular to subrounded		end core	cross-stratified	heavy iron staining at contact, heavy mineral banding	quartz, feldspar, not as much mica as in upper portions of this core, more similar amount to sands stratigraphically higher in the core	
159.2	48.5	160.0	48.8	0.8	0.2			0								

Top Depth (ft)	Top Depth (m)	Basal Depth (ft)	Basal Depth (m)	Thickness (ft)	Thickness (m)	Grain Size	▲ or ▼ ··	Facies	Sorting	Roundness	Color	Basal Contact	Primary Structures	Secondary Alteration	Comments	Driller's Log
160.0	48.8	162.1	49.4	2.1	0.6	sand: medium to coarse sand	▲	2	well	subangular to subrounded		gradational	cross-stratified	iron stained, heavy mineral bands	quartz, feldspar, muscovite, lithics, chert	8" missing: I measured with measuring tape
162.1	49.4	163.5	49.8	1.4	0.4	sand: coarse to very coarse sand	▲	2	well	subangular to subrounded		sharp	cross-stratified	iron stained, heavy mineral bands	quartz, feldspar, muscovite, lithics, chert	
163.5	49.8	163.7	49.9	0.2	0.1	sandy silt: medium brown silt to very fine sand		4			10YR 4/3	sharp	massive			
163.7	49.9	164.4	50.1	0.7	0.2	clay: clay with some silt		4			10YR 5/3	end core	massive	patches of iron and MnO stains	light brown to pink brown clay , very hard	
164.4	50.1	165.0	50.3	0.6	0.2			0								
165.0	50.3	167.8	51.2	2.8	0.9	sand with clay coats: medium to fine sand with thick clay coats coarsens to medium to coarse sand / clay coats thin toward the base		4			5YR 4/6 (brown to dark rust red)	gradational	massive	MnO staining, root traces, clay filled cracks/root traces near the basal contact where clay coats thin	at 167' there are thin clay intervals or lenses. 2mm clay filled fracture near base	full recovery hard clay in shoe--possible root traces
167.8	51.2	169.3	51.6	1.5	0.5	silty sand: silty fine sand		4			10YR 4/4 (orangis h brown)	sharp	massive	clay fill root traces, MnO staining		
169.3	51.6	170.0	51.8	0.7	0.2	clay		4			10YR 4/3 (mediu m orange brown)	end core	laminated	burrow/root traces, mottle faint iron staining	hard	

Top Depth (ft)	Top Depth (m)	Basal Depth (ft)	Basal Depth (m)	Thickness (ft)	Thickness (m)	Grain Size	▲ or ▼ ⁚	Facies	Sorting	Roundness	Color	Basal Contact	Primary Structures	Secondary Alteration	Comments	Driller's Log
170.0	51.8	171.0	52.1	1.0	0.3	clay		4			10YR 5/3 (light to medium brown) grades to 10YR 4/3 (dark brown)	sharp	massive	cracks or root traces filled with light orange stained clay. Mottled iron staining and some MnO staining	hard	15" missing: reddish coarse sand with pebbles in the shoe, very muddy core, may have removed too little
171.0	52.1	171.5	52.3	0.5	0.2	sand with clay coats: medium to very coarse sand with thick clay coats		4			7.5YR 4/6	sharp		heavily iron stained, root traces, heavy MnO stains near the basal contact.		
171.5	52.3	172.4	52.6	0.9	0.3	clay		4			10YR 5/3 (mediu m brown)	sharp	laminated	heavily iron stained, root traces		
172.4	52.6	173.7	53.0	1.3	0.4	sand with clay coats: coarse to very coarse sandand some pebbles (1cm diameter) with thick clay coats		4			7.5 YR 4/6	end core			clay coats are thicker here than they were above in the core.	
173.7	53.0	175.0	53.4	1.3	0.4			0								

Top Depth (ft)	Top Depth (m)	Basal Depth (ft)	Basal Depth (m)	Thickness (ft)	Thickness (m)	Grain Size	▲ or ▼ ⠒	Facies	Sorting	Roundness	Color	Basal Contact	Primary Structures	Secondary Alteration	Comments	Driller's Log
175.0	53.4	176.7	53.9	1.7	0.5	sand with pebbles: coarse to very coarse sand with some gravel and pebbles		4?	poorly	subangular to subrounded	10YR 5/3 ish	end core			core is wet, not cohesive, was reworked, looks like clay coated or mixed with orangish clay	179 stoped coring, very hard sandy clay in the shoe-- core stuck in barrel, compressed 6", limited recovery in two tubes
176.7	53.9	176.9	53.9	0.2	0.1	sand: very coarse to medium		4?	poorly	subangular to subrounded		break in core		iron staining, MnO staining	small 1" chunk remained coherent by MnO staining, 1" of loose sand above it, next 9" are empty	
176.9	53.9	177.7	54.2	0.8	0.2			0								
177.7	54.2	178.7	54.5	1.0	0.3	sand: medium to very coarse sand mixed with clay and some pebbles		4?	poorly			sharp	cross-stratified	heavy mineral banding	1" of sand then grades to 3" of pebbles (1-2 cm) between two 1" bands of pebbly sand	
178.7	54.5	178.9	54.5	0.2	0.1	clay		4?			10YR 5/3 with some pinkish (7.5YR 5/6)	end core		faint iron staining	medium brown hard clay	
178.9	54.5	180.0	54.9	1.1	0.3			0								

Top Depth (ft)	Top Depth (m)	Basal Depth (ft)	Basal Depth (m)	Thickness (ft)	Thickness (m)	Grain Size	▲ or ▼ **	Facies	Sorting	Roundness	Color	Basal Contact	Primary Structures	Secondary Alteration	Comments	Driller's Log
180.0	54.9	181.0	55.2	1.0	0.3	silty clayey sand: medium to coarse sand with thick to thin clay coats		4?	moderately well	subangular to subrounded	10YR 4/3	gradational	massive		clay coating decreses with depth	
181.0	55.2	182.6	55.7	1.6	0.5	sand: coarse to very coarse	▲	2	moderately well	subangular to subrounded		gradational	massive	elongate burrows? Filled with dark mineral (MnO)	quartz dominated, green mineral present but no abundant	
182.6	55.7	184.2	56.2	1.6	0.5	sand: coarse to medium that coarsens to a coarse sand	▲	2	moderately well to well	subangular to subrounded		end of core	massive	non visible		
184.2	56.2	185.0	56.4	0.8	0.2	coarse sand in shoe, top of core may be cemented		0								
185.0	56.4	188.5	57.5	3.5	1.1	sand: medium to coarse sand		2	moderately well transitions to moderately	subangular to subrounded		gradational	massive, no heavy mineral bands	faint iron staining	darker sand compared to sand units near the top of the core; mostly quartz, and some feldspar, muscovite, lithics	
188.5	57.5	189.1	57.7	0.6	0.2	sand: medium		2	well	subangular to subrounded		end of core	massive, no heavy mineral bands	faint iron staining	darker sand compared to sand units near the top of the core; mostly quartz, and some feldspar, muscovite, lithics	
189.1	57.7	190.0	57.9	0.9	0.3	coarse sand in shoe		0								

Top Depth (ft)	Top Depth (m)	Basal Depth (ft)	Basal Depth (m)	Thickness (ft)	Thickness (m)	Grain Size	▲ or ▼ **	Facies	Sorting	Roundness	Color	Basal Contact	Primary Structures	Secondary Alteration	Comments	Driller's Log
190.0	57.9	192.8	58.8	2.8	0.9	sand: medium to coarse sand grades to coarse to very coarse sand		2	well to moderately	subangular to subrounded		sharp, heavily iron stained contact	massive	dark iron staining especially in the coarse to very coarse sand	occassional piece of gravel (~1-2 cm but 2cm max)	
192.8	58.8	193.7	59.1	0.9	0.3	sand: medium to coarse sand		2	well	subangular to subrounded		end of core				
193.7	59.1	195.0	59.5	1.3	0.4	coarse sand in shoe		0								
195.0	59.5	200.0	61.0	5.0	1.5	No recovery: sand in the shoe		0								
200.0	61.0	204.3	62.3	4.3	1.3	sand: medium to coarse sand coarsens to coarse sand; band of gravel at 61m (201')	▲	2	moderately to moderately well	subangular to subrounded		end of core	massive		90% quartz, feldspar, lithics, muscovite, reddish brown mineral (breaks easily); occassional pebbles	
204.3	62.3	205.0	62.5	0.7	0.2			0								
205.0	62.5	207.0	63.1	2.0	0.6	sand: coarse to very coarse sand; some bands of increased silt/clay content; band of gravel at base		2	moderately to moderately well	subangular to subrounded		end of core	massive		same composition as in previous core only muscovite is more abundant	
207.0	63.1	210.0	64.0	3.0	0.9			0								
210.0	64.0	212.5	64.8	2.5	0.8	clayey sand: medium to coarse sand mixed with clay (drill mud)		3	moderately to poorly	subangular to subrounded	clay- 10YR 5/2	gradational	massive		possibly drilling mud mixed in with the sand.	

Top Depth (ft)	Top Depth (m)	Basal Depth (ft)	Basal Depth (m)	Thickness (ft)	Thickness (m)	Grain Size	▲ or ▼	Facies	Sorting	Roundness	Color	Basal Contact	Primary Structures	Secondary Alteration	Comments	Driller's Log
212.5	64.8	213.0	64.9	0.5	0.2	sand: medium to very coarse sand		2	moderately	subangular to subrounded		gradational	massive		overall darker color, possibly large fraction of lithics.	
213.0	64.9	213.4	65.1	0.4	0.1	gravel: granule with occassional pebble mixed in near the base (<1 cm diameter)		1	moderately	subangular to subrounded		end of core	massive		overall darker color compared to overlying finer sands, similar composition possibly larger fraction of lithics.	
213.4	65.1	215.0	65.5	1.6	0.5	213.5' to 217' no recovery other than shoe, coarse sand contact with clay. Previous core must have fallen and is recovered. Clay in shoe full liner so there must be extra from previous push.		0								
215.0	65.5	215.5	65.7	0.5	0.2	clayey sand: coarse to very coarse sand mixed with clay		3			10YR 5/2	sharp	massive		mixed from trouble recovering core	
215.5	65.7	218.0	66.5	2.5	0.8	clay: some silt mixed in towards the base		3			10YR 4/3	gradational	laminated in some areas, breaks in blocks so may be massive in areas	iron stains throughout		

Top Depth (ft)	Top Depth (m)	Basal Depth (ft)	Basal Depth (m)	Thickness (ft)	Thickness (m)	Grain Size	▲ or ▼ **	Facies	Sorting	Roundness	Color	Basal Contact	Primary Structures	Secondary Alteration	Comments	Driller's Log
218.0	66.5	220.0	67.1	2.0	0.6	silty clay to clayey silt: amount of silt increases towards the base		3			10YR 4/3	end of core	massive	iron stains throughout, some iron staining in bands, root traces		
220.0	67.1	221.1	67.4	1.1	0.3	clay: some silt mixed in (very little) and a few coarse sand grains mixed in		3? 4?			10 YR 5/3 (looks a little pink/mauve)	sharp	massive	few iron stains	some filaments filled with off-white colored material (clay) near the edge of the core	
221.1	67.4	221.8	67.6	0.7	0.2	sandy clayey silt: sandy silt with some clay, clay content increases with depth to a thin clay layer at the base		3? 4?			10YR 4/3 (becomes more pink tinted as clay content increases)	sharp	massive	a few blotchy iron stains		
221.8	67.6	223.3	68.1	1.5	0.5	sand with clay coats: fine to very fine sand with medium clay coats		3? 4?			10YR 4/4		very thin clay beds (~1mm thick near the base)	iron stained through out		
223.3	68.1	225.0	68.6	1.7	0.5			0								
225.0	68.6	225.9	68.9	0.9	0.3	sand: medium to fine sand with a band of medium sand		3	moderately well	subangular to subrounded		sharp	massive	bands of faint iron staining in the band of medium grained sand	composition is still quartz dominated with feldspar, lithics, and a reddish mineral (too small to identify)	

Top Depth (ft)	Top Depth (m)	Basal Depth (ft)	Basal Depth (m)	Thickness (ft)	Thickness (m)	Grain Size	▲ or ▼ **	Facies	Sorting	Roundness	Color	Basal Contact	Primary Structures	Secondary Alteration	Comments	Driller's Log
225.9	68.9	228.2	69.6	2.3	0.7	gravel: coarse to very coarse sand and granule matrix supporting pebbles (1-4cm), amount of pebbles decreases with depth		1	poorly	matrix: subangular to subrounded pebbles: rounded to well rounded		end of core	massive	increase in iron staining at the base		
228.2	69.6	230.0	70.1	1.8	0.5	gravel in shoe, well rounded and matrix supported		0								
230.0	70.1	230.4	70.2	0.4	0.1	gravel/pebbles: gravel (<1cm) and pebbles (1-2cm) mixed with drill mud		1	poorly	subrounded to rounded		sharp			coated in drill mud with some sand grains, likely the sand supported gravel from above mixed with drilling mud	
230.4	70.2	231.6	70.6	1.2	0.4	sand: matrix supported pebbles (1-2cm), the matrix is fine to coarse with occassional matrix supported pebbles. Fines to a fine to coarse sand just below a band of pebbles at 70.7m (232')		2	poorly	matrix: subangular to subrounded pebbles: rounded to well rounded		sharp	some coarser pebble bands , but otherwise appears massive	iron staining especially prominent in areas with pebbles, also some black stains (MnO)		

Top Depth (ft)	Top Depth (m)	Basal Depth (ft)	Basal Depth (m)	Thickness (ft)	Thickness (m)	Grain Size	▲ or ▼ ••	Facies	Sorting	Roundness	Color	Basal Contact	Primary Structures	Secondary Alteration	Comments	Driller's Log
231.6	70.6	232.3	70.8	0.7	0.2	gravel: matrix supported pebbles (1-4cm) that interchange with bands of coarse to very coarse sand		1	poorly	matrix: subangular to subrounded pebbles: rounded to well rounded		sharp	massive	iron staining especially prominent in areas with pebbles, also some black stains (MnO)		
232.3	70.8	233.4	71.2	1.1	0.3	gravel: clast supported pebbles, very little matrix		1	poorly	subrounded to rounded		gradational	massive	iron staining especially prominent in areas with pebbles, also some black stains (MnO)	cobble (5cm diameter at 71 m (233')	
233.4	71.2	233.8	71.3	0.4	0.1	sand: coarse to very coarse		2	moderately	subangular to subrounded		end of core	massive	iron staining especially prominent in areas with pebbles, also some black stains (MnO)		
233.8	71.3	234.2	71.4	0.4	0.1	sand: coarse to very coarse sand, some coarser granules		2	moderately	subangular to subrounded		gradtaional	massive	none visible	visibly less quartz, more lithics give the unit and overall darker appearance, less mica visible	
234.2	71.4	234.8	71.6	0.6	0.2	gravel: fine gravel or granules, clast supported		1	moderatly to moderately well	angular to subangular, some are subrounded		end of core	massive		visibly less quartz, more lithics give the unit and overall darker appearance, less mica visible	
234.8	71.6	255.0	77.7	20.2	6.2	missing--no recovery		0								

Top Depth (ft)	Top Depth (m)	Basal Depth (ft)	Basal Depth (m)	Thickness (ft)	Thickness (m)	Grain Size	▲ or ▼ **	Facies	Sorting	Roundness	Color	Basal Contact	Primary Structures	Secondary Alteration	Comments	Driller's Log
255.0	77.7	259.6	79.1	4.6	1.4	sandy, clayey silt: silty sand to clayey silt grades to silty medium to fine sand, silt and clay increase with depth (from 78 m or 256')		3? 4?			10YR 4/4 transitions to 4/3	end of core	thinly laminated from 78 to 78.4m (256-257'), the rest of the core is massive	faint iron staining throughout with some root traces, heavily iron stained at contact were clay content increases 78m (256')		
259.6	79.1	260.0	79.3	0.4	0.1			0								
260.0	79.3	260.4	79.4	0.4	0.1	gravel: matrix supported pebbles (1-3cm) mixed with some drill mud, matrix sands are very coarse to medium		1	poorly	pebbles: well rounded to subrounded matrix: subangular to subrounded		sharp	massive	faint iron staining		
260.4	79.4	261.2	79.6	0.8	0.2	sand: silty sand to coarse to medium sand	▲	2	moderatley well	subangular to subrounded		sharp	cross-stratified	faint iron staining	compositions still shows and increase in lithics compared to upper sands (~80% quartz, feldspars, and more lithics than previously)	
261.2	79.6	261.6	79.8	0.4	0.1	gravel: matrix supported pebbles (1-3cm), matrix sands are very coarse to medium		1	poorly	pebbles: well rounded to subrounded matrix: subangular to subrounded		sharp	massive	faint iron staining		

Top Depth (ft)	Top Depth (m)	Basal Depth (ft)	Basal Depth (m)	Thickness (ft)	Thickness (m)	Grain Size	▲ or ▼ **	Facies	Sorting	Roundness	Color	Basal Contact	Primary Structures	Secondary Alteration	Comments	Driller's Log
261.6	79.8	262.0	79.9	0.4	0.1	sand: medium to coarse sand		2	moderatley well	subangular to subrounded		sharp	massive	faint iron staining	compositions still shows and increase in lithics compared to upper sands (~80% quartz, feldspars, and more lithics than previously)	
262.0	79.9	262.3	80.0	0.3	0.1	gravel: matrix supported pebbles (1-3cm), matrix sands are very coarse to medium		1		pebbles: well rounded to subrounded matrix: subangular to subrounded		sharp	massive	dark black stain near the basal contact		
262.3	80.0	265.0	80.8	2.7	0.8	silty sand: sandy silt transitions to silty sand (silt decreases with depth)		3			10YR 4/3	end of core	massive	iron staining and some root traces	very hard, well indurated (all of the core is in one half of the barrel)	
265.0	80.8	266.6	81.3	1.6	0.5	silty sand: medium to fine silty sand		3	moderately well	subrounded to rounded	overall 10YR 4/4	gradational	thinly laminated	faint iron staining	visible muscovite (glittery), quartz, orthoclase (pink feldspar or some pinkish red mineral)	

Top Depth (ft)	Top Depth (m)	Basal Depth (ft)	Basal Depth (m)	Thickness (ft)	Thickness (m)	Grain Size	▲ or ▼ **	Facies	Sorting	Roundness	Color	Basal Contact	Primary Structures	Secondary Alteration	Comments	Driller's Log
266.6	81.3	269.3	82.1	2.7	0.8	sand: medium sand		2	moderately well to well	subangular to subrounded		end of core	more massive at the top and transitions to cross-stratified, heavy mineral bands along the cross-strata	faint iron staining	mostly quartz (~90%), feldspar, lithics, muscovite, orangish pink salmon colored mineral	
269.3	82.1	270.0	82.3	0.7	0.2			0								
270.0	82.3	274.0	83.5	4.0	1.2	sand: coarse to medium sand		2	moderately well to well	subangular to subrounded		end of core	massive with some thin clay beds within the basal 12.7cm (5in)		compositions similar to above: mostly quartz (~90%), feldspar, lithics, muscovite, orangish pink salmon colored mineral	
274.0	83.5	275.0	83.8	1.0	0.3			0								
275.0	83.8	275.4	84.0	0.4	0.1	sand: medium to coarse sand		2	well sorted	subangular to subrounded		sharp	massive (hard to tell, too thin)		compositions similar to above: mostly quartz (~90%), feldspar, lithics, muscovite, orangish pink salmon colored mineral	

Top Depth (ft)	Top Depth (m)	Basal Depth (ft)	Basal Depth (m)	Thickness (ft)	Thickness (m)	Grain Size	▲ or ▼	Facies	Sorting	Roundness	Color	Basal Contact	Primary Structures	Secondary Alteration	Comments	Driller's Log
275.4	84.0	280.0	85.4	4.6	1.4	clay		4			2.5YR 5/3 to 7.5YR 5/3 (transitions from pinkish/ red to brown towards base of clay)	end of core	massive	root traces/filaments filled with off white mineral, mottled with MnO near the top more concentrated MnO near the base of the clay	very hard/ well indurated, breaks in a very blocky pattern	
280.0	85.4	283.0	86.3	3.0	0.9	clay		3? 4?			2.5YR 5/3	gradational	massive	root traces and filaments filled with off-white and pink stained clay	cobble(5cm wide and 7cm long) dark black to gray with lighter mineral bands at 85.5m (280.5')	
283.0	86.3	285.0	86.9	2.0	0.6	clay to silty clay		3? 4?			2.5YR 5/3	end of core	massive	calcite concretion (reacts readily with HCl) that is ~2cm wide and 7cm long and one that is less prominent at 86.4m (283.5)	softer clay, more malleable than overlying clay, still breaks in a blocky pattern	

Top Depth (ft)	Top Depth (m)	Basal Depth (ft)	Basal Depth (m)	Thickness (ft)	Thickness (m)	Grain Size	▲ or ▼ **	Facies	Sorting	Roundness	Color	Basal Contact	Primary Structures	Secondary Alteration	Comments	Driller's Log
285.0	86.9	290.0	88.4	5.0	1.5	silty clay		3? 4?			2.5YR 5/3	end of core	massive	similar cacite concretions as seen in overlying core (at 87.8 and 88.3 m (288' and 289.5')), root traces and filaments filled with off-white and pink stained clay, some MnO stains		
290.0	88.4	295.0	89.9	5.0	1.5	in shoe: pinkish clay		0								
295.0	89.9	300.0	91.5	5.0	1.5	black fragments		0								
300.0	91.5	305.0	93.0	5.0	1.5	no core		0								
305.0	93.0	310.0	94.5	5.0	1.5	no core		0								
310.0	94.5	315.0	96.0	5.0	1.5	no core		0								
315.0	96.0	316.0	96.3	1.0	0.3	silty clay		?? ?			2.5YR 5/2	gradational	thinly laminated	MnO specs throughout	very well indurated, very hard to break	
316.0	96.3	320.0	97.6	4.0	1.2	sandy silt: very fine to fine sandy silt with some clay		?? ?	moderately well to well	subangular to subrounded	10YR 4/3	end of core		small filaments or root traces filled with off-white (slightly stained) mineral, some MnO specs as seen above	similar to above, the upper portion of this unit is very well indurated through 97.3m (319'), but the last 0.3m is softer with root traces/ cracks filled with white mineral (clay)	

** ▲ or ▼ indicate a fining upward (▲) or a fining downward (▼) trend within sections of the core.

Table B2: Lithologic descriptions of the proximally located soft sediment core MRWA. The facies column uses a number to denote the hydrofacies and areas where core was not recovered. The numbers include: (0) no core recovered, (1) gravel flood deposits, (2) sandy channel deposits, (3) silty sands, silty clays, and clay overbank deposits, (4) pedogenically altered deposits.

See table on following page.

Top Depth (ft)	Top Depth (m)	Basal Depth (ft)	Basal Depth (m)	Thickness (ft)	Thickness (m)	Grain Size	▲ or ▼ :	Facies	Sorting	Roundness	Color	Basal Contact	Primary Structures	Secondary Alteration	Comments	Driller's Log
0	0.0	4	1.2	4	1.2	sand with clay coats: medium to coarse sand with thin clay coats coarsens with depth to coarse to very coarse sand near the base	▲	3	moderatly well to moderate	subangular to subrounded	overall 10YR 3/3 to 4/3 (changes from darker to light)	end of core	massive		90% quartz, some feldspar, muscovite, lithics	missing 1' (I measured)
4	1.2	5	1.5	1	0.3			0								
5	1.5	5.8	1.8	0.8	0.2	sand with clay coats: coarse to very coarse sand that fines to medium to coarse sand with medium thick clay coats		3	moderately well to well	subangular to subrounded	10YR 5/4	sharp, at an angle	appears mostly massive, but possibly cross-stratified	faint iron staining	slightly less orange staining at the base	missing 3.6'
5.8	1.8	6.4	2.0	0.6	0.2	sand with clay coats: very coarse to coarse sand with thin clay coats		3	moderately well to well	subangular to subrounded	10YR 5/4	end of core	possibly cross-stratified-- upper contact is at an angle	faint orange hue from iron staining		
6.4	2.0	10	3.0	3.6	1.1			0								
10	3.0	11.3	3.4	1.3	0.4	clay and clayey silt: clay grades to clayey silt with very fine sand which grades to fine to very fine silty, clayey, sand	▲	3	fines sands at base seem well sorted		2.5 Y 5/3	sharp		root traces throughout, iron staining concentrated in the root traces	clay to silt to very fine sand pattern seems to repeat itself twice (see below)	missing 4.5" (I measured)

Top Depth (ft)	Top Depth (m)	Basal Depth (ft)	Basal Depth (m)	Thickness (ft)	Thickness (m)	Grain Size	▲ or ▼ :	Facies	Sorting	Roundness	Color	Basal Contact	Primary Structures	Secondary Alteration	Comments	Driller's Log
11.3	3.4	13	4.0	1.7	0.5	clay and clayey silt: clay grades to clayey silt with very fine sand which grades to fine to very fine silty, clayey, sand	▲	3	fines sands at base seem well sorted		2.5 Y 5/3	sharp		root traces through out, heavily iron stained at the silty sand basal contact with clay below (at ~13')		
13	4.0	14.7	4.5	1.7	0.5	clay to silt and very fine sand: clay grades to silt then very fines sand then back to silt		3			2.5Y 5/4	end of core	appears massive but may be thinly laminated	root traces through out and faint iron staining accenting where the root traces are		
14.7	4.5	15	4.6	0.3	0.1			0								
15	4.6	16	4.9	1	0.3	silty sand: silt to very fine silty sand with some coarse patches of sand mixed into the silt	▲	3			2.5Y 5/1 to 5/2	sharp	appears massive with thin sand lenses randomly dispersed	some faint heavy mineral banding near the top (2.5Y) and some faint iron staining		
16	4.9	18.4	5.6	2.4	0.7	sand: coarse to medium sand that grades to medium to fine sand	▼	2	well	subangular to subrounded		end of core	c-m sand: cross-bedding delineated by heavy mineral banding m-f sand: massive	patches of iron staining in the medium to coarse sand	sand is 90% - 95% quartz	missing 1'9" (I measured)
18.4	5.6	20	6.1	1.6	0.5			0								
20	6.1	20.6	6.3	0.6	0.2	silty sand: medium to fine sand with some silt	▲	3	moderately well		2.5Y 5/3		cross-stratified			2'6" missing

Top Depth (ft)	Top Depth (m)	Basal Depth (ft)	Basal Depth (m)	Thickness (ft)	Thickness (m)	Grain Size	▲ or ▼ :	Facies	Sorting	Roundness	Color	Basal Contact	Primary Structures	Secondary Alteration	Comments	Driller's Log
20.6	6.3	21.2	6.5	0.6	0.2	sand: medium sand		2	well	subangular to subrounded			cross-stratified deliniated by heavy mineral banding		gray clay content increases toward the base of the unit	
21.2	6.5	22.5	6.9	1.3	0.4	clay: clay grades to a fine silt then to a coarser silt		3			2.5Y 5/2	end of core	massive	some root traces delineated by iron staining		
22.5	6.9	25	7.6	2.5	0.8			0								
25	7.6	27	8.2	2	0.6	sandy clay: clay mixed with medium to fine sand	▲	3			2.5Y5/2 to 5/3	contact is denoted by thick band of calcite at 27'2"-27'4"	massive	iron stained (heaviest aroud 27-28' where calcite is), burrows	at 26'4", there is a pocket of clean sand in a tear drop shape. The sand is medium to coarse and moderately well sorted. There is also a sharp contrast of heavily iron stained clay and mildly splotched iron stained clay. At 26'8" , there is a thinly veined network of calcite filled cracks in the clay that is approximately an inch and a half thick. Reacts readily with HCl.	1'5" missing
27	8.2	28.4	8.7	1.4	0.4	sandy silt: silt with very fine sand that coarsens to medium to fine sandy silt		3			2.5Y 5/4	end of core		iron stains througout, root traces		

Top Depth (ft)	Top Depth (m)	Basal Depth (ft)	Basal Depth (m)	Thickness (ft)	Thickness (m)	Grain Size	▲ or ▼ :	Facies	Sorting	Roundness	Color	Basal Contact	Primary Structures	Secondary Alteration	Comments	Driller's Log
28.4	8.7	30	9.1	1.6	0.5			0								
30	9.1	30.5	9.3	0.5	0.2	silty sand: silty medium to fine sand		3			2.5Y 6/3	gradation al		mottled iron staining, and root traces		
30.5	9.3	31.5	9.6	1	0.3	sand: medium to fine sand		2	well	subangular to subrounded		sharp	cross-strata delineated by heavy mineral banding	faint orange tint throughout		
31.5	9.6	32.3	9.8	0.8	0.2	sandy silt: very fine sandy silt that grades to a thin clay coated medium to coarse sand		3			2.5Y 5/3	sharp		root traces and iron staining throughout	thin clay band between the silt and the sand	1'4" missing
32.3	9.8	33.6	10.2	1.3	0.4	clay: with some minor sand and silt mixed in		3			2.5Y 5/3	end of core	appears massive	root traces, burrows, iron staining	soft, malleable, has a fuzzt appearance (silt)	
33.6	10.2	35	10.7	1.4	0.4			0								
35	10.7	36	11.0	1	0.3	sand: medium to fine sand grades into very fine sand		2	well	subangular to subrounded		gradation al	massive	iron staining dispersed through out the unit but concentrated near the clean sand filled cracks.	large medium to fine clean sand filled cracks dispersed through the unit	
36	11.0	37	11.3	1	0.3	silt	▼	3			2.5Y 5/3	gradation al	thiny laminated	root traces, iron staining that delineates the root traces and seems to decrease with depth.		
37	11.3	38	11.6	1	0.3	silty clay		3			5Y 6/2	sharp	thinly laminated	very faint iron staining		

Top Depth (ft)	Top Depth (m)	Basal Depth (ft)	Basal Depth (m)	Thickness (ft)	Thickness (m)	Grain Size	▲ or ▼ :	Facies	Sorting	Roundness	Color	Basal Contact	Primary Structures	Secondary Alteration	Comments	Driller's Log
38	11.6	38.7	11.8	0.7	0.2	sand: medium to fine clean sand		2	well	subangular to subrounded		gradation al		faint iron staining	sand is 90% - 95% quartz, white feldspar (plag?) with a little muscovite	
38.7	11.8	40	12.2	1.3	0.4	silt: very fine silt	▼	3			2.5Y 5/3	end of core	thinly laminated, can see very thin milimeter scale bands of very fine, lightly colored silt	faint iron staining, possible burrows filled with lightly colored very fine silt	hard to see what the whole surface looks like. Some of the silt had been smeared over the surface.	
40	12.2	40.8	12.4	0.8	0.2	clayey silt: very fine clayey silt		3			2.5Y 6/2	sharp	thinly laminated	faint iron staining	clay content increases toward the paleosol at the base of the unit	
40.8	12.4	43.7	13.3	2.9	0.9	sand with clay coats: coarse to medium sand with thick clay coats, medium sand coarsens to coarse then fines back to medium sand		4			7.5YR 6/2 (or 10YR 5/3)	end of core		iron staining, more distinct than above, root traces	pinkish color clay becomes increasingly brown with depth, irnon staining gives the unit and orange tint	
43.7	13.3	45	13.7	1.3	0.4			0								
45	13.7	47.2	14.4	2.2	0.7	sand with clay coats: medium to fine sand with thick clay coats		3			2.5Y 5/2	sharp	massive		the top foot of core has small nodules of hardened clay coated grains less than 1cm long. It is concentrated in an ~5" section.	

Top Depth (ft)	Top Depth (m)	Basal Depth (ft)	Basal Depth (m)	Thickness (ft)	Thickness (m)	Grain Size	▲ or ▼ :	Facies	Sorting	Roundness	Color	Basal Contact	Primary Structures	Secondary Alteration	Comments	Driller's Log
47.2	14.4	48	14.6	0.8	0.2	silty sand: very fine to fine silty sand		3			2.5 Y 6/2 to 5/2 ish	sharp but at an angle--possibly erosional	massive			
48	14.6	48.7	14.8	0.7	0.2	silty sandy clay: alternating clay, medium to fine sand, and fine silt each from 1.5" to 3"		3			2.5 Y 6/2 to 5/2 ish	end of core	thinly laminated	some heavy mineral banding in the sand and silt		
48.7	14.8	50	15.2	1.3	0.4			0								
50	15.2	50.8	15.5	0.8	0.2	sand: very fine to fine sand		2			2.5Y 6/2	gradation al	thinly laminated	slightly irnon stained, heavy mineral banding	band of fine to mendium sand at 50.3', thin bands of calcareous material	
50.8	15.5	52	15.9	1.2	0.4	sandy to clayey silt: very fine sandy silt that fines to clayey silt	▲	3			2.5Y 5/2	gradation al	thinly laminated	slightly iron stained	thin bands of calcareous material, abundant mica gives the core a glittery sheen	
52	15.9	53	16.2	1	0.3	clay		3			2.5Y 5/2	gradation al	massive			
53	16.2	53.7	16.4	0.7	0.2	clay: calcareous clay		3			2.5Y 7 or 8/2	sharp			soft, reacts readily with HCl	
53.7	16.4	54	16.5	0.3	0.1	sandy clay: medium to coarse sand mixed with clay		3	moderately well	subangular to subrounded						
54	16.5	55	16.8	1	0.3			0								
55	16.8	56	17.1	1	0.3	sand with clay coats: medium to coarse sand with thick clay coats		3			2.5Y 4/3	gradation al	massive		clay coats decrease with depth, brown color	

Top Depth (ft)	Top Depth (m)	Basal Depth (ft)	Basal Depth (m)	Thickness (ft)	Thickness (m)	Grain Size	▲ or ▼ **	Facies	Sorting	Roundness	Color	Basal Contact	Primary Structures	Secondary Alteration	Comments	Driller's Log
56	17.1	57.8	17.6	1.8	0.5	sand: fine to very coarse sand		2	moderate to poorly	subangular to subrounded		sharp	massive	slightly iron stained	90% quartz, feldspar, few lithics, muscovite	
57.8	17.6	58.2	17.7	0.4	0.1	clayey sand: silty clay to clay with medium to coarse sand		3			2.5Y 4/2	end of core	massive	root traces and faint iron mottling throughout	very hard	
58.2	17.7	60	18.3	1.8	0.5			0								
60	18.3	61.2	18.7	1.2	0.4	clayey silt: clayey silt to very fine sand grades to medium to fine sandy clay	▲	3			2.5Y	sharp	massive		very hard at the base	
61.2	18.7	62.4	19.0	1.2	0.4	clayey silt: coarsens to medium to fine sandy silt	▲	3			2.5Y	end of core	thin laminations	calcite filled cracks	clay content decreases with depth; NO PHOTO	
62.4	19.0	65	19.8	2.6	0.8			0								
65	19.8	67.2	20.5	2.2	0.7	sandy silt		3			2.5Y 6/3	gradation al	massive	minimal iron stains at contact were silt transitions to clay unit	2" unit of clay at 65.4'; more brownish in this unit and becomes increasingly gray with depth	
67.2	20.5	68.9	21.0	1.7	0.5	sandy clay: some silt		3			2.5Y 6/2	gradation al	massive	iron stains and some root traces	more gray, clay is very hard in basal few inches	
68.9	21.0	69.8	21.3	0.9	0.3	sandy silt: some clay content toward the base		3			5Y 5/2	end of core	massive	iron staining and root traces	more gray	
69.8	21.3	70	21.3	0.2	0.1			0								
70	21.3	70.5	21.5	0.5	0.2	silty sand: silty fine sand with some medium sand mixed in near the top of the core		3			2.5Y 5/3	gradation al	massive			

Top Depth (ft)	Top Depth (m)	Basal Depth (ft)	Basal Depth (m)	Thickness (ft)	Thickness (m)	Grain Size	▲ or ▼ :	Facies	Sorting	Roundness	Color	Basal Contact	Primary Structures	Secondary Alteration	Comments	Driller's Log
70.5	21.5	71.4	21.8	0.9	0.3	sand: medium to fine sand		2					cross-stratified with some heavy mineral banding		90% quartz, feldspar, muscovite, some lithics, overall color is more dingy that the sands decribed higher up in the core (more fines?)	
71.4	21.8	75	22.9	3.6	1.1			0								
75	22.9	77	23.5	2	0.6	sand with clay coats: medium to coarse sand with thick clay coats		4			5YR 5/4	sharp		root traces and iron staining throughout	pinkish red paleosol becomes more brown in color with depth, paleosol is hard at the top and heavily altered but softens toward the base	
77	23.5	77.4	23.6	0.4	0.1	clay		3			2.5YR 6/3	sharp		heavy iron stained band at top contact		
77.4	23.6	78.4	23.9	1	0.3	sandy silt		3			2.5YR 5/3	gradation al		blotches of iron staining		
78.4	23.9	79.2	24.1	0.8	0.2	silty sand: medium to very coarse sand with silt that decreases with depth		3			2.5YR 5/3	end of core	very little faint iron staining			
79.2	24.1	80	24.4	0.8	0.2			0								
80	24.4	81.3	24.8	1.3	0.4	silty sand: medium to coarse sand with silt	▲	3	poorly	subangular to subrounded	2.5Y 5/3 to 5/4 ish	sharp	massive	faint iron staining		

Top Depth (ft)	Top Depth (m)	Basal Depth (ft)	Basal Depth (m)	Thickness (ft)	Thickness (m)	Grain Size	▲ or ▼ **	Facies	Sorting	Roundness	Color	Basal Contact	Primary Structures	Secondary Alteration	Comments	Driller's Log
81.3	24.8	82.2	25.1	0.9	0.3	silty clay: clay to silty clay (possibly some very fine sand or coarse silt)		3			2.5Y 6/2	end of core	massive	faint iron staining and root traces		
82.2	25.1	85	25.9	2.8	0.9			0								
85	25.9	85.4	26.0	0.4	0.1	sand with clay coats: sand with thick clay coats		4			7.5YR 6/2	sharp				
85.4	26.0	86.1	26.3	0.7	0.2	clayey silt: clayey silt with some medium to fine sand; clay decreases with depth		3			2.5Y 6/3	gradation al		iron staining throughout		
86.1	26.3	87.2	26.6	1.1	0.3	sandy silt: medium to fine sandy silt	▼	3			10YR	gradation al		mottled iron staining		
87.2	26.6	88	26.8	0.8	0.2	clay: mixed with sand		3			2.5Y 5/4	gradation al			core is crumbled	
88	26.8	89.1	27.2	1.1	0.3	sandy silt: silt with medium to fine sand		3			2.5Y 5/4	gradation al		iron staining	core is crumbled and no obvious primary structures	
89.1	27.2	90	27.4	0.9	0.3	clayey silt		3			2.5Y 5/3	end of core	thin laminations	mottled iron staining	core is no longer crumbled	
90	27.4	90.4	27.6	0.4	0.1	sand: very coarse to graules (granule-2mm)		2	poorly	subangular to subrounded		sharp				

Top Depth (ft)	Top Depth (m)	Basal Depth (ft)	Basal Depth (m)	Thickness (ft)	Thickness (m)	Grain Size	▲ or ▼ :	Facies	Sorting	Roundness	Color	Basal Contact	Primary Structures	Secondary Alteration	Comments	Driller's Log
90.4	27.6	94.6	28.8	4.2	1.3	sand: medium to very coarse sand		2	poorly	subangular to subrounded	(OVERA LL appears 2.5Y 6/2)	end of core	cross-stratified with some heavy mineral banding	faint iron staining	medium sand near top is well sorted and slightly iron stained, grades to coarse and then very coarse sand, small bands of coarsening throughout, 90% quartz, feldspar, muscovite, few lithics, very light in color	
94.6	28.8	95	29.0	0.4	0.1			0								
95	29.0	96	29.3	1	0.3	sand: coarse to very coarse sand, some granuals mixed in near the top of the core		2	moderately to poorly	subangular to subrounded	(OVERA LL appears 2.5Y 6/2)	sharp	thin laminations, heavy mineral banding		thin laminations delineated by thin bands of clay (2.5Y 4/1)	
96	29.3	97.1	29.6	1.1	0.3	sand with clay coats: medium to coarse sand with thick clay coats		3			2.5Y 5/3	sharp	massive		not reddish in color but is clay mixed with sand	
97.1	29.6	98	29.9	0.9	0.3	sand: coarse to medium sand possibly with some silt		2	moderately well	subangular to subrounded		gradation al	massive	iron stained		
98	29.9	98.4	30.0	0.4	0.1	clayey silt: silt with some medium to coarse sand in it, fines to clayey silt		3			2.5Y 6/3	end of core	massive	faint iron staining		
98.4	30.0	100	30.5	1.6	0.5			0								

Top Depth (ft)	Top Depth (m)	Basal Depth (ft)	Basal Depth (m)	Thickness (ft)	Thickness (m)	Grain Size	▲ or ▼ :	Facies	Sorting	Roundness	Color	Basal Contact	Primary Structures	Secondary Alteration	Comments	Driller's Log
100	30.5	103	31.3	2.8	0.9	sandy silt: silt with very fine to fine sand grades to very fine sand with some silt	▲	3	moderately well		2.5Y 5/2	sharp	thinly laminated near top of the core where there is more silt; appears to be cross-stratified near basal contact where there is more sand, heavy mineral banding throughout	heavily iron stained	this unit has a lot of mica that gives the core a glittery sheen; there are some thin bands of coarse sand (~5mm wide)	
103	31.3	104	31.6	1	0.3	sand: medium to coarse sand, possibly some silt mixed in		2	moderately to poorly	subangular to subrounded	OVERALL 2.5Y 4/1	gradational	cross-stratified with heavy mineral banding	blotches of iron staining	90% quartz, feldspar, little muscovite, few lithics	
104	31.6	105	31.9	0.9	0.3	sand: coarse to very coarse sand		2	moderately to poorly	subangular to subrounded	OVERALL 2.5Y 6/2 to 5/2	end of core	cross-stratification with thin bands of medium to coarse sand dispersed throughout (103.5' to 104')		at 104.2' there is a 2.5" band of medium sand	
105	31.9	105	32.0	0.3	0.1			0								
105	32.0	106	32.4	1.2	0.4	sand: medium to coarse sand grades to coarse to very coarse sand	▲	2	moderately to poorly	subangular to subrounded		sharp	no apparent structural features	very little if any iron stainging, maybe slight faint orange tinge		

Top Depth (ft)	Top Depth (m)	Basal Depth (ft)	Basal Depth (m)	Thickness (ft)	Thickness (m)	Grain Size	▲ or ▼ :	Facies	Sorting	Roundness	Color	Basal Contact	Primary Structures	Secondary Alteration	Comments	Driller's Log
106	32.4	107	32.6	0.8	0.2	sand: medium to coarse sand grades to a coarse sand then back to a medium sand, below the anomalous unit of fine silty sand, the sand is coarse to very coarse	▲	2	moderately to poorly	subangular to subrounded		sharp	cross-stratified, heavy mineral banding		at 107", there is a 3" think unit of very fine sand with silt that coursens to a fine sand (2.5Y 6/3). The top and bottom contacts are sharp and it appears to be an isolated unit within the coarser sand deposit.	
107	32.6	109	33.1	1.7	0.5	sand: medium sand that grades to coarse sand, some silt mixed in with bottom 6"	▲	2	moderately to poorly	subangular to subrounded	sand with silt mixed in has an overall color of 2.5Y 5/3	end of core	within the top 1/4 of medium sand: cross-stratification , heavy mineral banding; the rest of the sand is massive			
109	33.1	110	33.5	1.3	0.4			0								
110	33.5	115	34.9	4.5	1.4	sand with clay coats: medium to fine sand with thick clay coats that decrease with depth		4	sand in clay seems poorly sorted	subangular to subrounded	7.5YR 5/6 transition s to 5/4	sharp	massive	some MnO staining that increases the induration of the core	clay coats decrease with depth from thick to thin. The color of the core reflects this change.	
115	34.9	115	35.0	0.3	0.1	clay: with some medium to coarse sand grains mixed in (not as much sand incorporated as above)		4			7.5YR 5/4	end of core	massive			

Top Depth (ft)	Top Depth (m)	Basal Depth (ft)	Basal Depth (m)	Thickness (ft)	Thickness (m)	Grain Size	▲ or ▼ :	Facies	Sorting	Roundness	Color	Basal Contact	Primary Structures	Secondary Alteration	Comments	Driller's Log
115	35.0	115	35.1	0.2	0.1		↓	0								
115	35.1	119	36.2	3.7	1.1	sand with clay coats: coarse to fine sand with thick clay coats; clay coats decrease with depth; basal sands have a very thin clay coat		4			7.5YR 5/4 trans to 5/3; more brown at the base 10YR 5/4	end of core		heavily iron stained and root traces toward the top of the core; mottled iron staining near the base; some large filiaments filled with either clean sand or off-white colored clay (no reaction with HCl)	some of the iron staining as well as some of the thin sand lenses appear to be on an angle	
119	36.2	120	36.6	1.3	0.4			0								
120	36.6	120	36.6	0.2	0.1	clay: clay with some sand		4			7.5YR 5/4	sharp				
120	36.6	121	37.0	1.1	0.3	clay: some very coarse to medium sand interbeds		3			2.5Y (clay is light brown to gray brown and sand is burnt orange)	sharp	interbeds of sand	some iron staining	contacts of the sand and clay units are hard to see, but the different units are distinct	
121	37.0	122	37.2	0.8	0.2	clay: yellowish off-white/gray clay		3			2.5Y	sharp	possible thin laminations	some iron staining and root traces		
122	37.2	123	37.4	0.5	0.2	sand with clay coats: very coarse to coarse sand with thin clay coats; fines to medium sand		4			7.5YR	sharp				

Top Depth (ft)	Top Depth (m)	Basal Depth (ft)	Basal Depth (m)	Thickness (ft)	Thickness (m)	Grain Size	▲ or ▼ :	Facies	Sorting	Roundness	Color	Basal Contact	Primary Structures	Secondary Alteration	Comments	Driller's Log
						with thicker clay coats										
123	37.4	123	37.4	0.2	0.1	clay: some sand and granules mixed in		4			10YR	sharp				
123	37.4	125	38.0	1.8	0.5	sand with clay coats: very coarse to medium sands with some pebbles mixed in have very thin clay coats		4	moderate	subangular to subrounded	7.5YR (orange-red)	sharp	cross-stratification and heavy mineral banding in the basal sevreal inches	heavily iron stained		
125	38.0	125	38.1	0.4	0.1	clay: some granuoles mixed in (max 1cm long, most <5mm)		3			2.5Y (light brown)	end of core		heavily iron stained (dark reddish brown colored in spots)	NOTE: The entore 5' core is very segmented. It looks like interchanges of sand and clay that have been pedogenically altered. The whole core is very orange in color (excluding the light brown clay with slight iron staining)	

Top Depth (ft)	Top Depth (m)	Basal Depth (ft)	Basal Depth (m)	Thickness (ft)	Thickness (m)	Grain Size	▲ or ▼ :	Facies	Sorting	Roundness	Color	Basal Contact	Primary Structures	Secondary Alteration	Comments	Driller's Log
125	38.1	128	39.0	3	0.9	sand with clay coats: coarse to very coarse sand with thin clay coats		4	moderate	subangular to subrounded	staining (5YR 4/6, 5YR 5/6, 5YR 5/7, 5YR 5/4) unstained has overall appearance of 2.5Y 7/2	sharp			looks like 3 stacked 5-6" fining upward packages: at the base are more coarsely grained sedimnets mixed with a little clay, this fines to a poorly sorted mix of very coarse to medium sand with thin clay coats--an overall orangish red color	
128	39.0	130	39.5	1.6	0.5	sand: medium to coarse grained with NO clay coats		2	well	subangular to subrounded	OVERALL without secondary alteration 2.5Y 7/2	end of core	cross-stratification with some heavy mineral banding	the unit is stained with various bands of bright orange to mauve while some bands are left unstained and remain whitish in color		
130	39.5	130	39.6	0.4	0.1			0								
130	39.6	132	40.2	1.8	0.5	sand: coarse to medium sand with some fine sand mixed in		2	moderately	subangular to subrounded	OVERALL 2.5YR 7/6	sharp	cross-stratification and some heavy mineral banding; also some clay banding (salmon colored)	iron staining (less iron staining than above)	similar to sands described in above core; 90% quartz, feldspar, muscovite, few lithics	

Top Depth (ft)	Top Depth (m)	Basal Depth (ft)	Basal Depth (m)	Thickness (ft)	Thickness (m)	Grain Size	▲ or ▼ :	Facies	Sorting	Roundness	Color	Basal Contact	Primary Structures	Secondary Alteration	Comments	Driller's Log
132	40.2	133	40.5	1.2	0.4	silty clay: that grades to some sandy silt in basal couple inches		3			2.5Y 5/3 (basal silt is 2.5Y 5/2)	sharp-- small patches of sand from the underlyin g unit are embedde d in the basal silt	thinly laminated, some thin layers of the salmon colored clay described above	bands of iron staining, root traces, and some MnO stains		
133	40.5	133	40.7	0.4	0.1	sand: fine to very fine sand		2	moderately well	subangular to subrounded		end of core		lightly iron stained		
133	40.7	135	41.2	1.6	0.5			0								
135	41.2	137	41.9	2.4	0.7	sand: medium to fine sand with clay or clayey silt interbeds (2cm or less in thickness)		2	modertaely	subangular to subrounded	OVERAL L2.5Y 5/3 (iron staining 10YR 4/4)	sharp	clay or clayey silt interbeds (2cm or less in thickness)	iron staining in bands		
137	41.9	139	42.5	1.9	0.6	silty clay		3			2.5Y 5/3 transition s to 5Y 5/1	sharp	massive with interbeds of very fine sand and silt (1cm thick or less) to 138.4' then grades to thinly laminated clay and silty clay	iron staining is banded in silty clay		
139	42.5	140	42.6	0.3	0.1	sand: fine to very fine sand		2	moderately	subangular to subrounded	very light in color	sharp	massive	mottled iron staining		
140	42.6	140	42.6	0.2	0.1	silty clay: with some very fine sand mixed in		3			2.5Y 5/3	end of core				

Top Depth (ft)	Top Depth (m)	Basal Depth (ft)	Basal Depth (m)	Thickness (ft)	Thickness (m)	Grain Size	▲ or ▼ :	Facies	Sorting	Roundness	Color	Basal Contact	Primary Structures	Secondary Alteration	Comments	Driller's Log
140	42.6	140	42.7	0.2	0.1			0								
140	42.7	142	43.3	2.1	0.6	silty clay: some thin silt interbeds at top of core (~1cm thick); in last 8" of the core interbeds are clayey silt to very fine sand and 1-4cm thick		3			2.5Y 5/3	sharp	thinly laminated, interbeds	banded iron staining, black filaments, and root traces		
142	43.3	143	43.5	0.7	0.2	sand: very fine to fine sand		2	well	subangular to subrounded	2.5Y 5/3	sharp	thinly laminated, thin 1mm beds of silty sand at the top of the unit	faint iron staining especially in the interbeds		
143	43.5	143	43.7	0.5	0.2	sandy silt: some very fine sand grains		3			2.5Y 5/3	sharp	some thin bands of very fine sand	root traces		
143	43.7	144	43.8	0.5	0.2	sand: fine to very fine sand		2	well	subangular to subrounded	OVERAL L 2.5Y 5/2 ish	sharp		large elongate iron stained root traces		
144	43.8	144	44.0	0.6	0.2	sandy silt		3			2.5Y 4/2	sharp	band of fine to very fine sand at the base	root traces continue from overlying sandy layer		
144	44.0	145	44.2	0.6	0.2	clayey sandy silt: can roll a stringer but it falls apart		3			2.5Y 4/3	end of core	thin laminations	iron staining throughout		
145	44.2	147	44.7	1.7	0.5	silty clay: with silt interbeds		3			2.5Y 5/3	sharp	silt interbeds (1cm thick or less); thinly laminated	iron staining and root traces		

Top Depth (ft)	Top Depth (m)	Basal Depth (ft)	Basal Depth (m)	Thickness (ft)	Thickness (m)	Grain Size	▲ or ▼ :	Facies	Sorting	Roundness	Color	Basal Contact	Primary Structures	Secondary Alteration	Comments	Driller's Log
147	44.7	148	45.1	1.1	0.3	sandy silt fines to silty clay		3			2.5Y 5/3	sharp	thinly laminated	iron staing is banded in the clayey silt and spotted in the silt		
148	45.1	149	45.3	0.9	0.3	sandy silt		3			2.5Y 5/2	sharp	thinly laminated	iron staining along laminations, root traces (filaments), brown mottling at base		
149	45.3	150	45.6	0.8	0.2	clayey silt		3			2.5Y 5/2	sharp	thinly laminated	iron stains along laminations		
150	45.6	150	45.7	0.5	0.2	silty sand		3			2.5Y 5/2	end of core	massive?	iron staining		
150	45.7	151	46.0	1	0.3	silty clay: with an interbed of silt (<1cm; ~5mm)		3			2.5Y 5/3	gradtaional	thiny laminated	root traces, iron staining		
151	46.0	152	46.2	0.5	0.2	clay		3			2.5Y 4/3	gradational		root traces, iron staining, MnO staining	very hard, brittle, crumbles	
152	46.2	152	46.3	0.5	0.2	sand silty clay: medium to fine sand mixed in with silty clay, more sand towards the base		3			2.5Y 5/3	sharp (at an angle- - erosional ?)	thin laminations decrease towards the base (becomes more massive)	root traces, some iron staining	very hard	
152	46.3	153	46.6	1	0.3	sandy silt: silt with some very fine sand		3				end of core	appears massive	bands (streaks) of iron staining	at 152.8' there is a 2cm band of medium to fine clean sand	
153	46.6	155	47.3	2	0.6			0								

Top Depth (ft)	Top Depth (m)	Basal Depth (ft)	Basal Depth (m)	Thickness (ft)	Thickness (m)	Grain Size	▲ or ▼ :	Facies	Sorting	Roundness	Color	Basal Contact	Primary Structures	Secondary Alteration	Comments	Driller's Log
155	47.3	158	48.0	2.6	0.8	sand: fine to medium sand (with coarse grains) grades to medium to coarse sand	▲	2	moderately	subangular to subrounded	OVERAL L 2.5Y 6/3	sharp	cross-stratified with some heavy mineral banding in finer grained sands	a few bands of faint iron staining	90% quartz, feldspar, muscoite (bands of it in the mediumt o fine sand), minor lithics, some red minerals and greenish gray minerals	
158	48.0	159	48.5	1.6	0.5	sand: medium to fine sand grades to medium to coarse sand then to coarse to very coarse sand	▲	2	moderately	subangular to subrounded	OVERAL L 2.5Y 5/2 ish	end of core	cross-stratified with some heavy mineral banding in finer grained sands	a few bands of faint iron staining	90% quartz, feldspar, muscoite (bands of it in the mediumt o fine sand), minor lithics, some red minerals and greenish gray minerals	
159	48.5	160	48.8	0.8	0.2			0								
160	48.8	161	49.1	1	0.3	sand: medium to very coarse sand		2	moderatly to poorly	subangular to subrounded	OVERAL L 2.5Y 6/3	sharp	massive	faint iron staining; some possibly MnO staining at the basal contact	90% quartz, feldspar, more lithics than previous core of sands, some green mineral and some red orange mineral	
161	49.1	162	49.4	1	0.3	gravel: matrix supported gravel (1cm long maximum), matrix is very coarse to granule		1	poorly	gravel is well rounded; matrix is subangular to subrounded		gradation al	massive			
162	49.4	162	49.5	0.4	0.1	sand: very coarse to granule		2	moderately	subangular to subrounded		sharp		heavily iron stained at base		

Top Depth (ft)	Top Depth (m)	Basal Depth (ft)	Basal Depth (m)	Thickness (ft)	Thickness (m)	Grain Size	▲ or ▼ :	Facies	Sorting	Roundness	Color	Basal Contact	Primary Structures	Secondary Alteration	Comments	Driller's Log
162	49.5	165	50.2	2.4	0.7	silty clay: some very fine sand mixes in near the base		3			2.5Y 4/3 to 4/4	end of core		root traces or filaments filled with clay or MnO, faint iron stains near the top, more mottled iron staining throughout near base of unit		
165	50.2	165	50.3	0.2	0.1			0								
165	50.3	167	50.9	1.9	0.6	silty clay: some sand grains (a very gritty clay)		3			10YR 5/3	gradation al	massive	mottled iron staining, root cracks or filaments filled with clay	breaks in blocks and is very hard	
167	50.9	168	51.2	1.1	0.3	sand with clay coats: coarse to medium sand with thick clay coats, sand size decrases to medium sand with depth, clay coats also decrease with depth		3			10YR 5/4	end of core (next core is mini core of continue d 165-170 interval)	massive	iron staining, root traces, black to very dark brown mottling, some filaments filled with MnO (black mineral) as well	soft/ malleable	
168	51.2	170	51.7	1.7	0.5	sand with clay coats: coarse to medium sand with thick clay coats, sand size decrases to medium sand with depth, clay coats also decrease with depth		3			10YR 5/4	mini core of above interval continue d-end of core	massive	iron staining, root traces, black to very dark brown mottling, some filaments filled with MnO (black mineral) as well	soft/ malleable	
170	51.7	170	51.8	0.3	0.1			0								

Top Depth (ft)	Top Depth (m)	Basal Depth (ft)	Basal Depth (m)	Thickness (ft)	Thickness (m)	Grain Size	▲ or ▼ :	Facies	Sorting	Roundness	Color	Basal Contact	Primary Structures	Secondary Alteration	Comments	Driller's Log
170	51.8	172	52.4	2	0.6	sand with thick clay coats: medium to fine sand with thick clay coats; clay decreases with depth		3			10YR 5/4 transitions to 4/4	gradational		mottled iron staining	very soft and malleable	
172	52.4	175	53.3	2.7	0.8	sand: medium to fine grades to fine to medium then back to medium to fine that coarsens to medium to coarse		2	moderately	subangular to subrounded	2.5Y 4/3	end of core	cross-stratified in the finer sands with some heavy mineral bands, massive in coarser sands		random granules mixed in (< 1cm long); 85% quartz with more lithics, red minerals, green minerals, feldspar, muscovite, salmon colored mineral	
175	53.3	175	53.4	0.3	0.1			0								
175	53.4	176	53.7	1.1	0.3	sand: medium to fine grained, occassional granule		2	moderately	subangular to subrounded	OVERALL 2.5Y 5/2	gradational	cross-stratified, heavy mineral banding		whole composition of the core is similar: 85% quartz with more lithics, red minerals, green minerals, feldspar, muscovite, salmon colored mineral	

Top Depth (ft)	Top Depth (m)	Basal Depth (ft)	Basal Depth (m)	Thickness (ft)	Thickness (m)	Grain Size	▲ or ▼ :	Facies	Sorting	Roundness	Color	Basal Contact	Primary Structures	Secondary Alteration	Comments	Driller's Log
176	53.7	177	54.0	1.1	0.3	sand: with some matrix supported gravel bands, sand is very coarse to coarse sand		2	poorly	gravel is well rounded to rounded and the sand is subangular to subrounded	OVERAL L 2.5Y 5/2	sharp– band of gravel delineate s contact	massive, gravel seems to be aligned in bands		whole composition of the core is similar: 85% quartz with more lithics, red minerals, green minerals, feldspar, muscovite, salmon colored mineral	
177	54.0	178	54.1	0.3	0.1	sand: medium to fine sand		2	moderately well	subangular to subrounded	OVERAL L 2.5Y 5/2	end of core	massive		whole composition of the core is similar: 85% quartz with more lithics, red minerals, green minerals, feldspar, muscovite, salmon colored mineral (orthoclase?)	
178	54.1	180	54.9	2.5	0.8			0								

Top Depth (ft)	Top Depth (m)	Basal Depth (ft)	Basal Depth (m)	Thickness (ft)	Thickness (m)	Grain Size	▲ or ▼ :	Facies	Sorting	Roundness	Color	Basal Contact	Primary Structures	Secondary Alteration	Comments	Driller's Log
180	54.9	180	55.0	0.3	0.1	sand: medium to coarse grained sand mixed with a few pieces of gravel (sparsly distributed)		2	poorly	subangular to subrounded, pebbles are rounded to well rounded	OVERAL L 2.5Y 5/3	gradation al	massive		similar composition to core above: 85% quartz with more lithics, red minerals, green minerals, feldspar, muscovite, salmon colored mineral (orthoclase?); gravel pieces are 1-3cm long and are quartz, andesite?	
180	55.0	183	55.7	2.5	0.8	gravel: matrix supported gravel (1-3 cm long); matrix is coarse to very coarse sand		1	poorly	matrix is subangular to subrounded; pebbles are rounded to well rounded	OVERAL L 2.5Y 3/1	sharp	massive	dark gray staning on the basal 12.7cm (5")	some clay mixed in the basal sand and gravel	
183	55.7	184	55.9	0.7	0.2	silty clay: few sparse patches of very fine sand		3			2.5Y 6/2	sharp	possible thin beds of alternating clay 1-2mm			
184	55.9	184	56.0	0.1	0.0	gravel: matrix supported gravel (1-3 cm long); matrix is coarse to very coarse sand		1	poorly	matrix is subangular to subrounded; pebbles are rounded to well rounded		end of core	massive			
184	56.0	185	56.4	1.4	0.4			0								

Top Depth (ft)	Top Depth (m)	Basal Depth (ft)	Basal Depth (m)	Thickness (ft)	Thickness (m)	Grain Size	▲ or ▼ **	Facies	Sorting	Roundness	Color	Basal Contact	Primary Structures	Secondary Alteration	Comments	Driller's Log
185	56.4	185	56.5	0.3	0.1	gravel: matrix supported gravel (1-3 cm long); matrix is coarse to very coarse sand		1	poorly	matrix is subangular to subrounded; pebbles are rounded to well rounded		sharp	loosly packed--no longer consolidate d			
185	56.5	186	56.8	1.1	0.3	clay: increasing silt fraction		6			2.5Y 6/2	gradation al		MnO staining and some iron staining	very hard clay	
186	56.8	189	57.5	2.2	0.7	silty clay: with thin 1mm bands of very fine sand sporadically		6			5Y 5/1	gradation al			looks fuzzy--from silt and very fine sand	
189	57.5	190	57.9	1.4	0.4	blue silty clay: few specs of sand (muscovite) intermixed and some very thin lenses of sand		6			gley 1 5/10Y	end of core	thinly laminated	elongate burrows, bioturbation?, no iron staining		
190	57.9	195	59.5	5	1.5	blue silty clay: few specs of sand (muscovite) intermixed and some very thin lenses of sand		6			gley 1 5/10Y darkens to gley 1 4/10Y	end of core	thin lenses and elongate tube like features filled with off-white very fine sand, some very fine sand beds more abundant in the top 1m (4')	some faint iron staining in the first 1m (4')		

** ▲ or ▼ indicate a fining upward (▲) or a fining downward (▼) trend within sections of the core.

Appendix C: Drillers' Well Log Analysis

Incised Valley Fill (IVF) Character: Driller's Logs

A relatively coarse grained incised-valley fill (IVF) deposit was identified beneath the city of Modesto using geophysical logs (Burow *et al.* 2004; Figure C1). The logs show a very coarse grained gravel base that gradually fines upward to sand then fine silt and clay. To further investigate the location of the identified IVF in the Modesto area, I evaluated approximately 10,000 driller's well logs from the California Department of Water Resources (provided by the US Geological Survey). While well logs are notorious for irregular quality and potential inaccurate subsurface descriptions, drilling through thick gravel, such as that expected with the IVF basal deposits, would cause a significant change in the drill rig character and possibly require a change in the drill bit. Thus, I assume that thick gravels are consistently more accurately recorded than other deposits within driller' well logs.

However, due to the potential variable quality of well logs, a subjective ranking system from 1 (highest quality) to 4 (lowest quality) was created to filter out the best quality logs. Ranks were also assigned in-between each of these four main categories. The intermediate groups were reserved for the few logs that were slightly greater in quality or slightly lower in quality than the category to which they would be assigned. Subjective ranks were assigned to each well based on the following factors that impact the quality of the logs and thus their rank:

- **Gravel thickness**
  - Gravel 5 meters or greater indicated possible IVF deposits present.
- **Drilling method**
  - Cable tool drilling logs were considered more reliable than mud-rotary logs because the cable tool drilling method produces a sample for the

driller that is not mixed in drilling mud and allows more detail to be described.

- **Stratigraphy—character of the IVF**
  - The fining upward succession of thick gravel overlain by thick sand then silt or clay was expected in IVF deposits (Weissmann *et al.,* 2002b, 2004).
- **Driller**
  - Some drillers consistently recorded more detail than others. Lack of quality for a particular driller was also assessed by the uniqueness of each log. Wells within the same section were noted to have exactly the same stratigraphy recorded by the same driller, which is unlikely in the fluvial fan deposits.
- **Total depth of the log**
  - Some of the logs did not record to the depth of expected incised valley fill bases. Logs from wells that were 60 meters deep or greater were given preference. Some of the logs terminated within the basal gravel, and therefore were not useful for defining the absolute depth of the IVF.
- **Level of detail in the log**
  - The level of detail in a log was measured by the lithologic description and the amount of detail in the vertical succession of units. The presence or absence of color and sediment size descriptors was noted in the ranking process. Some of the driller's produced logs that lacked very little detail vertically. For example, a well with a depth of 100 meters or more was described as 3 or 4 thick units of sand and clay. This resolution makes identification of the IVF much more difficult.

It is important to note that the logs were assigned ranks on a combination of the above factors. No one category outweighed the others consistently in importance. An incomplete log that shows IVF stratigraphy, a log recorded by a driller that consistently produced poor quality logs but that clearly shows the IVF stratigraphy, or a log where the stratigraphy appears slightly irregular could all receive the same ranking. Although this method is subjective, very few wells (<100) that recorded thick gravel units were difficult to describe given the above guidelines. A description of wells ranked 1 through 4 is included below.

<u>Rank 1 Wells</u>

A well assigned a rank of 1 denotes the best representation of the incised-valley fill (Figure C2).

- A thick gravel base fining upward to sand then silt and clay.
- The drilling method was mostly cable tool.
- Several geophysical logs are also included in this category.

Rank 2 Wells

A well assigned a rank of 2 denotes a good representation of the incised-valley fill (Figure C3).

- A moderately thick gravel base fining upward to sand then silt and clay.
- Wells in this category show a slightly less distinct fining upward trend of the IVF: thin sand or sand and clay alternating overlie the gravel.
- The drilling method recorded on the driller's logs was mostly mud-rotary and some cable tool.

Rank 3 Wells

A well assigned a rank of 3 denotes a poor representation of the incised-valley fill (Figure C4).

- A thin sandy gravel base fining upward to clay or sand then silt and clay.
- Wells in this category show a less distinct fining upward pattern of the IVF: thin sand or thick clay overlie the gravel.
- The drilling method recorded on the driller's logs was mostly mud-rotary and some cable tool.

Rank 4 Wells

A well ranked 4 denotes the poorest representation of a possible incised-valley fill (Figure C5).

- Contains relatively thin gravel and does not resemble the ideal fining-upward succession contained within the incised-valley fill deposits.
- The drilling method recorded on the driller's logs was mud-rotary.

Figure C1: Resistivity log of selected test holes near Modesto, San Joaquin Valley, California. (Adapted from Burow, et al., 2004)

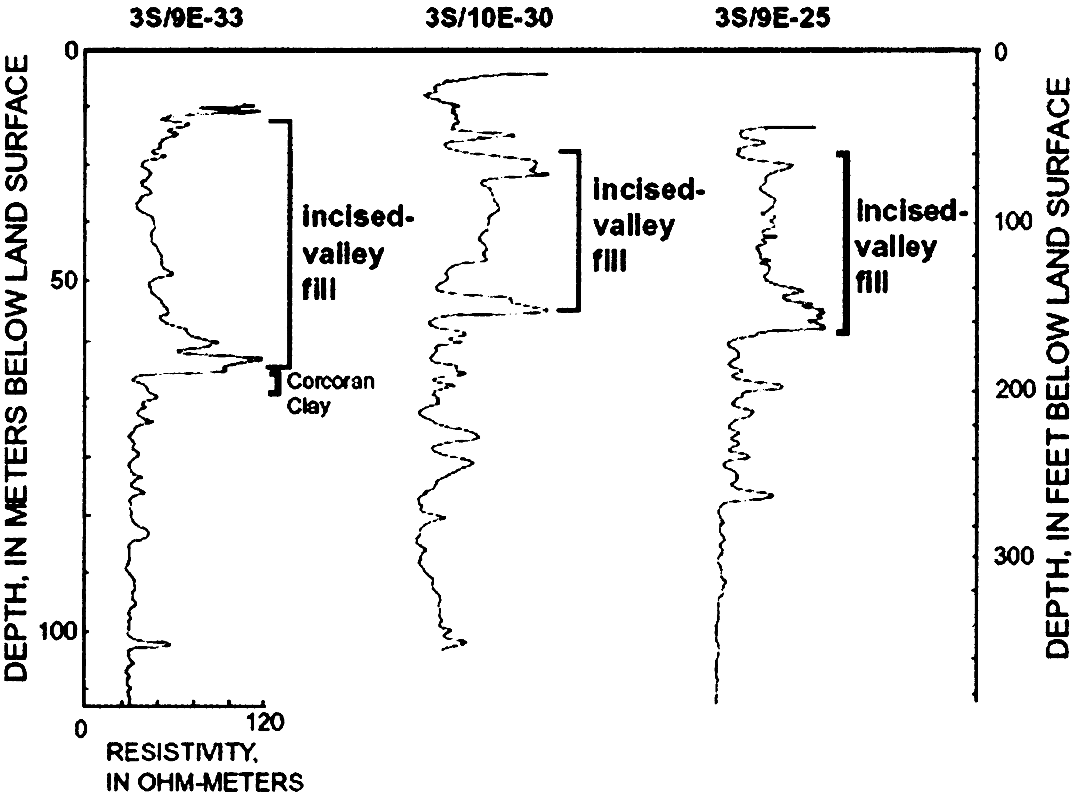

Figure C2: Driller's Well Log: Rank 1 example log. This log was drilled with a cable tool and includes detail as well as the expected IVF stratigraphy. NOTE: The well logs record depth from the surface in feet.

(12) WELL LOG: Total depth 268 ft. Completed depth 264 ft.

from ft.	to ft.	Formation (Describe by color, character, size or material)
0	5	topsoil
5	7	clay
7	10	silty sand
10	12	sand
12	13	silty clay
13	22	sand
22	33	brn. silty clay
33	36	hard clay
36	39	sand & gravel
39	48	set sand
48	66	clay
66	110	coarse sand
110	126	sand & cobbles
126	134	sand & gravel
134	153	sand
153	180	sand & colbbles
180	191	brn. clay
191	193	set sand
193	194	sand & gravel
194	199	brn. clay
199	202	set sand & gravel
202	219	clay
219	221	sand & gravel
221	223	brn. clay
223	225	silty clay
225	230	silty sand & gravel
230	232	brn. clay
232	235	sand & gravel
235	247	red clay
247	253	set silty clay
253	264	red clay
264	268	sand
268	+	clay

FINES

SAND

GRAVEL

OUTSIDE CORC CLAY AREA

Figure C3: Driller's Well Log: Rank 2 example log.

(12) **WELL LOG:** Total depth 370 ft. Depth of completed well 350 ft.

from ft.	to ft.	Formation (Describe by color, character, size or material)
0	2	Silty clay
2	7	Clay
7	9	Sandy clay
9	16	Sand
16	20	Gravel and Sand
20	22	Sandy gravel
22	26	Clayey sand
26	39	Clay
39	47	Clayey sand
47	54	Clayey sand, dense
54	58	Clayey sand and gravel, dense
58	61	Sand, dense
61	65	Clayey sand, red
65	75	Clayey sand, tan
75	81	Sand
81	86	Clayey sand
86	95	Sand
95	115	Claey sand
115	127	Sandy clay
127	132	Gravel
132	153	Sand & Gravel, dense
153	165	Clay
165	171	Clayey Sand& Gravel, hard
171	187	Clayey Sand & Gravel, vy hd
187	192	Clay, swelling
192	212	16 Mesh Clayey Sd & Grvl, vy hd
212	214	Sand, loose
214	256	Clayey Sd & Grvl, vy hard
256	258	Sandy gravel, loose
258	295	Clayey sand and gravel
295	297	Gravel to 3"
297	306	Clayey Sd & Grvl, Grvl 3/8"
306	326	Silty sand
326	329	Sand, loose
329	357	Silty sand w/ layers loose S
357	370	Clayey sand and gravel

OUTSIDE CORC. CLAY AREA

FINES

SAND

GRAVEL

Figure C4: Driller's Well Log: Rank 3 example log.

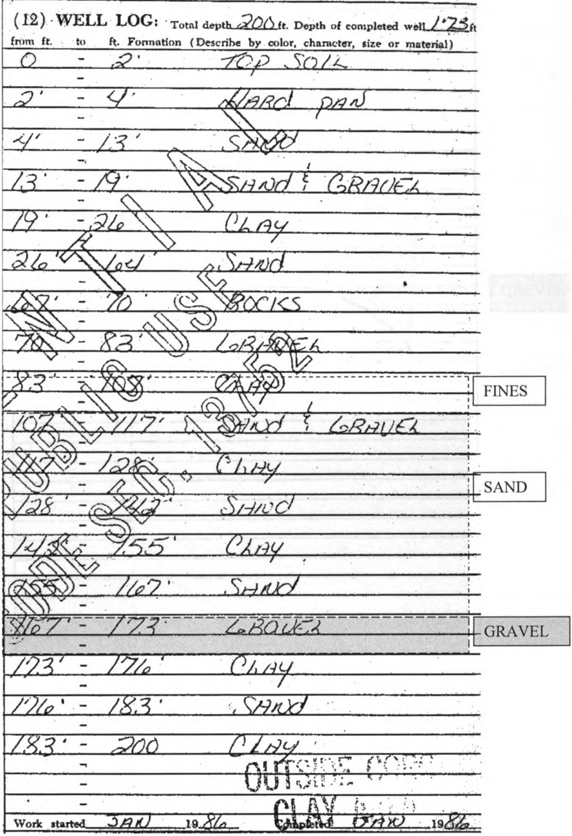

(12) WELL LOG: Total depth 200 ft. Depth of completed well 173 ft

from ft.	to ft.	Formation (Describe by color, character, size or material)
0	2'	TOP SOIL
2'	4'	HARD PAN
4'	13'	SAND
13'	19'	SAND & GRAVEL
19'	26	CLAY
26'	64'	SAND
68'	70'	ROCKS
70'	83'	GRAVEL
83'	107'	CLAY
107'	117'	SAND & GRAVEL
117'	128'	CLAY
128'	142'	SAND
142'	155'	CLAY
155'	167'	SAND
167'	173'	GRAVEL
173'	176'	CLAY
176'	183'	SAND
183'	200	CLAY

Work started JAN 1986 Completed JAN 1986

Figure C5: Driller's Well Log: Rank 4 example log.

GEOLOGIC LOG

ORIENTATION (✓) X VERTICAL ___ HORIZONTAL ___ ANGLE ___ (SPECIFY)

DEPTH TO FIRST WATER ______ (Ft.) BELOW SURFACE

DEPTH FROM SURFACE		DESCRIPTION
Ft.	to Ft.	*Describe material, grain size, color, etc*
0	7	Soil
7	16	Sand
16	30	clay
30	36	Sand
36	50	Clay & Sand Streaks
50	102	Clay
102	112	Gravel & Rocks
112	118	clay
118	123	Sand
123	150	Clay & Shale
150	167	Gravel & Rocks
167	185	Clay
185	192	Sand & Gravel
192	198	Sandy Clay
198	200	Set up Gravel
200	235	clay

GRAVEL

TOTAL DEPTH OF BORING 235 (Feet)

TOTAL DEPTH OF COMPLETED WELL 210 (Feet)

Appendix D: Sequence Boundary Surface Generation

The stratigraphy of the area was modeled by generating surfaces of the sequence boundary paleosols. These boundaries include the continuous paleosol surface and the incised valley sides and base.

Riverbank Paleosol with Modesto IVF

To generate the Riverbank paleosol, the ground surface was assumed to be a sufficient estimate of the Riverbank fan surface because the overlying Modesto formation that covers the area is only a thin veneer across the fan surface (*Bennett*, 2003; *Weissmann et al.*, 2006; Bennett *et al.* in press). This assumption allowed the Riverbank paleosol surface to be created using the modern 30-meter DEM.

1. The DEM raster file, or grid, was clipped manually in ArcMap with the N-Bands Raster Clipper tool, which can be downloaded from the ESRI website (Multi-Bands Raster Clipper v1.2 for ArcMap 9.x at http://arcscripts.esri.com/details.asp?dbid=13474).
2. Because the file size of the 30-meter DEM grid was very large, the 30-meter resolution of the DEM was increased using the AGGREGATE expression in ArcMap Spatial Analyst.
    a. In spatial analyst, select raster calculator and type in the following map algebra syntax: aggregate ([name of grid], [cell factor], [aggregation type], truncate, data).
    b. The cell factor (13.333) was calculated to make the cell size 400 meters (400/30=13.333).

c. The aggregation type "mean" was chosen as the method for calculating the output value of each cell.

d. "Truncate" refers to how the calculator will manage boundaries. The truncate option reduces the number of rows and/or columns by one. This option allows truncation of the input grid at the bottom and right boundaries so that the number of rows and columns will be a multiple of the cell factor. This means that the output grid may be smaller then the input. In the case of the input 30-meter DEM, the grid was clipped sufficiently large enough to account for the potential shortening by this function.

e. The "data" parameter specifies that if the 30-meter DEM had a NoData value, it would be ignored in the calculation of the new output grid.

3. The new coarser grid was converted to a point shapefile in Arc GRID with the GRIDPOINTSHAPE function or in ArcMap Spatial Analyst.

   a. The syntax required for this is: GRIDPOINTSHAPE ([name of grid to be converted]).

   b. An alternate method is available in ArcMap to convert the raster file to a point shape file. In the Spatial Analyst menu, select "Convert" then select "Raster to Feature". Be sure the "Output geometry type" is point. The "field" specified should be the column with the elevation data.

4. Using the shapefile of rank 1 and 2 wells delineating the presence of the Modesto Formation IVF basal gravel between 24 to 38 m (80 to 125 ft) (Appendix A), polygon shapefiles of the proposed incised valleys (both the IVF scenarios, the

small Modesto Formation valley, and the larger valley) were created. The width of the valley was approximated from measurements of the modern valley: 0.7 to 1.6 kilometers. Because there was little information on the actual IVF width, we assume that the current valley is a good representation of the geometry of past interglacial incised-valleys.

5. The polygon shapefiles were then converted to point shapefiles.
    a. To do this, the polygons were first converted to grids (raster files). In Spatial Analyst, select "Convert" then "Feature to Raster". The grid cell size specified was 200 meters.
    b. To convert the raster file to a point shape file, return to the same menu, only this time select "Raster to Feature". Be sure to convert the file to a point shapefile. The "field" specified for the conversion does not matter because raster file did not have any relief. The elevation of the valley bottom will be manually added in the following steps. The result is a grid with rows and columns of points (or ghost wells) spaced 200 meters apart delineating the location of the IVF.
6. Once the IVFs were delineated as a 200-meter spaced point shapefile, elevations of "ghost" wells were assigned to the valley bottom with a gradient of 0.0004 ("ghost" wells were used to enforce our conceptual model of the incised valley geometry). The gradient value was obtained from measurements of the modern interglacial river gradient in Weissmann et al. (2006). To assign the elevations, the rank 1 and 2 well shapefile was plotted with the ghost well point shapefile. Rank 1 and 2 wells with elevations that matched the expected gradient of the

basal gravel were used as anchors to calculate and then assign elevations to the "ghost" wells situated between them (see description of RB valley below and Figure D1 for image of implementation of "ghost" wells).

7. To insert the IVF point into the Riverbank paleosol surface, the polygon coverage was used to select all points in the DEM within the area of the Modesto IVF polygon.
    a. In ARC Map the "Select by Location" feature was used to select all points that "are contained by" the polygon. A buffer of 50 meters was applied. Once the points were selected, they were removed.
8. The Modesto IVF point shapefile was then used to fill in the valley floor elevation points.
9. The point shapefile that resulted from the merging of the DEM and the Modesto IVF was then used to generate a grid of the surface in ArcMap Geostatistical Wizard using the Local Polynomial Function A cell size of 300 meters was chosen. The resulting surfaces are shown below in figures 1 through 4.

Upper Turlock Lake Paleosol with Riverbank IVF

The Upper Turlock Lake (UTL) surface was not generated from a preexisting surface, and therefore was created in a series of steps with multiple sources of data.

1. First, the elevation of the Corcoran clay was used to estimate the elevation of the Turlock Lake surface. The Corcoran clay elevation was estimated by sorting out "blue clay" or "blue silt" from the USGS texture database (described in *Burow et al.*, 2004). These data were saved in an individual database and plotted in ArcMap using the plot XY data option. In ArcMap, points were selected by depth

("Select by attributes"). An estimated depth of 60 meters (~200 feet) for the Corcoran Clay was obtained from *Burow et al.* (2004), so a range of 55 to 67 meters (180 to 220 feet) was applied to select the Corcoran Clay. The elevations were calculated from the "land surface elevation" minus the "top depth" of the Corcoran clay. Because this database search limited the depth range for the Corcoran clay, most of the points plotted were clustered in a band that runs the length of the study area approximately 100km east of the San Joaquin River.

2. To determine the elevation of the upper Turlock Lake (UTL) paleosol, the thickness between the Corcoran Clay and the Turlock Lake paleosol was added to each of the points in the Corcoran Clay database, using the "calculate values" feature in the ARC Map attributes table. MRWA, the core drilled in the distal portion of the fan, is located in the area where most of the Corcoran Clay points were identified in the database; therefore the thickness added to the Corcoran Clay points was obtained from the MRWA core descriptions. The MRWA thickness between the UTL top and the top of the Corcoran Clay was estimated to be 23.5 meters (77 feet). Estimates from Lettis (1982) verify that this is a reasonable value.
3. Once all of the Corcoran Clay data points had been converted to UTL top elevations, other data points were added. Supplementary points added to the database of UTL elevations include (1) the land surface elevations of the outcropping UTL from soil maps (*Weissmann et al.*, 2006) and (2) the elevation of the UTL approximated in the two cores described (MREA and MRWA). The

combination of these data in a point shapefile (Figure D2) was used as the input to generate the UTL surface in Arc GRID.

4. In Arc GRID, the TREND surface interpolation function was used to make the UTL surface, which uses a polynomial regression technique to fit a least squares surface to the data set. This function was chosen because it creates a smooth surface in a raster file format. Because this method attempts to find a best fit for the entire surface, the resulting surface may not go through many of the input data points. A low root-mean square (RMS) error (~7.928) and general shape of the surface were used as indicators of the generated surface's accuracy.
   a. The syntax used in ARC GRID is as follows:
      i. **TREND (<point_cover | point_file>, {item}, {order}, {xmin, ymin, xmax, ymax})**
      ii. The <point cover> is the point shapefile of UTL elevations that was used to generate the surface.
      iii. The item is the elevation of the UTL surface in the shapefile that will be used to make the surface.
      iv. The order used was 2. This was used after experimentation with other orders, which produced unrealistic representation of the surface.
      v. The coordinates for the area to be interpolated were (-125696, 1564302, -35442, 1663440) in NAD 1983 Albers projection.
   b. The elevation of the TREND surface/ grid was checked with the Riverbank surface to be sure that they do not intersect, as realistically, the

UTL would not overlie the younger Riverbank Formation. To ensure that the UTL was not above the Riverbank in any locations, ArcMap's "Raster Calculator" in Spatial Analyst was used.

   i. In Raster Calculator, the following expression was used:

      1. con ([UTL grid] <= [Riverbank grid], [UTL grid], [Riverbank grid]).

      2. This conditional statement says that if the UTL grid is less than or equal to the Riverbank, then the output grid should be assigned the UTL grid elevation, if not, the output grid should be assigned the Riverbank elevation.

5. The raster file of the UTL fan surface that was created in TREND was then converted to a point shapefile in ArcMap in Spatial Analyst (see above in step 3b of the **Riverbank Paleosol with Modesto IVF**).

6. Similarly to the methods described above for the Riverbank paleosol surface, polygon shapefiles of the proposed Riverbank incised valleys were used create "ghost" wells assigned elevations of the IVF bottom gradient (Figure D1). The IVFs were added to the UTL fan surface (See steps 4-9 in **Riverbank Paleosol with Modesto IVF**).

   a. One difference between the generation of this valley bottom and the Modesto valley is the correction for subsidence. Because the Riverbank Formation is older (~130 to 450 ka) (Lettis, 1988; Weissmann *et al.*, 2002b), the impacts of subsidence were calculated into the gradient. The valley bottom was assigned a gradient of 0.0017. Subsidence was calculated from a rate of 0.2 mm/yr, or 0.0002 m/yr (*Lettis*, 1988) over a span of approximately 330 ka. This results in about 66 meters of subsidence, which increases the slope by 0.0013. When added to the modern valley gradient of 0.0004 is equal to 0.0017.

7. The resulting surfaces are shown below in figures D3 through D6.

Figure D1: This figure shows a map view of the use of ghost wells used to delineate the IVF. In this example, the black dots show the ghost wells used to delineate the RB IVF. The surrounding gray dots represent the elevation of the paleolsol surface. This point data was used to interpolate the Turlock Lake sequence boundary surface.

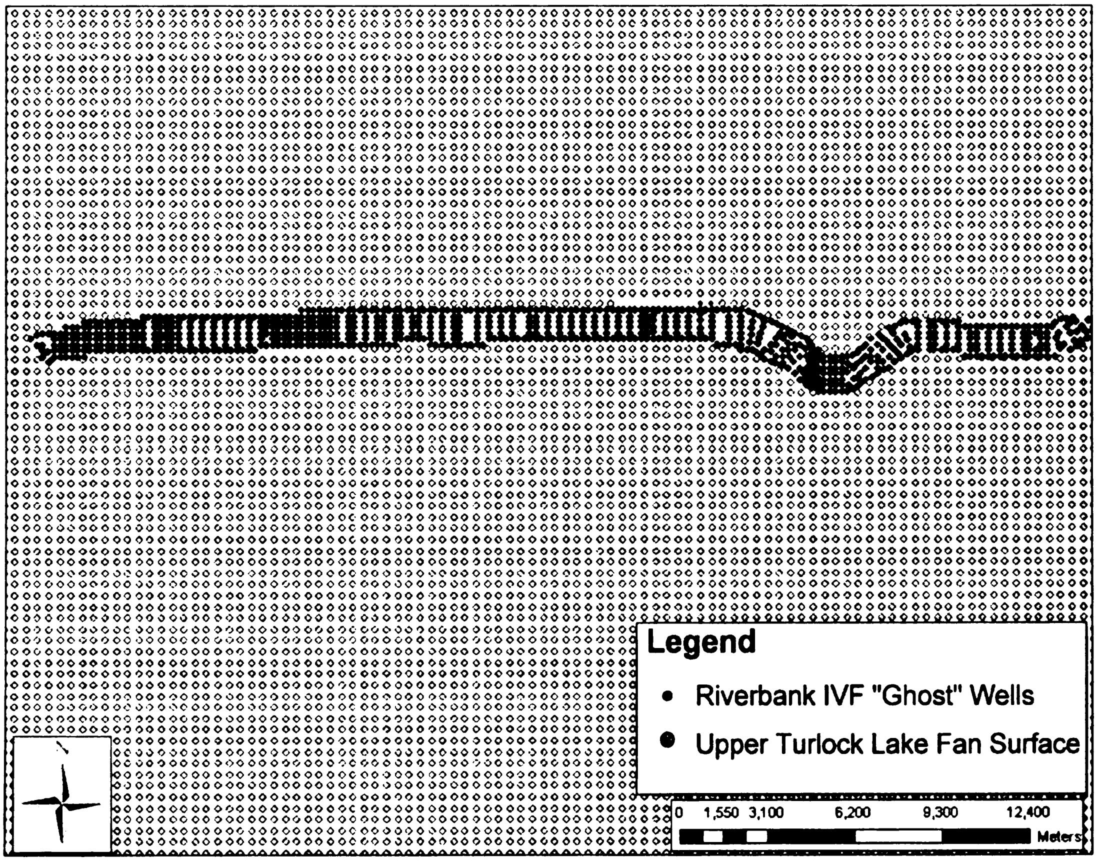

Figure D2: This map shows the location of the Corcoran Clay wells found in the USGS database. The dense clusters of points in the eastern portion of the map mark areas where the Turlock Lake formation outcrops. These points were used to interpolate the UTL sequence boundary surface.

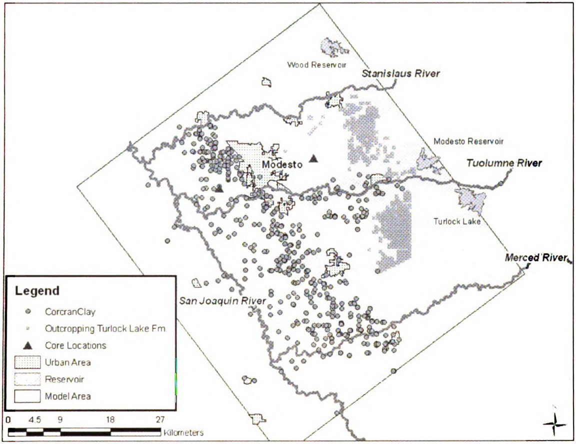

Figure D3: The Riverbank Formation surface with the Tuolumne River large Modesto IVF above the upper Turlock Lake Formation surface with the Tuolumne River Riverbank IVF (RBML). NOTE: Surfaces are exploded 100 meters.

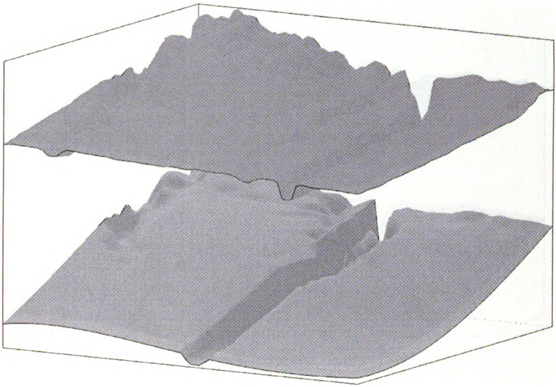

Figure D4: The Riverbank Formation surface with the Tuolumne River small Modesto IVF above the upper Turlock Lake Formation surface with the Tuolumne River Riverbank IVF (RBMS). NOTE: Surfaces are exploded 100 meters.

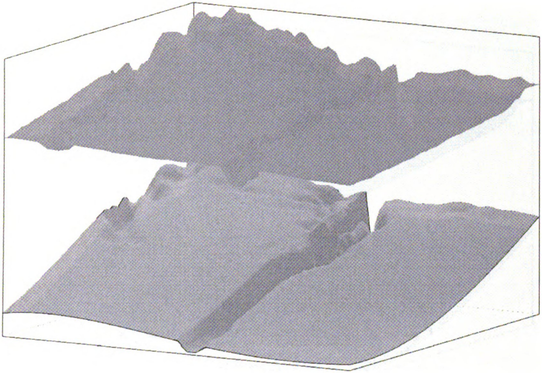

Figure D5: The Riverbank Formation surface with the Tuolumne River large Modesto IVF above the upper Turlock Lake Formation surface with the Tuolumne River Riverbank IVF and the Stanislaus River Riverbank IVF (RBSTML). NOTE: Surfaces are exploded 100 meters.

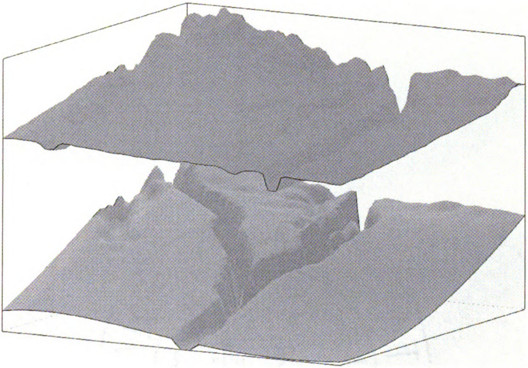

Figure D6: The Riverbank Formation surface with the Tuolumne River small Modesto IVF above the upper Turlock Lake Formation surface with the Tuolumne River Riverbank IVF and the Stanislaus River Riverbank IVF (RBSTMS). NOTE: Surfaces are exploded 100 meters.

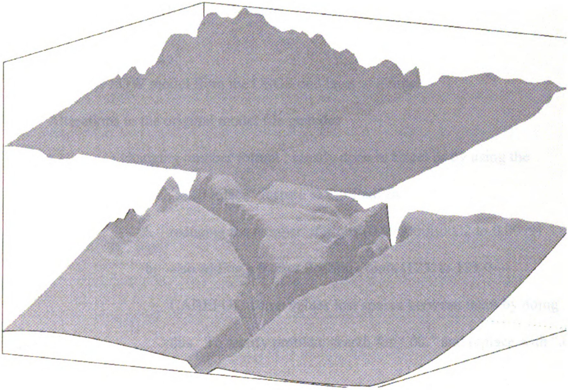

Appendix E: USGS Model

Details of the USGS model are described in Chapter 2 of this thesis. The following appendix details how the original USGS MODFLOW model was opened. To open the original USGS MODFLOW model:

Open the MODFLOW model from the USGS one layer at a time.

Alterations to the original model file include:

(1) changing number format : mostly done in Excel or by using the "Search and replace" feature in EditPadPro
   a. reducing the number of digits (0.990000E0002 to 0.0099)
   b. also adding a 0 after floating points (123. to 123.0—CAREFUL: some values lost spaces between them by doing this. To rectify problem search for ".00." and replace with ".0 .0")

(2) reducing the number of spaces in between numbers: done in Excel and the "Search and replace" feature in EditPadPro--(save as a comma delimited file and then replace commas with spaces)
   a. e.g.- from 5 or more to just one

(3) Reducing the number of hard returns within a row of data (files are set up so that they list data by row (153 rows) for each layer (16 layers). There are also 137 columns. To complete step 3, I used a script that Anthony wrote in Matlab—see "dat_read.m" in C:\users\Amy\May312005\USGSModelFiles\Tuolumne060605\USGS_used_4_final_model.

(4) ALSO MAKE EXTERNAL FILES INTERNAL—I cut and pasted all of the external files into the .bcf file. GMS would not read the external files.

To generate Kdatasets.gpr

Once the model will read the discrete (.dis) and (.bcf) file by using the above methods, the K values must be imported separately. GMS would only read one layer of K data at a time. (I think this is because they are read in as 3D data sets, which makes K values in all other layers zero.)

(1) Open the MODFLOW model in GMS with the K, Leakance, and Wetdry values for ALL layers "INTERNAL". MODFLOW will only read the first layer with values into the model. This means that ONLY the K, leakance, and wetdry values for layer 1 will be read into GMS when it opens.

(2) Once GMS opens, save this model as "Kdatset.gpr"—CLOSE THE MODEL

(3) Go into the "Kdatset.mfs" file using Microsoft Explorer to set the origin (ORG -83756.2 1573010 0.0) and the rotation angle (ROT 37).

(4) Re-open the model "Kdataset.gpr".

(5) Click on the 2D grid module.

(6) Click on the "Grid" dropdown menu and "Create grid". Enter the following:

a. X origin: -83756.2 Y origin: 1573010 Z origin: 0.0

b. Length: 54800 Length: 61200

c. Number of cells: 137 Number of cells: 153

d. IN BOTTOM RIGHT CORNER, FILL IN ROTATION ANGLE: 37

(7) Go into the 3D grid module and click on the "MODFLOW" dropdown menu. Select "BCF Package" and view AND export the K, leakance, and wetdry values for Layer 1. EXPORT the values from "Layer to 2D data set"—File names should be something like "layer1_k", "layer1_leak", and "layer1_wetdry".

(8) Go into the 2D grid module and right click on each of the 2D data sets just generated, and EXPORT the data as and ASCII file (CAREFUL—the default file type is Binary—BE SURE TO CHANGE THIS!!!).

(9) Once the data have been saved as ASCII files they can be imported into any model later (see step 13). After data has been saved, SAVE "Kdataset.gpr" and CLOSE out of the model.

(10) Open the original MODFLOW .bcf file. This time, delete all of the values for layer 1 (including K, leakance, and wetdry). Fill in "CONSTANT 0.0 (free) 0" for each of those data sets. Now Layer 2 data should be the first data set visible in the .bcf file. Save and close this file.

(11) Open a new GMS file. Open the original MODFLOW file (.nam) . (This step is similar to step 1).

(12) Repeat steps 7-10 for each successive layer. NOTE: Only Layers 1 through 7 have "wetdry" data. Layers 8 through 16 are confined and have transmissivity values, NOT hydraulic conductivity values.

(13) Once all of the ASCII files have been generated, they can be opened in GMS as 3D data sets.

(14) Open "Kdataset.gpr" then go to "File—Open" and select the ASCII file to import. Once all files are open as 3D data sets, they will need to be converted into 2D data sets (next step). *This is necessary because importing a 3D data set into the BCF package will make all values in other layers zero. Transforming to a 2D ensures that only the values of the 2D layer to which you import the data will be changed.*

(15) To convert from 3D to 2D, click on the file to be converted so that the text is bolded.

(16) Go to the "Data" dropdown menu and select "3D data to 2D data".

(17) ***BETTER WAY:*** **Go into the 3D grid module and click on a data set. Go to the DATA drop down menu. Select "3D data to 2D data". In dropdown box, select "Value from k layer" then in the adjacent box, match the layer of K values to the layer specified in the data set to be converted. Save the file as, for example: "lay1_layer1_k" or "lay8_layer8_trans". This results in a 2D array ASCII file when exported.** *OLD WAY—DID NOT WORK: Make sure the file you want to convert is selected, and that the "Maximum value in the ij column" is selected and click "OK". When a 2D data set is saved as a 3D data set, a value of zero is filled in for all unknown numbers. Any K, leakance, or wetdry number for a given layer will be greater than 0, therefore the maximum number in the ij column will be K (or leakance, or wetdry) for the layer file being converted.*

(18) SAVE the new 2D file with the old 3D file name.

(19) Once all of the layers have been converted into 2D grid, go back to the 3D grid module and click on the MODFLOW dropdown menu. Go to the "BCF Package" and begin importing the 2D data to each layer.

a. NOTE: to do this go into each layer (1-7) and (1) click "hydraulic conductivity", "leakance" or "wetdry" (2) select the appropriate layer (3) click "2D data set to layer" and pick the data set you want to fill in. DO NOT FILL IN HYDRAULIC CONDUCTIVITY FOR LAYERS 8 THROUGH 16.

b. FOR (8-16) fill in the "transmissivity" and the "leakance" ONLY

(20) SAVE ALL WORK PERIODICALLY.

To open sequence boundary surfaces in GMS

(1) in 2D scatter point module

(2) Select "File" then "Open"

(3) "Import as scatter points"

(4) assign scatter point file a name

(5) with this data set active, go to "Interpolation" drop down menu

(6) Select "Interpolate -> 2D grid"

(7) Select interpolation method

a. "Inverse distance weighted" and leave default options

i. "Nodal Function" should stay as "Gradient plane"

ii. "Computation of nodal function coefficients" should stay as "Use subset of points"

iii. "Computation of interpolation weights" should stay as "Use subset of points"

(8) repeat until all data files have been opened in GMS

(9) Next, export the 2D grid data to an ASCII file and save for use within the code.

Appendix F: Model Generation

The following documentation details the inputs for the model adapted from the USGS. The initial model from the USGS was developed by Steve Phillips (Steve Phillips, Hydrologist; U.S. Geological Survey, 6000 J Street, Placer Hall, Sacramento, CA 95819-6129; sphillip@usgs.gov; phone: 916-278-3002; fax -3071).

A. Flow Package

The Layer Property Flow (LPF) was chosen to allow more flexibility in entering parameters (the Block-Centered Flow (BCF) package was used in the USGS model). Values such as the vertical hydraulic conductivity were incorporated into the model without conversion of the original "vcont" values (or Kv/ thickness), but rather through the Kh/Kv ratio that calculates the vertical conductance based on the layer elevations.

B. Solver

Preconditioned Conjugate Gradient 2 (PCG2) solver was used for this model (the USGS model also used the PCG2 solver). The initial solution for the adapted model was generated using the geometric multigrid (GMG) solver and starting heads all equal to the elevation of layer 1. The solution generated using the GMG was then used as a starting head and allowed the rest of the models to be solved with the PCG2 solver.

C. Discretization

Changes to the discretization of the USGS model were made in layers where the IVFs are located (approximately layers 2 through 7 in the old model) (See Figure 10 in Chapter 2). The new discretization is finer and better models the IVFs. The adapted model layers 2 through 16 (old layers 2 through 7) use the IVF base as a layer surface. The original layers 2 through 7 in the USGS model were assigned as a percent thickness between the ground surface elevation and the top of the Corcoran Clay layer. In the adapted model, the slope of the layers 2 through 5 match the Modesto small IVF base and 6 through 16 match the slope of the Riverbank IVF base.

One problem that arose with the new discretization was the new layers intersected with some of the older layers due to varying gradients. To fix this, layers 17 through 22 (USGS model layers 8 through 11) were slightly altered in the eastern portion of the model to prevent intersection of layer elevations. Layers 23 through 27 (USGS layers 12 through 16) were well below the IVF and were not affected by the gradient of the new surfaces, thus the original USGS top and bottom elevations were preserved in the adapted model.

The following instructions describe how the modified model was discretized.

1) Open a new model in GMS 5.0.
    a) Create a 3D grid with at least 8 layers.
    b) In the MODFLOW super file, be sure to set the correct origin and rotation
        i) Rotation 37 degrees,
        ii) ORIG
            (1) (x) -83795.7
            (2) (y)1572727.3
            (3) (z)0.0 (from well code)
        iii) length
            (1) (x length) 54800
            (2) (y length) 61200
        iv) Cells 400 by 400m

v) (x) 137 columns (y) 153 rows

c) Be sure the LPF package is activated.

d) Import the top and bottom elevation from the old model. Import layers 11-16 of the old model as the basal layers of this model. (export data and import to my model)

2) Use the base of IVF to determine the dip of the upper most grid layers.

i) To do this, use the IVF base grid surface (same as the data used for the calculations of the gravel, sand and fines top elevation of the IVF).

(1) Generate in Arc GRID using the TREND function

(2) Assign coordinates so that the surface generated will cover the entire model area.

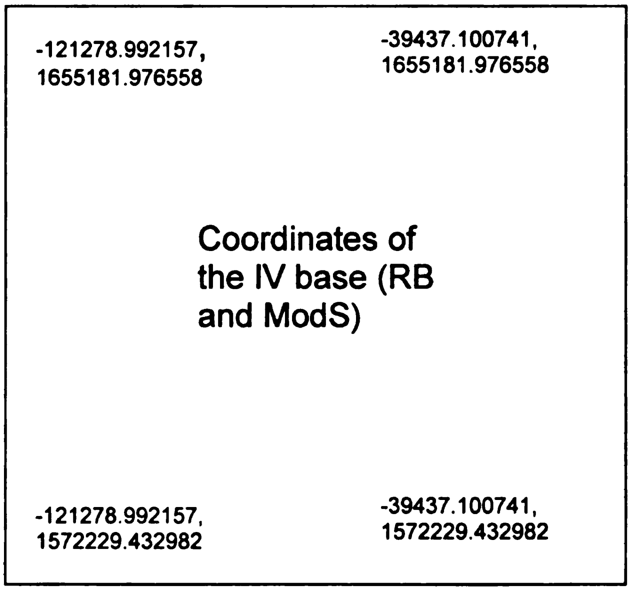

(a) RIVERBANK VALLEY and MODESTO VALLEY surface

(i) Resample original 12m cell surface from initial IV base (used in code and to make gravel, sand , and fines surfaces) to 50m cells

1. In ArcMap Toolbox—Data Management—Raster—Resample

(ii) Convert raster to point file in Arc GRID

(iii)Make TREND surface with 50m cells in Arc GRID

(iv)Resample trend surface to 300m cells

1. In ArcMap Toolbox go to—Data Management—Raster—Resample

(v) Check Riverbank surfaces using the raster calculator in ArcMap Spatial Analyst to find the absolute difference between the surfaces to be sure there is not a significant difference.

1. The maximum difference between the initial 12 m and the resampled 50m grid is minimal (calculates 0).
2. The maximum difference between the 50m grid and the trend surface is 0.012m.
3. The maximum difference between the 50m trend surface and the resampled 300m surface is 0.095m.
4. Difference between the original 12m cell surface and the final 300m surface was ~0.01m.

(vi)Check MODESTO surfaces using the raster calculator in ArcMap Spatial Analyst to find the absolute difference between the surfaces to be sure there is not a significant difference.

1. The maximum difference between the initial 12 m and the resampled 50m grid is 0.05m.

2. The maximum difference between the 50m grid and the trend surface is 0.017m.
3. The maximum difference between the 50m trend surface and the resampled 300m surface is 0.019m.
4. Difference between the original 12m cell surface and the final 300m surface was ~0.053m.

ii) INTERSECTION OF SURFACES: The Riverbank valley base and Modesto valley base surfaces intersect in the southern portion of the model grid. To fix this, there are two steps using the raster calculator in ArcMap will be used.

(1) Initial adjustment: The following conditional statement was used to calculate the new surface:

(a) con(RIVERBANK>= MODESTO, MODESTO – 5, RIVERBANK)

(2) Thin cells-- To fix thin areas between the Modesto IV base surface and the Riverbank IV base surface…

(a) m-r = [MODESTO]- [RIVERBANK]

(b) RIVERBANK below MODESTO fix thin cells = con([m-r] < 5, [MODESTO] - 5,[RIVERBANK])

iii) Convert raster file to ASCII file in ARC toolbox then import to GMS as scatter points and reinterpolate to the 2D grid using natural neighbor.

iv) Add layers between the Modesto IVF base and the Riverbank IVF base to make discretization fine enough to capture IVF character (minimum 0.5m thick cells)

v) Both of the IVF base surfaces intersect the Corcoran clay and layers 9 through 11. Use the GMS model checker to auto fix layer errors. In GMS model checker:

(1) Set a minimum thickness of 0.5 m for cell thickness.

(2) Fix layer errors from the top down and preserve the top layers (this is the best way to preserve the known data surfaces: the Modesto IVF, the Riverbank IVF and the Corcoran Clay)

D. Boundaries

The southern and western general head boundary cells in the modified model are the same as in the USGS model. Changes in the GHB conditions were made to the rivers in the central portion of the model and the northeastern boundary. The upper reaches of the Stanislaus, Tuolumne, and Merced Rivers in layer 1 where changed from specified fluxes to general head cells. The GHB condition was removed in several cells (~250) in the northern portion of the model.

The specified flux cells that represent the Stanislaus, Tuolumne, and Merced Rivers in layer 1 of the USGS model were changed to GHB cells in the adapted model (See Figure 8 in Chapter 2). The head elevations at these new locations were assigned based on the ground surface elevation. Using National Geographic TOPO! California, waypoints were marked along the river and imported into ArcMap and plotted as XY data. This point file was then opened in GMS5.0 and used to assign head elevations to the new GHB cells delineating the upper reaches of the rivers. These new head elevations were then added to the input file for the GHB code.

In the USGS model, lack of boundary cells along the rivers was justified because the rivers are disconnected from the aquifer in the area. However, the lack of a boundary in this portion of the model causes unrealistic volumes of water to collect within the river valleys. To maintain the condition that the rivers are not connected to the aquifer in the eastern portion of the model, conductances of the newly assigned GHB cells were reduced. Conductances were assigned using the same calculations as the original river cells (explained below), but without the vertical K river multiplier (vkrivmult) of 10, which lowered the cell conductances to reflect the disconnected surface and groundwater in the area. The cell conductances that were calculated this way include all of the GHB cells delineating the rivers to the eastern extent: cell *I 20 J78* on the Stanislaus River, *I 53 J 61* on the Tuolumne River, and *I 136 J73* on the Merced River (Table F1). The eastern most GHB cells along the river have even lower conductivities to represent the more consolidated geologic deposits in that area. These cells were not only calculated without the vertical K river multiplier but also divided by 2 (Table F2). This allows unrealistic volumes of water to fill the river valley, 5 to 8 meters at most. This condition is also present in the USGS model. To attempt to rectify this unrealistic situation, five cells were added to the head of the Tuolumne River, extending the GHB to the edge of the model. These cells are in Table 2. This helped to reduce the amount of water gained by the stream in the model, but did not correct the problem completely. The river in the adapted model still maintains losing and gaining reaches which is the most parsimonious condition that could be achieved for the model in this study.

In the northeastern-most portion of the USGS model, GHB cells are dry down to an elevation of 10 to 17 meters (33 to 56 feet). To avoid the drying of boundary cells,

some of the boundary cells assigned in the original USGS model were removed from layer 1 through layer 4 in the adapted model. The exact cells where the GHB condition was removed include:

- **Layer 1: I** 1; **J** 76 to 153
- **Layer 2: I** 1; **J** 81 to 153
- **Layer 3: I** 1; **J** 96 to 153
- **Layer 4: I** 1; **J** 111 to 153

General head boundaries were assigned using an adaptation of a code used to develop general head boundaries for the USGS model. Head elevations and cell conductances were assigned using a code adapted from the 16 layer USGS model to the 27 layer model used in this study. This code accounts for the location of the boundary (i.e. north and south lateral boundary, the San Joaquin River in the west, or the river cells in the top active layer).

Head was calculated with a vertical gradient of 0.05 meters of head per meter of depth. The head decreases from layer 1 to layer 17. Initial head values for layer 1 GHB were determined from stream gage data and the area topography (*S. Phillips*, pers. comm., 8/1/05). Layer 18 was set equal to layer 17 to prevent an unrealistic (at this model scale) head change between the low conductivity Corcoran Clay layer and the layer below it. The head was set to increase from layer 19 down to layer 27 in order to generate upward flow in these layers. The gradient of 0.05 meters of head per meter of depth (thickness) was added to the initial start head (values from layer 18). In a manner similar to the USGS approach, this increasing head value was constrained with the sub-condition that the calculated head value could not exceed the assigned head value in layer 1. If this condition occurred, the calculated head value for that layer would be ignored and the cell would be assigned a head equal to the head in layer 1).

Downward flow

ghbhead =ghbhead-(totthick*gradient) **(1)**

[for layers 1 through18 where head in layer 18 =head in layer 17]

Upward flow

ghbhead =ghbhead+(totthick*gradient) **(2)**

[for layers 19 through 27]

where ghbhead is the head assigned to the GHB cell, and totthick is the thickness from the center of the cell in layer 1 (for the downward flow) or layer 19 (for the upward flow) to the center of the layer for which the GHB head value is being calculated.

The conductance (ghbcond) through the GHB cells was determined depending on the location of the cell in the model: the top layer river cells had different conductance calculations that the rest of the GHB cells. In general, conductance is calculated using two variables: (1) the horizontal hydraulic conductivity assigned to the cell and (2) the cell thickness. Constants also included in the calculation are: (1) cell size (400m) and (2) general head boundary distance (400m).

Preserve Regional Lateral Flow from the East

ghbcond = KH*thick*cellsize/ ghbdist **(3)**

(For GHB cells assigned to northern and southern boundaries and western boundary below layer 1)

GHB cells that delineate rivers in layer 1 allow a small amount of vertical flow, while below layer 1 along the western model edge and for all layers along the north and south extent of the model, the boundary reflects the overall lateral flow from the east. To implement vertical flow, the conductance through layer 1 GHB cells at the location of the rivers was calculated using the vertical hydraulic conductivity, riverbed thickness (1m), river width (25m), and a vertical conductivity multiplier of 10.

Preserve Local Vertical Flow from Rivers

ghbcond = KV * ((cellsize*rivwidth) /bedthick)* vkrivmult (4)

(For GHB cells assigned to rivers in layer 1)

E. Hydraulic Conductivity data

See IVF Fortran code and Vertical Hydraulic Conductivity and Anisotropy Factor Fortran code

Horizontal Hydraulic Conductivities

Horizontal hydraulic conductivities were assigned using the IVF Fortran code (See Appendix G). This code assigns the IVF of the various scenarios based on the elevation at the center of a cell. The output file from this code preserves the general geometry and slope of the valley; however, some manual editing was needed for the hydraulic conductivity of the IVF Fortran output file. The main areas where edits were made are at the head and the mouth of the valley: the head of the valley from j137 to approximately j116 and the end of the valley from j49. The mouth of the valley, in particular lack fines at the top of the valley. General summary of where and why changes were made to the IVF HK files include:

- The stratigraphy at head of the valley was not as well defined as it was farther down valley. For example, the sand pinched out in some areas of the valley (e.g. J134 in the RBMS and RBSTMS model). The upper reaches of the IVF were edited to preserve the stratigraphy and lateral continuous nature of the valley.
- Lateral valley continuity was disrupted most commonly at bends in the river valley. In this case, the valley needed to be widened by a cell width (or 2 cell widths at the most) in areas to maintain connectivity (e.g. J116 in the Modesto small IVF).
- In all of the models, the Tuolumne River Riverbank IVF (RB) has fines largely nonexistent. Fines were added to the areas where they did not exist. The fines are likely under represented because the lower limit elevation of the fines may be slightly higher than the center of the cell. The unit may be too thin to be preserved with the discretization.

The need for manual edits of the IVF Kh file may have been caused by using a different surface generation method for the sequence boundary surfaces (surfaces including the IVF used in the IVF code) than was used to make the IVF base surface (which was used to make the upper layers of the model and in the IVF code to designate the location and Kh of cells in the IVF). Due to limited data, Arc GRID TREND was chosen as the surface generation tool for the IVF bottom surface that was entered in the model discretization. TREND was chosen over the ArcMap Geostatistical Wizard, which was used to create the sequence boundary surfaces, to allow manual designation of the output surface extent (step 2i2 above). The ArcMap Geostatistical Wizard will only extrapolate a surface to a predetermined extent outside of the input data points. Manually assigning the extent of the output surface provided the flexibility to create a surface large enough to cover the model extent. Using the same method of surface generation for both the sequence boundary surface and the IVF base surface for the new model discretization would be ideal, but it was not possible in this case due to a lack of input data points, which prevented the ArcMap Geostatistical Wizard from generating a surface large enough to cover the model area. Minimal lateral and vertical shifting of the valley mostly in the eastern portion of the model was the result of this discrepancy.

Vertical Hydraulic Conductivities

Because the LPF package is used for this model, a leakance value (vcont = Kv/thickness) is not specified. Instead, this model uses an anisotropy factor (Kh/Kv). To calculate this number for the model, a FORTRAN code (See Appendix H) was generated to first, calculate the vertical conductivity from the leakance parameter in the USGS data. This vertical conductivity was assigned to cells in the newly discretized model using the same method as the horizontal hydraulic conductivity: if the new model's cell centered elevation falls between the top and bottom layer elevations of the coarser USGS model the KV from the USGS model will be assigned to the adapted model. Then, the vertical hydraulic conductivity was used to calculate the anisotropy factor (Kh/Kv).

F. Recharge

All of the original recharge values from the USGS land-use approach were maintained in the model (Burow *et al.*, 2004). Recharge values range from 0 to 0.005 m/d or 1.825 m/yr (0.0164 ft/day or 5.986 ft/yr).

G. Evapotranspiration

The original ET values were maintained in the new model: maximum evaporation rate of 1.6 m/yr at land surface and the maximum extinction depth is 2.1 meters below the land surface. These values were assigned based on the water budget in Burow *et al.* (2004).

H. Wells

Pumping wells in this model are the same wells used for the USGS model and include: urban-supply, agricultural, and water-table-control, or have known "drainage". Pumping from the wells was calculated using the same FORTRAN code as was used for the USGS model. Appropriate layer numbers were changed for the newly discretized model (see code). The well code had to be run to produce a separate well file for each model scenario, as several wells intersect the IVF.

I. Reservoirs

Wood Reservoir, Modesto Reservoir, and Turlock Lake are all preserved in the adapted model. The reservoir file was used with the adapted model without any changes to the file format. The vertical conductance of the reservoir, however, was reduced. The values of 0.003 and 0.006 m^2/day were divided by 1.2 (value obtained by manually testing various vertical conductances to constrain the best value). The resulting vertical conductances are 0.0025 and 0.005 m^2/day.

The only other small alteration made in the file is in the heading. The unit number that specifies where the cell-by-cell flow should be recorded was changed to zero. This is the second number in the initial line of the reservoir data array.

Table F1: Cells where the conductance in the upper reaches of the Tuolumne River were reduced by 10 and then 2. It is assumed that the lithologic units here are more consolidated, therefore their conductance is lower.

i	j	k	head	original conductance		New Conductance (Divide by 10 then 2)
87	121	1	28	163.93		81.96500245
87	122	1	28	233.15		116.575
88	123	1	28	391.37		195.6849976
89	124	1	29	438.96		219.4800049
89	125	1	29	128.64		64.3200012
90	126	1	30	277.76		138.8799927
91	126	1	30	204.3		102.15
92	127	1	31	153.32		76.66000365
93	128	1	31	130.46		65.2299988
94	129	1	32	122.12		61.05999755
95	130	1	33	119.37		59.68499755
96	131	1	33	127.74		63.8700012
97	131	1	34	122.28		61.14000245
98	132	1	34	125.52		62.75999755
99	133	1	35	249.4916		124.7457861
99	134	1	36	269.4419		134.7209548
100	135	1	37	227.6779		113.8389331
100	136	1	37	304.0255		152.0127616
101	137	1	37	266.2508		133.1253762

Table F2: Table listing the cells added to the head of the Tuolumne River to attempt to reduce the amount of water within the river valley.

i	j	k	head	Conductance		Kh	Kh/Kv	Kv	con
99	133	1	35	249.4947		86.4	3463	0.024949	249.4947
99	134	1	36	269.4443		86.4	3206.6	0.026944	269.4443
100	135	1	37	227.674		86.4	3794.9	0.022767	227.674
100	136	1	37	304.022		86.4	2841.9	0.030402	304.022
101	137	1	37	266.2558		86.4	3245	0.026626	266.2558

Appendix G: Incised-Valley Fill FORTRAN Code

A. IVF Code Information

1. Use IVF_CODE to assign the original Kh from the USGS model to the cell in the adapted model with the same elevation as the USGS model cell. Be sure to use the code specific to the geologic scenario: without ST or with ST.
2. Files Needed
   a. Elevation data exported from the GMS 5.0.
   b. Kh data from the USGS in ASCII form exported from GMS (no IVF, this code will add them)
   c. Gravel, sand, and fines top elevations for the IVF
   d. File to delineate where the Tuolumne River Riverbank IVF and Stanislaus Riverbank IVF are located. This file assigns the Stanislaus IVF a value of 3 and the Tuolumne River IVF a value of 2.
3. Writes
   a. This will output a new Kh data set for each geologic scenario.

B. IVF Developing Stratigraphy and Assigning Hydraulic Conductivities

1. Development of Top Surfaces of gravel, sand, and fines.
   a. This code relies on the stratigraphy of the area to identify a cell located within the IVF. The code uses a series of logical statements to determine whether the IVF is within the IVF, and if it is, what part of the IVF is the cell located in based on elevation. To do this, the code uses the grid surfaces developed in Appendix D, as well as grid surfaces of the top of the gravel, sand, and fines fractions of the IVF.

b. These surfaces were generated by:

    i. First, creating grid surfaces for the IV base.

        1. Use the point shapefile of each IVF with the valley gradient assigned to generate a surface in Arc GRID using TREND.

        2. The syntax used is:

            a. **TREND (<point_cover | point_file>, {item}, {order}, {xmin, ymin, xmax, ymax})**

            b. The <point cover> is the point shapefile of IV basal elevations that was used to generate the surfaces in Appendix D.

            c. The item is the elevation of the IVF base in the shapefile that will be used to make the surface.

            d. The order used was 1.

            e. The coordinates for the area to be interpolated were (-125695, 1607364, -35303, 1632550) in NAD 1983 Albers projection.

    ii. Obtain the entire thickness of the valley

        3. Using the Raster Calculator function in ArcMap's Spatial Analyst, the thickness of the valley was calculated with the following equation:

            a. **Total IV Thickness** = abs ([fan surface (UTL or RB)] –[bottom of IV surface])

b. The fan surface was either the Riverbank or the UTL fan surface WITHOUT the IVF.

c. The bottom of the IV surface was the Riverbank Tuolumne River, Riverbank Stanislaus River, Modesto Large, or Modesto Small gravel base surface generated in step "i".

4. Percent thickness of each fraction of the IVF (gravel, sand, and fines) were calculated using the grid files in the raster calculator:

a. Gravel thickness= 0.4* [valley thickness]

b. Sand thickness= 0.45* [valley thickness]

c. Fines thickness = 0.15* [valley thickness]

5. Using the thickness calculated above, the elevation of the top of the gravel, sand, and fines surfaces were created by adding that thickness to the valley bottom (for the gravel) or to the elevation of the top of the unit below (for the sand and the fines)

a. Gravel top surface elevation = [bottom of IV valley] + [gravel thickness]

b. Sand top surface elevation = [gravel top elevation] + [sand thickness]

c. **Fines top surface elevation** = [sand top elevation] + [fines thickness]

2. Hydraulic Conductivity Values

   b. The hydraulic conductivity values assigned to the IVF were obtained from Weissmann *et al.* (2004).

      i. Gravel was assigned a Kh of 864 m/d (or $1 x 10^{-2}$ m/s)

      ii. Sand was assigned a Kh of 86.4 m/d (or $1 x 10^{-3}$ m/s)

      iii. Fines were assigned a Kh of 0.0864 m/d (or $1 x 10^{-6}$ m/s)

C. Preparing the files for use in the FORTRAN code

The resulting Riverbank and UTL surfaces with IVFs were used in a FORTRAN code to assign the hydraulic conductivities of the IVF. To preserve a consistent file format and interpolate the ArcMap generated grid to the model grid for the FORTRAN code, the surfaces were opened in GMS 5.0 and interpolated to an existing model grid.

1. To open the surfaces in GMS 5.0, the raster files were converted into an ASCII file.

   a. In Arc Toolbox, look in Conversion Tools, then select "Raster to ASCII" tool.

2. In GMS 5.0, the USGS grid must be defined.

   a. The grid is 153 rows by 137 columns of 400 $meter^2$ cells.

   b. In the 2D grid module, select the Grid dropdown menu, then "create Grid".

      i. Origin (x) -83795.7 (y)1572727.3

      ii. Length (x length) 54800 (y length) 61200

      iii. Number of Cells: (x) 137 columns (y) 153 rows

      iv. Rotation: 37

3. Next, the ASCII file was opened in GMS 5.0 as 2D scatter points.
4. The 2D scatter points were then interpolated to the grid generated by the USGS.
    a. In the 2D grid module, go to the "Interpolation" drop down menu, and select interpolate to 2D grid.
    b. Inverse distance weighted was used to interpolate the surface. A maximum of 1 meter difference in the actual versus interpolated surface was noted based on a random sampling of points.
5. The newly interpolated surfaces were then exported as ASCII files to be used in the IVF FORTRAN code to assign hydraulic conductivity values.
    a. Some file manipulation was necessary prepare the ASCII files from GMS for the code. The exported GMS ASCII files each contain a header providing information the type of data set the file is, the file name, and the number of data points (see sample below). This as well as the list of 1's and 0's, denoting active and inactive cells respectively, needed to be removed.
    b. **Sample GMS Header**

```
DATASET
OBJTYPE "grid2d"
BEGSCL
ND 20961
NC 20961
NAME "elevation2"
TS 0 0
```

AND for 3 dimensional grids

```
DATASET
OBJTYPE "grid3d"
BEGSCL
ND 565947
NC 565947
```

NAME "gmsfil"
TS 0 0

D. IVF FORTRAN CODE

1. General Description of Code

   a. The IVF code uses a series of conditional statements to assign hydraulic conductivity values to cells of the model located within the IVF. Figure G1 shows a flow chart of conditional statements that must be met to assign the predetermined Kh values for the IVF. The elevation of the center of the cell was used to determine (1) if the cell was in the IVF and (2) based on the location, which Kh value it should be assigned. Cells outside of the IVF were assigned Kh values from the USGS model. Cells within the IVF were assigned a Kh value for gravel (864 m/d), sand (86.4 m/d), or fines (0.084 m/d) (Figure G2). For example, if the cell were above the Turlock Lake surface, below the Riverbank surface, above the top of the gravel elevation and below or equal to the bottom elevation of the top of the sand, then the cell is in the IVF and would be assigned a Kh of sand. As is illustrated in figure G2, the fines represent a small fraction of the total IVF thickness and the likelihood of the center of the cell falling either below or above this relatively thin interval is high, thus the fines are under represented in this model.

Figure G1: A flow chart of the conditional statements used to define the Kh of the IVF based on its stratigraphic position. This example uses the Modesto large IVF and the Tuolumne River Riverbank IVF (RBML).

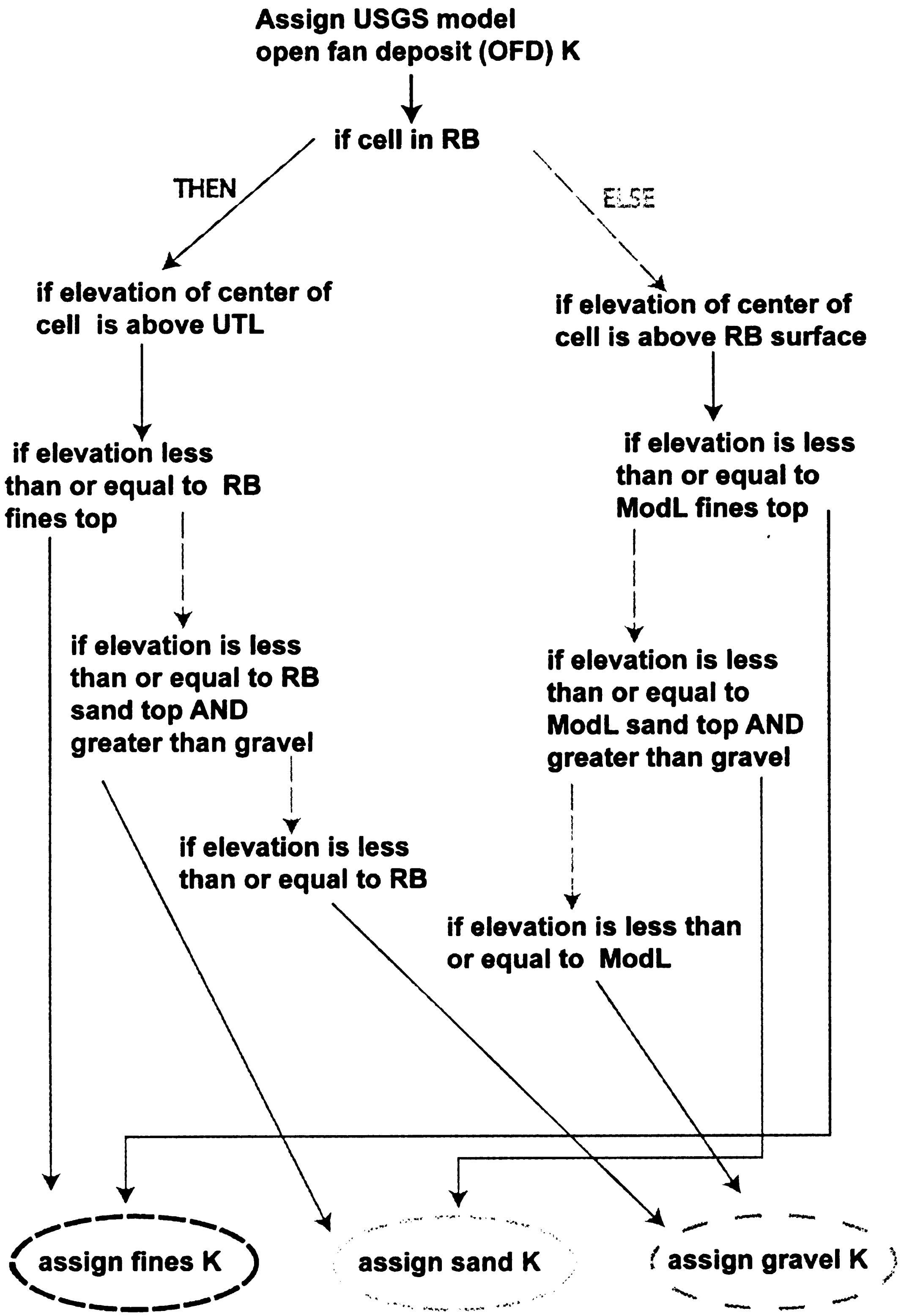

Figure G2: Cells located within the IVF were assigned a Kh based on the elevation of the center of the cell relative to the sequence boundary surfaces (in red), gravel (in orange), sand (in yellow), and fines (in blue) surfaces within the IVF. Shown in color.

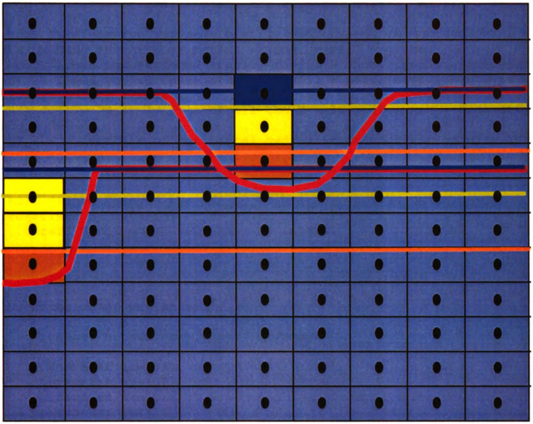

2. No IVF
    a. FORTRAN code

```
      program noIVF

c Program to create an output file to be
c used in 3D realization for a GMS 5.1
c groundwater model.
c DO NOT USE WITHOUT ADJUSTMENT FOR SPECIFICS
c
c PARAMETERS:
c gk = gravel hydraulic conductivity**;
c sk = sand conduct; fk = fines conduct**;
c pk=paleosol conduct**
c **from King's River model Weissmann, Zhang, Fogg, Mount (2004)
c HK1_40 = open fan deposit conduct from USGS model; nzusgs= vertical
discretization of USGS model;
c nx= number of rows
c ny= number of columns
c nz= my vertical discretization;
c
```

```
c Elevation from newly discretized USGS model (40 layers)= elevfil
c Riverbank top = rsfil
c Riverbank bottom of paleosol = rpfil
c Upper Turlock Lake top = usfil
c UTL base of paleosol = upfil
c Mod IV (large or small) fines top surface= mfsfil; mssfil = sand;
mgsfil = gravel
c ModS IV fines top surface= mfsfil (ONLY CHANGE TO MODESTO SMALL WHEN
FILE CHANGED IN PARFIL); mssfil = sand; mgsfil = gravel
c RB IV fines top surface= rfsfil; rssfil = sand; rgsfil = gravel
c ST IV fines top surface= stffil; stsfil = sand; stgfil = gravel (ONLY
WHEN PRESENT IN PARFIL)
c HK1_40fil= 3D array file of all the K values from newly discretized
USGS model
c HK_IVF = new file of horizontal hydraulic conductivities with IVF K
values inclusded
c
c
c EDIT 080905 Changed the HK1_40 to HK1_36.  nzz=36 Using newly
discretized HK data...
c ...nz=33 FInal model will have 33 layers.
c
c


c Declaration of variables

c     integer nznewd, nxy, nxyz, nxyzusgs

      parameter nx=153
      parameter ny=137
      parameter nz=27
      parameter nzz=16
      parameter nxy=nx*ny
      parameter nxyz=nx*ny*nz
      parameter nxyzz=nx*ny*nzz



      real elev(nxyzz)
      real elev2(nxyz)
      real HK1_16(nxyzz)
      real HK1_27(nxyz)

      character*40 elevfil
      character*40 elev2fil
      character*40 HK1_16fil
      character*40 HK1_27fil
      character*40 parfil1



      dx=400.
      dy=400.
      dz=0.5

c   Where are the data??????
```

```
      print*,'input par file name?:'  !  Open input and output files
      read(5,'(a40)') parfil1
      print*,'input file name:', parfil1
      open(1,file=parfil1,status='old')

      read(1,'(a40)') elevfil
      read(1,'(a40)') elev2fil
      read(1,'(a40)') HK1_16fil
      read(1,'(a40)') HK1_27fil


      close(1)
c

      open(18,file='dbg.txt',status='unknown')
      open(19,file='elevations',status='unknown')


c  Read data from ASCII file to fill arrays. Sequence boundaries!
      print*,'reading Parfil including ASCII files from GMS--read elev'
c     read(*, '(a40)') eleva
      open(1,file=elevfil,status='old', form='formatted')
c     print*, '1st doloop'
c      do i=1, 7
c           read (1,'(a40)') junk
c      enddo
                  do k=1,nzz
                        do j=1,ny
                              do i=1,nx
                                    ijk= i+((k-1)*nx*ny)+((j-1)*nx)
                                    read (1,*) elev(ijk)
                              enddo
                        enddo
                  enddo
      close(1)

      print*, 'open elev2fil'
      open(2,file=elev2fil,status='old', form='formatted')
           do k=1,nz
                  do j=1,ny
                        do i=1,nx
                              ijk= i+((k-1)*nx*ny)+((j-1)*nx)
                              read(2,*) elev2(ijk)
                        enddo
                  enddo
               enddo
      close(2)



      print*, 'open HK1_16fil'
      open (17,file=HK1_16fil,status='old', form='formatted')

            do k=1,nzz
                  do j=1,ny
                        do i=1,nx
```

```
                    ijk=i+((k-1)*nx*ny)+((j-1)*nx)
                    read(17,*) HK1_16(ijk)
                    enddo
                 enddo
              enddo

      close(17)


c fill in gms final grid array with proper hydraulic conductivity

      do k=1,nz
         do j=1,ny
            do i=1,nx
                  ij=i+((j-1)*nx)
                  ijk=((k-1)*nx*ny)+i+((j-1)*nx)

c Fill in USGS K values for bottom cells (USGS cells 12 through 16)
                if(k.ge.23) then
                kusgs=k-11
                ijkusgs=((kusgs-1)*nx*ny)+i+((j-1)*nx)
                HK1_27(ijk)=HK1_16(ijkusgs)
                else

c  Calculate elevation of cell and fill in USGS value as 'default'
c     ijk2 = cell number located below ijk
c     elevation = elevation of center of cell for rediscretized grid
                  ijk2=(k*nx*ny)+i+((j-1)*nx)
                  elevation = ((elev2(ijk)-
elev2(ijk2))/2)+elev2(ijk2)

c  Find out which usgs cell we are in and assign usgs K value
                  do kk=1,12
                     ijkk=((kk-1)*nx*ny)+i+((j-1)*nx)
                     ijkk2=(kk*nx*ny)+i+((j-1)*nx)
                    if(elevation.le.elev(ijkk).and.elevation.gt.elev
     *                   (ijkk2)) then
                         HK1_27(ijk)=HK1_16(ijkk)
                   write(15,'(4i4)') i,j,k,kk
                    endif
                   enddo
                endif
             enddo
             enddo
      enddo


c Prepare the gms input files

      print*, 'printing gms files'
      open(20,file=HK1_27fil,status='unknown')



c writing GMS full grid file
```

```
      do k=1,nz
            do j=1,ny
                  do i=1,nx
                        ijk=i+((j-1)*nx)+((k-1)*nx*ny)
                        write(20,'(E9.4)') HK1_27(ijk)
                   enddo
             enddo
      enddo


      print*,'gms files noIVF completed'
      print*,'Goodbye!'


      close(20)
      close(18)
      close(19)


      print*,'*****************************'
      print*,'GMS files written.'
      print*,'*****************************'
      print*,'(:'

      stop
      end
```

3. With the Riverbank IVF from the Stanislaus River
    a. FORTRAN code

```
      program IVF code wST

c Program to create an output file to be
c used in 3D realization for a GMS 5.1
c groundwater model.
c DO NOT USE WITHOUT ADJUSTMENT FOR SPECIFICS
c
c PARAMETERS:
c gk = gravel hydraulic conductivity**;
c sk = sand conduct; fk = fines conduct**;
c pk=paleosol conduct**
c **from King's River model Weissmann, Zhang, Fogg, Mount (2004)
c HK1_27 = open fan deposit conduct from USGS model; nzusgs= vertical
discretization of USGS model;
c nx= number of rows
c ny= number of columns
c nz= my vertical discretization;
c
c Elevation from newly discretized USGS model (40 layers)= elevfil
c Riverbank top = rsfil
c Riverbank bottom of paleosol = rpfil
c Upper Turlock Lake top = usfil
c UTL base of paleosol = upfil
```

```
c Mod IV (large or small) fines top surface= mfsfil; mssfil = sand;
mgsfil = gravel
c ModS IV fines top surface= mfsfil (ONLY CHANGE TO MODESTO SMALL WHEN
FILE CHANGED IN PARFIL); mssfil = sand; mgsfil = gravel
c RB IV fines top surface= rfsfil; rssfil = sand; rgsfil = gravel
c ST IV fines top surface= stffil; stsfil = sand; stgfil = gravel (ONLY
WHEN PRESENT IN PARFIL)
c HK1_27fil= 3D array file of all the K values from newly discretized
USGS model
c HK_IVF = new file of horizontal hydraulic conductivities with IVF K
values inclusded
c
c TO USE...
c (1) If changing vertical discretization: Check Lines 361 and 362
c (2) Edit 'parfil.par' to edit input files.
c



c Declaration of variables

c     integer nznewd, nxy, nxyz, nxyzusgs

      parameter nx=153
      parameter ny=137
      parameter nz=27
      parameter nzz=16
      parameter nxy=nx*ny
      parameter nxyz=nx*ny*nz
      parameter nxyzz=nx*ny*nzz


c     nxy=nx*ny
c     nxyz=nx*ny*nz
c     nxyzusgs=nx*ny*nzusgs

      real rs(nxy), rp(nxy), mfs(nxy), mss(nxy), mgs(nxy)
      real us(nxy), up(nxy), rfs(nxy), rss(nxy), rgs(nxy)
      real st3rb2(nxy)
      real stf(nxy)
      real sts(nxy)
      real stg(nxy)
      real elev(nxyzz)
      real elev2(nxyz)
      real HK1_16(nxyzz)
      real HK_IVF(nxyz)

      character*40 elevfil
      character*40 elev2fil
      character*40 usfil
      character*40 upfil
      character*40 rfsfil
      character*40 rssfil
      character*40 rgsfil
      character*40 stffil
      character*40 stsfil
```

```
      character*40 stgfil
      character*40 rsfil
      character*40 rpfil
      character*40 mfsfil
      character*40 mssfil
      character*40 mgsfil
      character*40 st3rb2fil
      character*40 HK1_16fil
      character*40 HK_IVFfil
      character*40 parfil1


c     character*40 parfil1, junk

c  K values for facies from Weissmann junk

      gk=864
      sk=86.4
      fk=0.0864
c     pk=0.0000001



      dx=400.
      dy=400.
      dz=0.5

c  Where are the data???????

      print*,'input par file name?:'  !  Open input and output files
      read(5,'(a40)') parfil1
      print*,'input file name:', parfil1
      open(1,file=parfil1,status='old')

      read(1,'(a40)') elevfil
      read(1,'(a40)') elev2fil
      read(1,'(a40)') usfil
      read(1,'(a40)') upfil
      read(1,'(a40)') rfsfil
      read(1,'(a40)') rssfil
      read(1,'(a40)') rgsfil
      read(1,'(a40)') stffil
      read(1,'(a40)') stsfil
      read(1,'(a40)') stgfil
      read(1,'(a40)') rsfil
      read(1,'(a40)') rpfil
      read(1,'(a40)') mfsfil
      read(1,'(a40)') mssfil
      read(1,'(a40)') mgsfil
      read(1,'(a40)') st3rb2fil
      read(1,'(a40)') HK1_16fil
      read(1,'(a40)') HK_IVFfil


      close(1)
c
```

```
      open(18,file='dbg.txt',status='unknown')
      open(19,file='elevations',status='unknown')


c  Read data from ASCII file to fill arrays. Sequence boundaries!
      print*,'reading Parfil including ASCII files from GMS--read elev'
c     read(*, '(a40)') eleva
      open(1,file=elevfil,status='old', form='formatted')
c     print*, '1st doloop'
c      do i=1, 7
c           read (1,'(a40)') junk
c      enddo
                  do k=1,nzz
                        do j=1,ny
                              do i=1,nx
                                    ijk= i+((k-1)*nx*ny)+((j-1)*nx)
                                    read (1,*) elev(ijk)
                              enddo
                        enddo
                  enddo
      close(1)

      print*, 'open elev2fil'
      open(2,file=elev2fil,status='old', form='formatted')
           do k=1,nz
                  do j=1,ny
                        do i=1,nx
                              ijk= i+((k-1)*nx*ny)+((j-1)*nx)
                              read(2,*) elev2(ijk)
                        enddo
                  enddo
               enddo
      close(2)

c     Open and read Upper Turlock Lake surface with Riverbank Valley
      print*, 'open usfil'
c     read(*, '(F15.5)') utl_rb1_300
      open(3,file=usfil,status='old', form='formatted')

                  do j=1,ny
                        do i=1,nx
                              ij=i+((j-1)*nx)
                              read(3,*) us(ij)
                        enddo
                  enddo
      close(3)

      print*, 'open upfil'
      open(4,file=upfil,status='old', form='formatted')

                  do j=1,ny
                        do i=1,nx
                              ij=i+((j-1)*nx)
                              read(4,*) up(ij)
                        enddo
                  enddo
```

```
close(4)


print*, 'open rfsfil'
open(5,file=rfsfil,status='old', form='formatted')

            do j=1,ny
                  do i=1,nx
                        ij=i+((j-1)*nx)
                        read(5,*) rfs(ij)
                  enddo
            enddo


close(5)

print*, 'open rssfil'
open(6,file=rssfil,status='old', form='formatted')

            do j=1,ny
                  do i=1,nx
                        ij=i+((j-1)*nx)
                        read(6,*) rss(ij)
                  enddo
            enddo

close(6)
print*, 'open rgsfil'
open(7,file=rgsfil,status='old', form='formatted')

            do j=1,ny
                  do i=1,nx
                        ij=i+((j-1)*nx)
                        read(7,*) rgs(ij)
                  enddo
            enddo

close(7)

print*, 'open stffil'
open(8,file=stffil,status='old', form='formatted')
            do j=1,ny
                  do i=1,nx
                        ij=i+((j-1)*nx)
                        read(8,*) stf(ij)
                  enddo
            enddo

close(8)

print*, 'open stsfil'
open(9,file=stsfil,status='old', form='formatted')
            do j=1,ny
                  do i=1,nx
                        ij=i+((j-1)*nx)
                        read(9,*) sts(ij)
                  enddo
```

```
            enddo

close(9)

print*, 'open stgfil'
open(10,file=stgfil,status='old', form='formatted')
            do j=1,ny
                  do i=1,nx
                        ij=i+((j-1)*nx)
                        read(10,*) stg(ij)
                  enddo
            enddo

close(10)

print*, 'open rsfil'
open(11,file=rsfil,status='old', form='formatted')

            do j=1,ny
                  do i=1,nx
                        ij=i+((j-1)*nx)
                        read(11,*) rs(ij)
                  enddo
            enddo


close(11)

print*, 'open rpfil'
open(12,file=rpfil,status='old', form='formatted')

            do j=1,ny
                  do i=1,nx
                        ij=i+((j-1)*nx)
                        read(12,*) rp(ij)
                  enddo
            enddo

close(12)

print*, 'open mfsfil'
open(13,file=mfsfil,status='old', form='formatted')

            do j=1,ny
                  do i=1,nx
                        ij=i+((j-1)*nx)
                        read(13,*) mfs(ij)
                  enddo
            enddo

close(13)

print*, 'open mssfil'
open(14,file=mssfil,status='old', form='formatted')

            do j=1,ny
                  do i=1,nx
```

```
                        ij=i+((j-1)*nx)
                        read(14,*) mss(ij)
                  enddo
            enddo

      close(14)

      print*, 'open mgsfil'
      open(15,file=mgsfil,status='old', form='formatted')

            do j=1,ny
                  do i=1,nx
                        ij=i+((j-1)*nx)
                        read(15,*) mgs(ij)
                  enddo
            enddo

      close(15)

      print*, 'open st3rb2fil'
      open (16,file= st3rb2fil, status='old', form='formatted')

            do j=1,ny
                  do i=1,nx
                        ij=i+((j-1)*nx)
                        read(16,*) st3rb2(ij)
                  enddo
            enddo

      close(16)


      print*, 'open HK1_16fil'
      open (17,file=HK1_16fil,status='old', form='formatted')

         do k=1,nzz
            do j=1,ny
                  do i=1,nx
                  ijk=i+((k-1)*nx*ny)+((j-1)*nx)
                  read(17,*) HK1_16(ijk)
                  enddo
            enddo
         enddo

      close(17)



c fill in gms final grid array with proper hydraulic conductivity

      do k=1,nz
         do j=1,ny
             do i=1,nx
                 ij=i+((j-1)*nx)
                 ijk=((k-1)*nx*ny)+i+((j-1)*nx)
```

```
c Fill in USGS Kh  values for bottom cells (USGS cells 12 through 16)
            if(k.ge.23) then
             kusgs=k-11
             ijkusgs=((kusgs-1)*nx*ny)+i+((j-1)*nx)
             HK_IVF(ijk)=HK1_16(ijkusgs)
            else

c  Calculate elevation of cell and fill in USGS value as 'default'
c     ijk2 = cell number located below ijk
c     elevation = elevation of center of cell for rediscretized grid
            ijk2=(k*nx*ny)+i+((j-1)*nx)
            elevation = ((elev2(ijk)-elev2(ijk2))/2)+elev2(ijk2)

c  Find out which usgs cell we are in and assign usgs K or T value
                do kk=1,12
                  ijkk=((kk-1)*nx*ny)+i+((j-1)*nx)
                  ijkk2=(kk*nx*ny)+i+((j-1)*nx)

      if(elevation.le.elev(ijkk).and.elevation.gt.elev
     *                         (ijkk2)) then
                               HK_IVF(ijk)=HK1_16(ijkk)
      write(15,'(4i4)') i,j,k,kk
                          endif
                enddo


c  Fill in UTL Formation Paleosol
c      if(elevation.le.us(ij).and.elevation.ge.up(ij)) gms(ijk)= pk

c Fill in Riverbank Formation Paleosol ModL IV
c      if(elevation.le.rs(ij).and.elevation.ge.rp(ij)) gms(ijk)= pk

c fill in Riverbank formation with RB IV (st3rb2 = 2 = inside tuol rb
valley)
      if(st3rb2(ij).eq.2) then
      if(elevation.lt.rfs(ij).and.elevation.gt.us(ij)) then
            if(elevation.le.rfs(ij).and.elevation.gt.rss(ij)) then
                  HK_IVF(ijk)= fk
            else if (elevation.le.rss(ij).and.elevation.gt.rgs(ij))
then
                        HK_IVF(ijk)= sk
c                       write(15,'(a6,e9.4)')'sands ',gms(ijk)
                  else if(elevation.le.rgs(ij)) then
                              HK_IVF(ijk)= gk
                  endif
            endif
      endif

c Fill in the Riverbank formation with ST IV
      if(st3rb2(ij).eq.3) then
            if(elevation.lt.stf(ij).and.elevation.gt.us(ij)) then
                  if (elevation.le.stf(ij).and.elevation.gt.sts(ij))
then
                        HK_IVF(ijk)= fk
            else if     (elevation.le.sts(ij).and.elevation.gt.stg(ij))
then
                              HK_IVF(ijk)= sk
```

```
                    else if (elevation.le.stg(ij)) then
                                HK_IVF(ijk)= gk
                endif
            endif
        endif

c Fill in the Modesto formation with Mod IVF
        if(elevation.gt.rs(ij)) then
            if (elevation.le.mfs(ij).and.elevation.gt.mss(ij)) then
                HK_IVF(ijk)= fk
                else
if(elevation.le.mss(ij).and.elevation.gt.mgs(ij))then
                    HK_IVF(ijk)= sk
                    else if (elevation.le.mgs(ij)) then
                        HK_IVF(ijk)= gk
              endif
         endif
        endif
             enddo
             enddo
        enddo



c Prepare the gms input files

        print*, 'printing gms files'
        open(20,file=HK_IVFfil,status='unknown')



c writing GMS full grid file

        do k=1,nz
            do j=1,ny
                do i=1,nx
                    ijk=i+((j-1)*nx)+((k-1)*nx*ny)
                    write(20,'(E9.4)') HK_IVF(ijk)
                enddo
            enddo
        enddo


        print*,'gms files completed'
        print*,'Goodbye!'


        close(20)
        close(18)
        close(19)


        print*,'*****************************'
        print*,'GMS files written.'
        print*,'*****************************'
        print*,'(:'
```

```
      stop
      end
```

4. Without the Riverbank IVF from the Stanislaus River
    a. FORTRAN code

```
      program IVF code noST

c Program to create an output file to be
c used in 3D realization for a GMS 5.1
c groundwater model.
c DO NOT USE WITHOUT ADJUSTMENT FOR SPECIFICS
c
c PARAMETERS:
c gk = gravel hydraulic conductivity**;
c sk = sand conduct; fk = fines conduct**;
c pk=paleosol conduct**
c **from King's River model Weissmann, Zhang, Fogg, Mount (2004)
c HK1_40 = open fan deposit conduct from USGS model; nzusgs= vertical
discretization of USGS model;
c nx= number of rows
c ny= number of columns
c nz= my vertical discretization;
c
c Elevation from newly discretized USGS model (40 layers)= elevfil
c Riverbank top = rsfil
c Riverbank bottom of paleosol = rpfil
c Upper Turlock Lake top = usfil
c UTL base of paleosol = upfil
c Mod IV (large or small) fines top surface= mfsfil; mssfil = sand;
mgsfil = gravel
c ModS IV fines top surface= mfsfil (ONLY CHANGE TO MODESTO SMALL WHEN
FILE CHANGED IN PARFIL); mssfil = sand; mgsfil = gravel
c RB IV fines top surface= rfsfil; rssfil = sand; rgsfil = gravel
c ST IV fines top surface= stffil; stsfil = sand; stgfil = gravel (ONLY
WHEN PRESENT IN PARFIL)
c HK1_40fil= 3D array file of all the K values from newly discretized
USGS model
c HK_IVF = new file of horizontal hydraulic conductivities with IVF K
values inclusded
c
c
c EDIT 080905 Changed the HK1_40 to HK1_36.  nzz=36 Using newly
discretized HK data...
c ...nz=33 FInal model will have 33 layers.
c
c



c Declaration of variables
```

```
c     integer nznewd, nxy, nxyz, nxyzusgs

      parameter nx=153
      parameter ny=137
      parameter nz=27
      parameter nzz=16
      parameter nxy=nx*ny
      parameter nxyz=nx*ny*nz
      parameter nxyzz=nx*ny*nzz


c     nxy=nx*ny
c     nxyz=nx*ny*nz
c     nxyzusgs=nx*ny*nzusgs

      real rs(nxy), rp(nxy), mfs(nxy), mss(nxy), mgs(nxy)
      real us(nxy), up(nxy), rfs(nxy), rss(nxy), rgs(nxy)
      real st3rb2(nxy)
c     real stf(nxy)
c     real sts(nxy)
c     real stg(nxy)
      real elev(nxyzz)
      real elev2(nxyz)
      real HK1_16(nxyzz)
      real HK_IVF(nxyz)

      character*40 elevfil
      character*40 elev2fil
      character*40 usfil
      character*40 upfil
      character*40 rfsfil
      character*40 rssfil
      character*40 rgsfil
c     character*40 stffil
c     character*40 stsfil
c     character*40 stgfil
      character*40 rsfil
      character*40 rpfil
      character*40 mfsfil
      character*40 mssfil
      character*40 mgsfil
      character*40 st3rb2fil
      character*40 HK1_16fil
      character*40 HK_IVFfil
      character*40 parfil1


c     character*40 parfil1, junk

c  K values for facies from Weissmann junk

      gk=864
      sk=86.4
      fk=0.0864
c     pk=0.0000001
```

```
      dx=400.
      dy=400.
      dz=0.5

c  Where are the data???????

      print*,'input par file name?:'  !  Open input and output files
      read(5,'(a40)') parfil1
      print*,'input file name:', parfil1
      open(1,file=parfil1,status='old')

      read(1,'(a40)') elevfil
      read(1,'(a40)') elev2fil
      read(1,'(a40)') usfil
      read(1,'(a40)') upfil
      read(1,'(a40)') rfsfil
      read(1,'(a40)') rssfil
      read(1,'(a40)') rgsfil
c     read(1,'(a40)') stffil
c     read(1,'(a40)') stsfil
c     read(1,'(a40)') stgfil
      read(1,'(a40)') rsfil
      read(1,'(a40)') rpfil
      read(1,'(a40)') mfsfil
      read(1,'(a40)') mssfil
      read(1,'(a40)') mgsfil
      read(1,'(a40)') st3rb2fil
      read(1,'(a40)') HK1_16fil
      read(1,'(a40)') HK_IVFfil


      close(1)
c

      open(18,file='dbg.txt',status='unknown')
      open(19,file='elevations',status='unknown')


c  Read data from ASCII file to fill arrays. Sequence boundaries!
      print*,'reading Parfil including ASCII files from GMS--read elev'
c     read(*, '(a40)') eleva
      open(1,file=elevfil,status='old', form='formatted')
c     print*, '1st doloop'
c      do i=1, 7
c           read (1,'(a40)') junk
c      enddo
                 do k=1,nzz
                       do j=1,ny
                             do i=1,nx
                                   ijk= i+((k-1)*nx*ny)+((j-1)*nx)
                                   read (1,*) elev(ijk)
                             enddo
                       enddo
                 enddo
      close(1)
```

```
      print*, 'open elev2fil'
      open(2,file=elev2fil,status='old', form='formatted')
           do k=1,nz
                  do j=1,ny
                        do i=1,nx
                             ijk= i+((k-1)*nx*ny)+((j-1)*nx)
                             read(2,*) elev2(ijk)
                        enddo
                  enddo
               enddo
      close(2)

c     Open and read Upper Turlock Lake surface with Riverbank Valley
      print*, 'open usfil'
c     read(*, '(F15.5)') utl_rb1_300
      open(3,file=usfil,status='old', form='formatted')

                  do j=1,ny
                        do i=1,nx
                             ij=i+((j-1)*nx)
                             read(3,*) us(ij)
                        enddo
                  enddo
      close(3)

      print*, 'open upfil'
      open(4,file=upfil,status='old', form='formatted')

                  do j=1,ny
                        do i=1,nx
                             ij=i+((j-1)*nx)
                             read(4,*) up(ij)
                        enddo
                  enddo

      close(4)


      print*, 'open rfsfil'
      open(5,file=rfsfil,status='old', form='formatted')

                  do j=1,ny
                        do i=1,nx
                             ij=i+((j-1)*nx)
                             read(5,*) rfs(ij)
                        enddo
                  enddo


      close(5)

      print*, 'open rssfil'
      open(6,file=rssfil,status='old', form='formatted')

                  do j=1,ny
                        do i=1,nx
                             ij=i+((j-1)*nx)
```

```
                  read(6,*) rss(ij)
            enddo
      enddo

close(6)
print*, 'open rgsfil'
open(7,file=rgsfil,status='old', form='formatted')

      do j=1,ny
            do i=1,nx
                  ij=i+((j-1)*nx)
                  read(7,*) rgs(ij)
            enddo
      enddo

close(7)

print*, 'open rsfil'
open(11,file=rsfil,status='old', form='formatted')

      do j=1,ny
            do i=1,nx
                  ij=i+((j-1)*nx)
                  read(11,*) rs(ij)
            enddo
      enddo


close(11)

print*, 'open rpfil'
open(12,file=rpfil,status='old', form='formatted')

      do j=1,ny
            do i=1,nx
                  ij=i+((j-1)*nx)
                  read(12,*) rp(ij)
            enddo
      enddo

close(12)

print*, 'open mfsfil'
open(13,file=mfsfil,status='old', form='formatted')

      do j=1,ny
            do i=1,nx
                  ij=i+((j-1)*nx)
                  read(13,*) mfs(ij)
            enddo
      enddo

close(13)

print*, 'open mssfil'
open(14,file=mssfil,status='old', form='formatted')
```

```
                do j=1,ny
                      do i=1,nx
                            ij=i+((j-1)*nx)
                            read(14,*) mss(ij)
                      enddo
                enddo

      close(14)

      print*, 'open mgsfil'
      open(15,file=mgsfil,status='old', form='formatted')

                do j=1,ny
                      do i=1,nx
                            ij=i+((j-1)*nx)
                            read(15,*) mgs(ij)
                      enddo
                enddo

      close(15)

      print*, 'open st3rb2fil'
      open (16,file= st3rb2fil, status='old', form='formatted')

                do j=1,ny
                      do i=1,nx
                            ij=i+((j-1)*nx)
                            read(16,*) st3rb2(ij)
                      enddo
                enddo

      close(16)

      print*, 'open HK1_16fil'
      open (17,file=HK1_16fil,status='old', form='formatted')

          do k=1,nzz
                do j=1,ny
                      do i=1,nx
                      ijk=i+((k-1)*nx*ny)+((j-1)*nx)
                      read(17,*) HK1_16(ijk)
                      enddo
                enddo
          enddo

      close(17)


c fill in gms final grid array with proper hydraulic conductivity

      do k=1,nz
         do j=1,ny
             do i=1,nx
                 ij=i+((j-1)*nx)
                 ijk=((k-1)*nx*ny)+i+((j-1)*nx)
```

```
c Fill in USGS K  values for bottom cells (USGS cells 12 through 16)
            if(k.ge.23) then
             kusgs=k-11
             ijkusgs=((kusgs-1)*nx*ny)+i+((j-1)*nx)
             HK_IVF(ijk)=HK1_16(ijkusgs)
            else

c  Calculate elevation of cell and fill in USGS value as 'default'
c     ijk2 = cell number located below ijk
c     elevation = elevation of center of cell for rediscretized grid
            ijk2=(k*nx*ny)+i+((j-1)*nx)
            elevation = ((elev2(ijk)-elev2(ijk2))/2)+elev2(ijk2)

c  Find out which usgs cell we are in and assign usgs K or T value
                do kk=1,12
                  ijkk=((kk-1)*nx*ny)+i+((j-1)*nx)
                  ijkk2=(kk*nx*ny)+i+((j-1)*nx)

      if(elevation.le.elev(ijkk).and.elevation.gt.elev
     *                         (ijkk2)) then
                               HK_IVF(ijk)=HK1_16(ijkk)
      write(15,'(4i4)') i,j,k,kk
                        endif
                enddo


c  Fill in UTL Formation Paleosol
c      if(elevation.le.us(ij).and.elevation.ge.up(ij)) gms(ijk)= pk

c Fill in Riverbank Formation Paleosol ModL IV
c      if(elevation.le.rs(ij).and.elevation.ge.rp(ij)) gms(ijk)= pk

c fill in Riverbank formation with RB IV (st3rb2 = 2 = inside tuol rb
valley)
      if(st3rb2(ij).eq.2) then
      if(elevation.lt.rfs(ij).and.elevation.gt.us(ij)) then
            if(elevation.le.rfs(ij).and.elevation.gt.rss(ij)) then
                  HK_IVF(ijk)= fk
            else if (elevation.le.rss(ij).and.elevation.gt.rgs(ij))
then
                        HK_IVF(ijk)= sk
c                       write(15,'(a6,e9.4)')'sands ',gms(ijk)
                  else if(elevation.le.rgs(ij)) then
                              HK_IVF(ijk)= gk
                  endif
            endif
      endif


c Fill in the Modesto formation with Mod IVF
      if(elevation.gt.rs(ij)) then
            if (elevation.le.mfs(ij).and.elevation.gt.mss(ij)) then
                  HK_IVF(ijk)= fk
                  else
if(elevation.le.mss(ij).and.elevation.gt.mgs(ij))then
                        HK_IVF(ijk)= sk
                        else if (elevation.le.mgs(ij)) then
```

```
                                HK_IVF(ijk)= gk
                     endif
        endif
       endif
              enddo
              enddo
       enddo



c Prepare the gms input files

       print*, 'printing gms files'
       open(20,file=HK_IVFfil,status='unknown')



c writing GMS full grid file

       do k=1,nz
             do j=1,ny
                   do i=1,nx
                         ijk=i+((j-1)*nx)+((k-1)*nx*ny)
                         write(20,'(E9.4)') HK_IVF(ijk)
                    enddo
              enddo
       enddo


       print*,'gms files completed'
       print*,'Goodbye!'


       close(20)
       close(18)
       close(19)


       print*,'*****************************'
       print*,'GMS files written.'
       print*,'*****************************'
       print*,'(:'

       stop
       end
```

Appendix H: Code to Calculate Kv and Kh/Kv

```
        program KVcalc

c Program to create an output file to be
c used in 3D realization for a GMS 5.1
c groundwater model.
c DO NOT USE WITHOUT ADJUSTMENT FOR SPECIFICS
c
c NOTE: This code uses a parameter file.
c
c PARAMETERS:
c
c nx= number of rows
c ny= number of columns
c nz= my vertical discretization;
c nzusgs= number of layers in original USGS model from Steve Phillips in July of 2004
c
c Elevation from original USGS 16 layer model= elevfil
c Elevation from rediscretized 27 layer model= elev2fil
c
c This program is intended to generate KV and Kh/Kv parameters for the 27 layer model generated
c * from the rediscretization of a 16 layer USGS model.
c  kvert.dat = vertical K calculated from the vcont values in the original USGS model (kvert= vcont/
thickness)
c         thickness= the distance between the center of the two cells for which kvert is being calculated
c  khkv.dat = kvert from original USGS reassigned to my layers (kvert is based on the material, not the cell
thickness)
c  vcont.dat = leakance from the original USGS model


c Declaration of variables


        parameter nx=153
        parameter ny=137
        parameter nzusgs=16
        parameter nz=27
        parameter nxy=nx*ny
        parameter nxyz=nx*ny*nz
        parameter nxyzusgs=nx*ny*nzusgs


        real elev(nxyzusgs)
        real elev2(nxyz)
        real vcont(nxyzusgs)
        real corc01(nxy)
        real thick(nxyzusgs)
    real kh(nxyz)
    real hlfthick(nxyzusgs)
    real kv1_16(nxyzusgs)
    real kv1_27(nxyz)
    real khkv(nxyz)
```

```
      character*40 elevfil
      character*40 elev2fil
      character*40 vcontfil
      character*40 corc01fil
      character*40 thickfil
      character*40 khfil
      character*40 hlfthickfil
      character*40 kv1_27fil
      character*40 khkvfil
      character*40 parfil1


c Open parfil (input)

      print*,'input par file name?:'
      read(5,'(a40)') parfil1
      print*,'input file name:', parfil1
      open(1,file=parfil1,status='old')

      read(1,'(a40)') elevfil
      read(1,'(a40)') elev2fil
      read(1,'(a40)') vcontfil
      read(1,'(a40)') corc01fil
      read(1,'(a40)') thickfil
      read(1,'(a40)') khfil
      read(1,'(a40)') hlfthickfil

      close(1)



c Read data from ASCII file to fill arrays.
      print*,'reading Parfil'
   open(1,file=elevfil,status='old', form='formatted')
                  do k=1,nzusgs
                        do j=1,ny
                              do i=1,nx
                                    ijk= i+((k-1)*nx*ny)+((j-1)*nx)
                                    read (1,*) elev(ijk)
                              enddo
                        enddo
                  enddo
      close(1)


       open(2,file=elev2fil,status='old', form='formatted')
                  do k=1,nz
                        do j=1,ny
                              do i=1,nx
                                    ijk= i+((k-1)*nx*ny)+((j-1)*nx)
                                    read (2,*) elev2(ijk)
                              enddo
                        enddo
                  enddo
      close(2)
```

```
open (17,file=vcontfil,status='old', form='formatted')
           do k=1,nzusgs
                  do j=1,ny
                         do i=1,nx
                            ijk=i+((k-1)*nx*ny)+((j-1)*nx)
                            read(17,*) vcont(ijk)
                         enddo
                  enddo
           enddo

    close(17)

    open (3,file=corc01fil,status='old', form='formatted')
           do j=1,ny
              do i=1,nx
                     ij=i+((j-1)*nx)
                     read(3,*) corc01(ij)
                  enddo
           enddo

    close(3)

    open (4,file=thickfil,status='old', form='formatted')
           do k=1,nzusgs
              do j=1,ny
                 do i=1,nx
                        ijk=i+((k-1)*nx*ny)+((j-1)*nx)
                        read(4,*) thick(ijk)
                    enddo
                  enddo
           enddo

    close(4)

    open (5,file=khfil,status='old', form='formatted')
           do k=1,nz
              do j=1,ny
                 do i=1,nx
                        ijk=i+((k-1)*nx*ny)+((j-1)*nx)
                        read(5,*) kh(ijk)
                           enddo
                  enddo
           enddo

    close(5)

    open (6,file=hlfthickfil,status='old', form='formatted')
           do k=1,nzusgs
              do j=1,ny
                 do i=1,nx
                        ijk=i+((k-1)*nx*ny)+((j-1)*nx)
                        read(6,*) hlfthick(ijk)
                    enddo
                  enddo
           enddo
```

```
        close(6)

c Calculate Kv for the 16 layer USGS model from the vcont values.
c    ijk2 = cell number located below ijk
      print*,'Create KV1_16'
      do k=1,nzusgs
       do j=1,ny
         do i=1,nx
         ijk=((k-1)*nx*ny)+i+((j-1)*nx)
                              ijk2=(k*nx*ny)+i+((j-1)*nx)

       if((k.eq.7.or.k.eq.8).and.(corc01(ij).eq.1)) then
                                k8=8
c                               kcorc=0.0013
                                ijk8=(k8*nx*ny)+i+((j-1)*nx)
           kv1_16(ijk)=vcont(ijk8)*hlfthick(ijk8)
c            kv1_16(ijk)=kcorc
         else
           kv1_16(ijk) = vcont(ijk)*(hlfthick(ijk)+hlfthick(ijk2))
       endif

      open(15,file='kv1_16.dat',status='unknown')
      write(15,'(E14.5)') kv1_16(ijk)

         enddo
       enddo
      enddo
      close(15)

c  Calculate KV1_27 from the vcont values in the original USGS model.
      print*,'Create KV1_27 and KH/KV'

      do k=1,nz
           do j=1,ny
             do i=1,nx
                        ij=i+((j-1)*nx)
                        ijk=((k-1)*nx*ny)+i+((j-1)*nx)
                             ijk2=(k*nx*ny)+i+((j-1)*nx)

c Fill in values for KV1_27 with USGS values for bottom layers 23 through 27 (USGS cells 12 through 16)
c These cells are the same size and thickness as in the original model.
c KV can be directly assigned after multiplying by the thickness.
c  kusgs = the layer number in the USGS model
c  ijkusgs = reading array at the specified layer in USGS model
c  ijkusgs2 = reading array at the layer below ijkusgs

c      print*,'Fill in USGS KV1_27  values for bottom layers'
                     if(k.ge.23) then
                        kusgs=k-11
                        ijkusgs=((kusgs-1)*nx*ny)+i+((j-1)*nx)
c                       ijkusgs2= ((kusgs)*nx*ny)+i+((j-1)*nx)
                        kv1_27(ijk)=kv1_16(ijkusgs)

                 else
c  Calculate elevation of center of cell and fill in correlative USGS value
```

```
c     elevation = elevation of center of cell for rediscretized grid

                    elevation = ((elev2(ijk)-elev2(ijk2))/2)+elev2(ijk2)

c  Find out which USGS cell we are in and assign KV value calculated from vcont
c Layer 8 is the Corcoran clay in the USGS model.  KV is calculated differently according to...
c ...'kvc_calib_merten.f' from the USGS model.
c      print*,'Find out which usgs cell we are in and assign Kv1_27'
                      do kk=1,12
                      ijkk=((kk-1)*nx*ny)+i+((j-1)*nx)
                      ijkk2=(kk*nx*ny)+i+((j-1)*nx)

                        if(elevation.le.elev(ijkk).and.elevation.gt.elev
     *                       (ijkk2)) then
                kv1_27(ijk)= kv1_16(ijkk)
              endif
                      enddo

c           write(15,'(4i4)') i,j,k,kk
        endif


              enddo
                   enddo
          enddo

c  Calculate Kh/Kv
      print*,'Calc Kh/Kv'
      do k=1,nz
             do j=1,ny
                do i=1,nx
                       ijk=((k-1)*nx*ny)+i+((j-1)*nx)

        if(kv1_27(ijk).eq.0) then
           khkv(ijk) = kh(ijk)/ 0.0000001
        else
           khkv(ijk)= kh(ijk)/ kv1_27(ijk)
        endif

          enddo
             enddo
          enddo


c writing GMS full grid file
      print*, 'writing GMS full grid file'
      open(18,file='kv1_27fil.dat',status='unknown')
      open(20,file='khkv.dat',status='unknown')


         do k=1,nz
                do j=1,ny
                       do i=1,nx
                              ijk=i+((j-1)*nx)+((k-1)*nx*ny)
                              write(18,'(E14.5)') kv1_27(ijk)
                              write(20,'(E14.5)') khkv(ijk)
```

```
                    enddo
               enddo
          enddo


          print*,'gms files completed'
          print*,'Goodbye!'


     close(18)
     close(19)
     close(20)




     print*,'******************************'
     print*,'GMS files written.'
     print*,'******************************'
     print*,'(:'

     stop
     end
```

Appendix I: General Head Boundary Code

```
      PROGRAM ghb_all
c     MODIFIED from USGS kvc_calib_merten.f from Steve Phillips July 11, 2005 via e-mail.
c     Used to remake ghb files with new discretization for use in lpf model.
c     Deleted beginning of program--only need to calc. the ghb file for model.
c     ***Lines that begin with asterisks are edits by Amy Lansdale.
c
c
c  ***TO USE: (1) ALWAYS check input horizontal hydraulic conductivity file #29 on line 61
c           (2) Change input Kv file #99 in line 64
c
c ***Changed numbers of layers and added some variables.
      integer row,col,nsteps,lay,iunit,nghb,ghbloc(200,200),
     + bound(200,200,20),corc01(200,200)
      real KH(153,137,27),KV1_27(153,137,27), KH2(153,137,27)
     + ,thick(153,137,27),ghbhead(200,200,80),ghbcond(200,200,80),
     + botelev(153,137,40),top(153,137,40),head,ghbdist,
     + persat(153,137,40)


c
c ... grid geometry
      nrow=153
      ncol=137
      nlay=27
      ny=137
      nx=153
      nz=27

c
      ncorr=0
      print*, 'initialize variables'
c     initialize variables
    5 do 10 lay=1,nlay
        do 10 row=1,nrow
          do 10 col=1,ncol
            ghbhead(row,col,lay)=0.
                ghbcond(row,col,lay)=0.
            KH2(row,col,lay)=0.
            persat(row,col,lay)=0.


   10 continue


      open(95,file='ghb27fil.ghb')
      open(101,file='KH2fil.dat')


c     open files and read in external data

      print*, 'open ghb_locations.dat'
      open(94,file='ghb_locations3.dat')
```

```
      read(94,'()')
            do 40 row=1,nrow

         read(94,'(200i1)') (ghbloc(row,col),col=1,ncol)

  40 continue

c *****THIS MUST BE CHANGED FOR EACH GEOLOGIC SCENARIO OF IVF (rbmodL, rbstmodL,
rbmods, rbstmods).************
     print*, 'open HK_IVFfil, thick, and KV1_27'
c ***This input HK file should be the HK file for each of the various IVF scenarios.  CHECK before each
run of this code.
     open(29,file='Khrbstmlless50finalnodat.dat')
c *** "Thickin" should be recalculated for various discretizations.  See 'Thickness.f' code to calculate.
     open(30,file='thick27.dat')
     open(99,file='kv1_27rbstmlless50.dat')




     do 20 lay=1,nlay
      do 20 row=1,nrow

        read(29,*) (KH(row,col,lay),col=1,ncol)
        read(30,*) (thick(row,col,lay),col=1,ncol)
        read(99,*) (KV1_27(row,col,lay),col=1,ncol)


  20 continue



c ***Calculate the K vertical for layer 1 to 2 and 2 to 3 (original layer 1 to 2) only (needed below in USGS
code) using the harmonic mean...
c     print*, 'Calc KH2'

      do 80 lay=1,nlay
       do 90 row=1,nrow
             do 100 col=1,ncol
c ...***check to see if KH value is equal to zero to prevent zero divide. Make KH a very small number.
c ...***most of the cells with zeros are inactive.
               if (KH(row,col,lay).eq.0) then
               KH2(row,col,lay)= 0.000000000000001
               elseif (KH(row,col,lay).ne.0) then
               KH2(row,col,lay)= KH(row,col,lay)
               endif

 100     continue
  90   continue
  80  continue

       print*, 'Write KH2'



     do 175 lay=1,nlay
```

```
      do 175 row=1,nrow
          do 175 col=1,ncol
           write(101,'(3i5,g20.12)') lay,row,col, KH2(row,col,lay)

 175 continue



      close(101)



      print*, 'ghb calc'

c ***   generate ghb file; ghbloc indicates boundary type (4&5 are lateral,
c ***   2 is river)
c
c ...  Vertical gradient of 0.05 specified along N and S lateral boundaries;
c ...  downward to layer 33 (***was 9 in original model), and upward below 33 (***was 9 in original
model)
c ...  -- max head below 33 (***was 9 in original model) = water table
c
c          constants:
           bedthick=1.0
           cellsize=400.
           rivwidth=25.
           ghbdist=400.
           nghb=0
           gradient=0.05
           vkrivmult=10.

      open(93,file='ghb27in1_finalEDIT.dat')
      open(105, file='totthick.dat')
c     open(106, file='totthick2.dat')

 200 read(93,*,end=290) lay,row,col,head


c     print*, 'downstream river segments and western boundary'
c ...  downstream river segments and western boundary
           if((ghbloc(row,col).eq.2.and.lay.eq.1).or.ghbloc(row,col).eq.5)
     &  then
            nghb=nghb+1
            ghbhead(row,col,lay)=head



c ****Changed the original:
c        ghbcond(row,col,lay)=vcont(row,col,lay)*((thick(row,col,lay)/
c        2.)+(thick(row,col,lay+1)/2.))*((cellsize*rivwidth)/bedthick)
c        *vkrivmult   to...see below...
            if(ghbloc(row,col).eq.2.and.lay.eq.1) then
            ghbcond(row,col,lay)= KV1_27(row,col,lay)*((cellsize*rivwidth)
     &  /bedthick)*vkrivmult
```

```
c ***Layer in following if statement (now layer 16) was 7 (lay above C.C) in original code...
c ..."REMOVE" is the line that was used to calc K. Not needed here because all values in...
c... KH file are actual conductivities, not K and T values as was true..
c...in original code (lay 8-16 were T values).  K values were calc by dividing by thickness in GMS.


      else
        ghbcond(row,col,lay)=KH2(row,col,lay)*thick(row,
     &    col,lay)*cellsize/ghbdist
        endif
c ***REMOVED    KH(row,col,lay)=KH(row,col,lay)/thick(row,col,lay)



c ...  north and south lateral boundary
c     print*, 'north and south lateral boundary'

          else if(ghbloc(row,col).eq.4) then
           nghb=nghb+1

c ...    conductance first
c ... ***layer was 7, change to layer 16 which is equivalent to the layer above CC
c            print*,'conductance first'
c ***below conditional statement separates the unconfined portions of the aquifer (above Corcran clay)
from the confined...
c... portions of the model (Corcran clay and below). Because ALL of my KH values are K values...
c... not K and T values, I maintianed the USGS code format but multiply by thickness in both portions of
the statement.
           if(lay.le.16) then
            ghbcond(row,col,lay)=KH2(row,col,lay)*thick(row,col,lay)*
     &     cellsize/ghbdist
           else
            ghbcond(row,col,lay)=KH2(row,col,lay)*thick(row,col,lay)*cellsize/
     &       ghbdist
           endif

c     print*, 'now head'

cc ...   now head
           totthick=0
c ****Edit the application of a gradient to the head from the methods used in the USGS.
c ****The gradient is subtracted (to generate downward flow) and applied from layer 1 to
c ****...17 (the Corcoran Clay). Then the layer below the Corcoran clay (where the most
c ****...pumping occurs), is set equal to the head in the Corcoran Clay.
           if(lay.eq.1) then
             ghbhead(row,col,lay)=head
 210   continue
      else if(lay.le.17) then
            do 220 k=1,lay
             if(k.eq.1) then
              thickness=thick(row,col,k)/2.
             else if(k.eq.lay) then
              thickness=thick(row,col,k)/2.
             else
```

```
            thickness=thick(row,col,k)
          endif
          totthick=totthick+thickness

 220     continue
        ghbhead(row,col,lay)=ghbhead(row,col,1)-(totthick*gradient)
    write (105,*) lay,row,col,totthick
c          totthick=0

c ****The original USGS gradient had the head in the Corcoran clay higher than...
c ****...the head in the cells above it. Added this IF/THEN statement to rectify that.
      else if(lay.eq.18) then
        ghbhead(row,col,lay)=ghbhead(row,col,17)
     write (105,*) lay,row,col


       else

c ... ***Change to layer 19. Below layer 18, the gradient is positive (generates an upward flow).
          do 240 k=19,lay
           if(k.eq.19) then
            thickness=thick(row,col,k)/2.
           else if(k.eq.lay) then
            thickness=thick(row,col,k)/2.
           else
            thickness=thick(row,col,k)
           endif
           totthick=totthick+thickness

           write (106,*) lay,row,col,totthick

 240     continue
        ghbhead(row,col,lay)=ghbhead(row,col,18)+(totthick*gradient)
    write (105,*) lay,row,col,totthick
c         totthick=0

        if(ghbhead(row,col,lay).gt.ghbhead(row,col,1))
   &     ghbhead(row,col,lay)=ghbhead(row,col,1)
          endif
         endif

    write (105,*) lay,row,col,totthick


         goto 200


c        output ghb file, rivers first
c

 290     k=1
c **** Change the iunit to 40 (was 2 in the old code). This is where flow budget will be recorded.
c **** When the file is opened by GMS and resaved, it will rewrite 40.
         iunit=40
         np=0
         write(95,'(2i5)') nghb,iunit
```

```
      write(95,'(2i5)') nghb,np
      do 300 i=1,nrow
      do 300 j=1,ncol
       if(ghbloc(i,j).eq.2.) write(95,'(3i5,2g20.12)') k,i,j,
 &   ghbhead(i,j,k),ghbcond(i,j,k)
300 continue
      do 350 k=1,nlay
      do 350 i=1,nrow
      do 350 j=1,ncol
       if(ghbloc(i,j).eq.4.or.ghbloc(i,j).eq.5) write(95,'(3i5,2g20
 &   .12)') k,i,j,ghbhead(i,j,k),ghbcond(i,j,k)
350 continue
      print*,'******************************'
  print*,'Files written.'
  print*,'******************************'
      stop
  end
```

Appendix J: Well Code

```
        program wel_calib_all
c ***Lines that begin with astericks are edits by Amy Lansdale from the original code by Steve Phillips.
c *****TO USE: Change file #34 in line 36 to input horizontal hydraulic conductivity.
c
c
c    SPP 12/04 -- modified to distribute pumpage to adjacent layers for
c     wells pumping > spec rate in cells with < spec % of coarse materials
c     SPP 02/03 -- now called by runss_calib.sh
c        SPP 12/02 -- creates well file for MERSTAN SS model
c
c***Changed the array sizes to accomodate the 40 layer model. (Number of layers was set to 20 for the 16
layer model.)
        integer row,col,lay,ibound(200,200),icorc(200,200)
        real pumpage,tperf,bperf,x,y,bot(200,200,40),
   &  HK(200,200,40),tequiv(40),pumplay(40)
        character wellid*8,runtyp*1,onlycorc*1
c
        nrow=153
        ncol=137
        nlay=27
        xorigin=-83795.7
        yorigin=1572727.3
        nwells=0
        totpump=0.
        onlycorc='y'
c
c       read if single or multiple run, passed from script
c       read(*,*) runtyp
c       runtyp='s'
c
        open(30,file='wel.in')
        open(31,file='elevbot1_27nodat.dat')
        open(35,file='elevtop1_27nodat.dat')
        open(32,file='ibound.40')
        open(33,file='corc01.32')
c *****THIS FILE MUST BE CHANGED FOR EACH GEOLOGIC SCENARIO OF IVF (rbmodL,
rbstmodL, rbmods, rbstmods).************
        open(34,file='KHrbstmlplus50finalnodat.dat')
c       output files
        open(40,file='wel.tmp')
        open(41,file='wel27.wel')


c *****K and T input files--REMOVED ALL 07/21/05

c
c       read first array for "bot", which is top layer 1, ibound, icorc
        read(32,'( )')
        do 100 i=1,nrow
                read(35,*) (bot(i,j,1),j=1,ncol)
                read(32,*) (ibound(i,j),j=1,ncol)
                read(33,*) (icorc(i,j),j=1,ncol)
 100 continue
```

```
c
c         read rest of bottoms, and k
          do 150 l=1,nlay

          do 150 i=1,nrow
            read(31,*) (bot(i,j,l+1),j=1,ncol)
c                   iunit=50+l
c                   read(iunit,*) (HK(i,j,l),j=1,ncol)
 150 continue
c
c     read texture
      do 160 lay=1,nlay

          do 160 row=1,nrow
        read(34,*) (HK(row,col,lay),col=1,ncol)
 160  continue
c
c         read through list of wells one by one, determine equivalent transmissivities
c         to distribute by layer, and build well file
c ...  *** again, note that "bot" array starts with top of layer 1 ***
c
          read(30,'( )')
 200 read(30,*,end=99) wellid,x,y,tperf,bperf,pumpage
c
c         transform coordinates, and calculate row & column
c
          deltax=xorigin-x
          deltay=y-yorigin
          tdeltax=deltax
          xdist=((deltay*.601815023152048)-(deltax*.798635510047293))
          ydist=((deltay*.798635510047293)+(tdeltax*.601815023152048))
          col=int(xdist/400.)+1
          row=153-int(ydist/400.)
c
c         sweep through layers, calculating effective transmissivity based on thickness
c         of screened interval within each layer and K value for layers 1-7; layers 8-16
c     "K" values are "T" already
c
c
          if(ibound(row,col).ne.0) then
            sumtequiv=0.
          do 500 lay=1,nlay
                   if((tperf.gt.bot(row,col,lay+1)).and.(bperf.lt.bot(row,col,lay))) then
                            if(tperf.lt.bot(row,col,lay)) then
                                     z1=tperf
                            else
                                     z1=bot(row,col,lay)
                            endif
                            if(bperf.gt.bot(row,col,lay+1)) then
                                     z2=bperf
                            else
                                     z2=bot(row,col,lay+1)
                            endif
c ...           The old way
c                           tequiv(lay)=K(row,col,lay)
c                           if(lay.le.7) tequiv(lay)=tequiv(lay)*(z1-z2)
```

```
c                              sumtequiv=sumtequiv+tequiv(lay)

c ...          The new way
c****Change old layer 7 in USGS model to layer 16, which is still the layer above the Corcran Clay in the
newly...
c...discretized model.
                              if(lay.le.16) then
                               tequiv(lay)=HK(row,col,lay)*(z1-z2)
                              else
                               tequiv(lay)=HK(row,col,lay)*((z1-z2)/
     &                  (bot(row,col,lay)-bot(row,col,lay+1)))
                              endif
                              sumtequiv=sumtequiv+tequiv(lay)
                        else
                              tequiv(lay)=0.
                        endif
 500 continue
c
c         now distribute pumpage by layer, write to file, and read next well
c
c $$$ option 1: correct for wells screened only in corcoran
c
c    if(onlycorc.eq.'y') then
c
c ...  first check for wells screened only in corcoran (unrealistic) and,
c      if so, distribute pumpage to layers 7 - 9
c******Change 8 (USGS Corcran Clay) to 17, 7 (USGS lay abv Corcran Clay) to 16,...
c ....and 9 (USGS lay blw Corcran Clay) to 18.
      if((tequiv(17).ne.0.).and.(tequiv(16).eq.0.).and.(tequiv(18).eq.
     &   0.)) then
           if(icorc(row,col).ne.0) then
            thick16=bot(row,col,16)-bot(row,col,18)
            tequiv16=HK(row,col,16)*thick16
            tequiv17=HK(row,col,17)
            tequiv18=HK(row,col,18)
            sumtequiv=tequiv16+tequiv17+tequiv18
            tequiv(16)=1.
            tequiv(18)=1.
c       Layer 16 (USGS layer 7)
         pump=pumpage*(tequiv16/sumtequiv)
            write(40,'(3i5,g15.6)') 16,row,col,pump
            nwells=nwells+1
            totpump=totpump+pump
c       Layer 17 (USGS layer 8--CC)
         pump=pumpage*(tequiv17/sumtequiv)
            write(40,'(3i5,g15.6)') 17,row,col,pump
            nwells=nwells+1
            totpump=totpump+pump
c       Layer 18 (USGS layer 9)
         pump=pumpage*(tequiv18/sumtequiv)
            write(40,'(3i5,g15.6)') 18,row,col,pump
            nwells=nwells+1
            totpump=totpump+pump
           else
         pump=pumpage
c        Layer 17 (USGS layer 8)
```

```
              write(40,'(3i5,g15.6)') 17,row,col,pump
              nwells=nwells+1
              totpump=totpump+pump
            endif
      else
c
c ...   Check for other wells pumping in single layer at > specified rate and
c       within cells with < specified % coarse; if so, distribute pumpage
c       proportionally to adjacent layers. If adjacent layers already pumping,
c       activate nearest layers above and below.
c
c $$$   Specified values:
c
        specrate=-1000.
        specpct=0.8007E+01
c*******Change 'specpct=10.' which refers to the corase\fine fraction from the initial USGS input...
c.....to 'specpct=0.8007E+01'.  This is the calculated HK of a cell with a coarse\fine fraction of 10...
c.....CALCULATE HK from htextr (corase\fine fraction)-->
c.....htextr=10; fcoarse=10/100=0.1; ffine=1-0.1= 0.9...
c.....To calc. use arithmetic mean from page 6  in 'kvc_calib-merten.f'-->
c.....Ksand and Kclay from 'kvc_calib_merten_s.dat'
c ....HK = (ffcoarse)(Ksand)+(fffine)(Kclay)= (0.1*80)+ (0.9*0.008)= 8.0072 = 0.8007E+01

c $$$
  580    do 590 lay=1,nlay
        pumplay(lay)=0.
  590    continue
           do 600 lay=1,nlay
        if(tequiv(lay).ne.0.) then
          pumplay(lay)=pumpage*(tequiv(lay)/sumtequiv)
          if((pumplay(lay).lt.specrate).and.(HK(row,col,lay)
     &      .lt.specpct)) then
          thick=bot(row,col,lay)-bot(row,col,lay+1)
          tequiv(lay)=HK(row,col,lay)
          if(lay.le.16) tequiv(lay)=tequiv(lay)*(thick)
          sumtequiv=tequiv(lay)
c         activate closest non-pumping layers, recalculating tequiv
          l=lay-1
  610        if(tequiv(l).eq.0.) then
           thick=bot(row,col,l)-bot(row,col,l+1)
           tequiv(l)=HK(row,col,l)
           if(l.le.16) tequiv(l)=tequiv(l)*(thick)
           sumtequiv=sumtequiv+tequiv(l)
          else
           thick=bot(row,col,l)-bot(row,col,l+1)
           tequiv(l)=HK(row,col,l)
           if(l.le.16) tequiv(l)=tequiv(l)*(thick)
           sumtequiv=sumtequiv+tequiv(l)
                 l=l-1
           goto 610
          endif
          l=lay+1
  620        if(tequiv(l).eq.0.) then
           thick=bot(row,col,l)-bot(row,col,l+1)
           tequiv(l)=HK(row,col,l)
           if(l.le.16) tequiv(l)=tequiv(l)*(thick)
```

```
            sumtequiv=sumtequiv+tequiv(l)
          else
            thick=bot(row,col,l)-bot(row,col,l+1)
            tequiv(l)=HK(row,col,l)
            if(l.le.16) tequiv(l)=tequiv(l)*(thick)
            sumtequiv=sumtequiv+tequiv(l)
                 l=l+1
            goto 620
          endif
        endif
      endif
 600   continue
c
c ...   Write out pumpage
c
          do 650 lay=1,nlay
      if(tequiv(lay).ne.0.) then
        pump=pumpage*(tequiv(lay)/sumtequiv)
            write(40,'(3i5,g15.6)') lay,row,col,pump
        nwells=nwells+1
        totpump=totpump+pump
      endif
 650   continue
    endif
  endif
        goto 200
c
c       end of input file has been reached, so write headers to well file,
c       and transfer previous output to this file
c
 99     nunit=2
        nparam=0
        rewind (40)
  write(41,'(2i5)') nwells,nunit
        write(41,'(2i5)') nwells,nparam
        do 1000 i=1,nwells
                read(40,'(3i5,g15.6)') lay,row,col,pump
                write(41,'(3i5,g15.6)') lay,row,col,pump
1000 continue
  write(*,'(a,g20.6)') 'total pumpage = ',totpump

  print*,'****************************'
  print*,'Files written.'
  print*,'****************************'
        stop
        end
```